UNIVERSITA' DEGLI STUDI DI GENOVA

Dipartimento di Medicina Sperimentale

Corso di Dottorato di Ricerca in *Biotecnologie in Medicina Traslazionale*

Curriculum *Medicina Rigenerativa ed Ingegneria dei Tessuti* (5465)

Coordinatore Chiar.mo Prof. Rodolfo Quarto

Platelet lysate activity in the wound-healing process: activation of endothelial and adipose tissue progenitor and differentiated cells

Dottorando

Alessio Romaldini

Tutor Accademico

Chiar.mo Prof. **Ranieri Cancedda**

Tutor Esterni

Dott.ssa **Fiorella Descalzi**

Dott.ssa **Maddalena Mastrogiacomo**

XXX ciclo

23 Marzo 2018

Con Affetto
Ai Miei Genitori…

TABLE OF CONTENTS

1. INTRODUCTION

1.1. Principles of Wound Healing

Wound healing is the physiological body's response to damage in order to restore, i.e. *to regenerate*, both the structure and the function of an injured tissue, a diseased organ or a missing part of the body. In all animals, regenerative mechanisms occur following the injury but their efficiency is dramatically variable depending on the biological complexity. In fact, the lower animals have an extraordinary regenerative potential while the higher ones preserve a limited potential. For example, *Hydra* lets any isolated fragments of body or aggregates of dissociated cells regenerate a complete and viable organism. There are evidences that the regeneration process in *Hydra* occurs almost exclusively by morphallaxis, i.e. the transformation of existing tissues into newly organized structures (Bosch, 2007). Analogously, the freshwater planarians can regenerate an entire body from almost any body piece after cutting. In a different way from *Hydra* model, the regeneration in planarian occurs by proliferation of undifferentiated cells producing a new tissue called blastema, which will grow and differentiate to replace the most distal structures lost when the organism has been cut. The remaining part of the old tissue readapts to the new one by cell death, proliferation and differentiation (Salo et al., 2009). In addition to phylogenetic development, the regenerative potential also depends on ontogenetic development of the organism. In particular, the newt has the ability to repeatedly regenerate its limbs independently of its age, while other amphibians such as axolotl, which can regenerate limbs in the larval stage, deteriorate or lose such ability after metamorphosis (Tanaka et al., 2016). In mammals, the regenerative capacity is limited and the rapid repair of the injury by deposition of fibrotic tissue often prevents the tissue regeneration, especially when the injury is extended. In after-birth humans, the amputated digit tips can regrow revealing a nearly perfect healing of nail bed, bone, and subcutaneous tissue, when the loss occurs in the first decade of life and before sexual maturity (Kisch et al., 2015). In the adult humans, any epithelia, bones, liver and the hematopoietic system represent tissues with the highest regenerative capacity (Eming et al., 2014). In general, such differences in the regenerative potential of humans throughout their lifespan could be explained referring to the content of undifferentiated cells within tissues, which are more abundant in the foetal and neonatal life than in adults (Cancedda et al., 2017). In any way, the rapid response to a severe damage by fibrotic repair could represent a survival advantage because it prevents lethal infections, stops quickly the bleeding and inhibits the mechanical deformation of tissues (Gurtner et al., 2008). Moreover, the complete

regeneration of extended portions of tissues or parts of body would be energetically unsustainable for a complex organism.

1.2. Molecular Mechanisms of Wound Healing

The classical model of wound healing is composed of three distinct but overlapping phases: i) inflammation, ii) new tissue formation, iii) remodelling. In all tissues, apart from hyaline cartilage, the first phase starts immediately after the damage by haemostasis in order to stop the blood extravasation. Haemostasis is initially achieved by vasoconstriction, then with the formation of a platelet plug and finally with the activation of coagulation cascade and the formation of a fibrin clot. When platelets encounter exposed collagen and von Willebrand factor in the sub-endothelial layer of a damaged vessel and remain entrapped in the fibrin clot, they activate and release a cocktail of more than 300 bioactive soluble molecules in the surrounding microenvironment by degranulation triggering the real healing process (Golebiewska and Poole, 2015). In particular, platelet-derived molecules together with microbial components and the activation of complement regulate the migration of innate myeloid-lineage cells from nearby tissues and from the circulation. Neutrophils are the first inflammatory cells recruited after the tissue damage and clean the wound site from pathogenic microorganisms and apoptotic cells. The recruitment of neutrophils is initially induced by damage-associated molecular patterns (DAMPs), released at the injury site, and then by CXC-chemokine ligand 8 (CXCL8) family chemokines and leukotrienes, released from surrounding tissue cells. Early-arriving neutrophils are then themselves activated to both directly and indirectly promote further secretion of CXCL8 family chemokines and leukotriene B4 (LTB4) inducing neutrophil recruitment from the circulation and amplification of the response (de Oliveira et al., 2016). Macrophages, derived mainly from monocytes of peripheral blood, arrive a little later and clear the wound of all matrix and cell debris, including fibrin and apoptotic neutrophils by phagocytosis. In response to various stimuli, monocytes/macrophages undergo a reprogramming which leads to the emergence of a spectrum of distinct functional phenotypes: the classically activated M1 phenotype, induced by IFNγ alone or in concert with microbial stimuli (e.g. LPS) or cytokines (e.g. GM-CSF), the alternatively activated M2 phenotype, induced by cytokines such as IL-4 and IL-13, and the "M2-like" phenotype, which shares some but not all signature features of M2 cells. In general, M1 cells are efficient producers of effector molecules (reactive oxygen and nitrogen intermediates) and inflammatory cytokines (IL-1β, TNF, IL-6), participate as inducer and effector cells in polarized Th1 responses and mediate resistance against intracellular parasites and tumours. Instead, M2 cells take part in polarized Th2 responses, parasite clearance, the dampening of inflammation, the promotion of tissue remodelling, angiogenesis, tumour progression and immunoregulation (Mantovani et al., 2013). Mast cells, derived from circulating basophils, are

recruited with a somewhat later time course respect to neutrophils and macrophages and have been postulated to act during the later post-inflammatory phases of the healing process (Martin and Leibovich, 2005). Each of these inflammatory cell types releases cocktails of growth factors and cytokines that regulate the progression of the physiological response to injury. At the wound site, an inflammatory microenvironment is hence established that mobilizes or recruits local and circulating endothelial cells, stem/progenitor cells and other cells with healing potential (Cancedda et al., 2017). The second phase of wound healing is characterized by the differentiation of fibroblasts into myofibroblasts and the formation of new blood vessels from the pre-existing vasculature. Myofibroblasts are contractile cells, with stress fibres containing α-smooth muscle actin, that move the edges of the wound close and also deposit collagen and other components of the extracellular matrix (ECM) (Darby et al., 2014). During the wound closure process, biomechanical forces elicited by myofibroblasts induce looping and splitting angiogenesis, which are processes of angiogenesis faster than sprouting occurring during the early embryonic development (Kreuger and Phillipson, 2015). Simultaneously, the reprogramming of resident differentiated cells and the recruitment of stem/progenitor cells out from their niche lead them to proliferate and reconstitute the missing parts of the damaged tissue. In the remodelling phase, collagen is remodelled and realigned along tension lines and apoptosis removes unnecessary cells (Atala et al., 2010).

When the tissue injury is severe or repetitive or if the wound-healing response itself becomes dysregulated, a progressively irreversible fibrotic response occurs at the expense of tissue regeneration. The outcome of fibrosis is the formation of a pathological tissue, known as scar tissue, showing an aberrant structure characterized by few cells, mainly fibroblasts, embedded in excessively collagen-rich ECM, which prevents the repaired tissue recovering its original function. In this scenario, ECM-secreting myofibroblasts are central to the pathogenesis of all fibrotic diseases but it is not completely clear which molecular and immunological mechanisms induce the uncontrolled differentiation of quiescent fibroblasts into actively proliferating ECM-producing myofibroblasts (Wynn and Ramalingam, 2012). Some evidences show that a prolonged disturbance in the coagulation cascade can lead to fibrosis and deficiencies in the clotting pathway can also contribute to it. Moreover, acute inflammatory reactions play an important part in triggering fibrosis. In fact, if the inflammatory macrophages and neutrophils are not quickly eliminated, they can exacerbate the inflammatory response that leads to scarring (Wynn and Ramalingam, 2012).

1.3. Regenerative Medicine: Classical and Innovative Approaches

The mission of regenerative medicine is to envisage and provide next-generation therapeutic solutions to physicians against wound-healing-related diseases, in which the wound-healing process

is poor or impaired, or against critical-size injuries. In this context, patients affected by visual and hearing impairments, difficult-to-heal large tissue defects, chronic skin wounds, or fibrotic diseases represent examples of target for the regenerative medicine.

Historically, the first successful experience of regenerative medicine is represented by the therapeutic application of autologous cultured human epithelium in two children who sustained burns on more than 95% of their bodies (Gallico et al., 1984). That approach based on the *ex vivo* expansion of autologous stem/progenitor cells before their use on the patient is commonly named "Cell Therapy". Another approach, indicated as "Tissue Engineering", uses biomaterials combined or not with expanded cells and biologically active molecules to recreate a functional tissue.

In this field, the Regenerative Medicine Lab of IRCCS Ospedale Policlinico San Martino at Genova (Italy) was among the pioneers all over the world and the major results were about the use of autologous and allogenic cultured human epidermal cells in the treatment of partial and full skin thickness burns (De Luca et al., 1989), the use of autologous graft of cultured urethral epithelium for the treatment of posterior hypospadias (Romagnoli et al., 1990), the restoration of the human corneal surface with autologous corneal epithelial sheets (Pellegrini et al., 1997) and the reconstruction of large bone segments with the use of autologous bone marrow stromal cells (Quarto et al., 2001). Although the successful outcomes of these experimental therapies and others reported in literature, a very few number of them reached the status of Advanced Therapy Medicinal Products (ATMPs), i.e. those "*medicines for human use that are based on genes or cells*" (http://www.ema.europa.eu/ema/). In the European Union, only four ATMPs with orphan designation (Glybera, Strimvelis, Zalmoxis, and Holoclar) have obtained the marketing authorisation by the European Medicines Agency (EMA) and a ten-year market exclusivity (Farkas et al., 2017). The major constraints for the broad use of these experimental therapies are the high costs of *ex vivo* cell manipulation in GMP (Good Manufacturing Practice)-qualified structures and the complexity/morbidity of surgical procedures (Cancedda et al., 2017).

The new frontier of regenerative medicine heads towards approaches able to modulate the scar response and reactive and enhance dormant endogenous regenerative mechanisms since the molecular regeneration regulators are conserved in mammals, including humans. This prospect appears very encouraging because it would allow to practise a personalized medicine and to develop less invasive therapeutic treatments potentially administered at home. However, classical strategies (tissue engineering and cell therapy) remain the best solution in extreme and very critical situations, such as skin burns or critical-size bone defects. In this innovative prospect, platelet by-products represent promising clinical tools because they are based on that well-balanced cocktail of

bioactive molecules physiologically released by activated platelets at the wound site. The use of autologous Platelet Rich Plasma (PRP) for the treatment of soft and hard tissue lesions is the most representative example of clinical application of this approach. Although PRP is broadly used in the clinical practise for the treatment of knee and hip osteoarthritis (Laver et al., 2017) and tendon and ligament injuries (Yuan et al., 2013) or in aesthetic (Frautschi et al., 2016), oral and maxillofacial surgery (Mihaylova et al., 2017), the outcomes reported in the literature about its efficacy are controversial especially because of the un-standardized preparation of PRP and variability of the current PRP treatment protocols. The PRP was also proposed as a tool for enhancing the healing of chronic wounds even if there are in literature some contradictory outcomes considering the aetiologies of wounds, (Martinez-Zapata et al., 2012) (Suryanarayan et al., 2013) (Suthar et al., 2017).

1.4. Aim of the Ph.D. Project

The new therapeutic approaches for the treatment of chronic wounds are based on *in situ* administration of bioactive molecules, incorporated or not in natural/synthetic dressings (Eming et al., 2014). In this field, the platelet derivatives have a strong potentiality because of their composition and beneficial effects. Starting from this preliminary consideration, my group of research has taken an interest in those endogenous regenerative mechanisms activated by platelet-derived factors during the healing of injured skin in order to provide a rationale for clinical use of platelet derivatives for the treatment of chronic wounds. In particular, they have previously reported that platelet lysate enhanced wound closure rates of human keratinocytes in association with a high expression of the inflammatory cytokine IL-8 and of the antimicrobial lipocalin NGAL, through a pathway involving both p38 MAPK and NF-κB, under inflammatory conditions. These preliminary data suggest that platelet lysate possibly promotes wound healing by the induction of re-epithelialization and the enhancement of inflammatory response at wound site that leads to secretion of factors involved in healing and in warding off bacterial infection (El Backly et al., 2011).

Starting from these encouraging findings, I focused my attention during my Ph.D. period on two different cell systems – endothelial and adipose stromal cells – physiologically involved in skin healing evaluating their response to platelet-derived factors under conditions mimicking as much as possible the wound microenvironment in order to mainly clarify the regenerative pathways possibly participating to the healing of chronic wounds.

In the first study, I analysed the effect exerted by platelet lysate (PL) on the inflammatory, proliferative and angiogenesis-related response of primary human umbilical vein endothelial cells

(HUVECs) since endothelial cells are the first cell population responding to platelet-derived factors. Considering that injured blood vessel repair and re-establishment of blood circulation are crucial for tissue repair, the goal of this study was to elucidate the contribution of resident endothelial cells to new vessel formation since the mechanisms of angiogenesis are not currently well defined.

In the second study, I focused my attention on human subcutaneous adipose tissue to examine its role in supporting the repair process of skin wounds since this tissue is located beneath the skin and physiologically contribute to re-establish the homeostasis of the damaged skin. Starting from this consideration, I defined a clinically relevant model for studying the *in vitro* response of subcutaneous adipose tissue to an injury. In particular, I used some early injury-associated stimuli, which were human serum (HS), platelet lysate (PL) and interleukin-1α (IL-1α), for mimicking as much as possible *in situ* wound microenvironment. These stimuli were tested separately or combining them on primary human adipose-derived stromal cells (hASCs) with the aim of investigating their proliferative and differentiation capabilities and their inflammation-related secretory activity. To reduce the gap between the results obtained in *in vitro* experiments and the regenerative mechanisms possibly activated *in vivo* following the injury, I decided to test the same stimuli on *in toto* human adipose tissue (hATs) cultured *ex vivo*.

Both these studies were conceived for identifying those pathways need to be activated and those ones to be limited for the healing of injured skin and for providing, hence, a rationale for the therapeutic treatment of chronic wounds by using platelet derivatives.

1.5. References – Chapter 1

Atala, A., Irvine, D. J., Moses, M., and Shaunak, S. (2010). Wound Healing Versus Regeneration: Role of the Tissue Environment in Regenerative Medicine. *MRS Bull.* 35, 597–606. doi:10.1557/mrs2010.528.

Bosch, T. C. G. (2007). Why polyps regenerate and we don't: Towards a cellular and molecular framework for Hydra regeneration. *Dev. Biol.* 303, 421–433. doi:10.1016/j.ydbio.2006.12.012.

Cancedda, R., Bollini, S., Descalzi, F., Mastrogiacomo, M., and Tasso, R. (2017). Learning from Mother Nature: Innovative Tools to Boost Endogenous Repair of Critical or Difficult-to-Heal Large Tissue Defects. *Front. Bioeng. Biotechnol.* 5, 1–13. doi:10.3389/fbioe.2017.00028.

Darby, I. A., Laverdet, B., Bonté, F., and Desmouliere, A. (2014). Fibroblasts and myofibroblasts in wound healing. *Clin. Cosmet. Investig. Dermatol.*, 301. doi:10.2147/CCID.S50046.

De Luca, M., Albanese, E., Bondanza, S., Megna, M., Ugozzoli, L., Molina, F., et al. (1989). Multicentre experience in the treatment of burns with autologous and allogenic cultured epithelium, fresh or preserved in a frozen state. *Burns* 15, 303–9. Available at:

http://www.ncbi.nlm.nih.gov/pubmed/2686683.

de Oliveira, S., Rosowski, E. E., and Huttenlocher, A. (2016). Neutrophil migration in infection and wound repair: going forward in reverse. *Nat. Rev. Immunol.* 16, 378–391. doi:10.1038/nri.2016.49.

El Backly, R., Ulivi, V., Ph, D., Tonachini, L., Ph, D., Mastrogiacomo, M., et al. (2011). Platelet Lysate Induces In Vitro Wound Healing of Human Keratinocytes Associated with a Strong Proinflammatory Response. 17. doi:10.1089/ten.tea.2010.0729.

Eming, S. A., Martin, P., and Tomic-Canic, M. (2014). Wound repair and regeneration: mechanisms, signaling, and translation. *Sci. Transl. Med.* 6, 265sr6. doi:10.1126/scitranslmed.3009337.

Farkas, A. M., Mariz, S., Stoyanova-Beninska, V., Celis, P., Vamvakas, S., Larsson, K., et al. (2017). Advanced Therapy Medicinal Products for Rare Diseases: State of Play of Incentives Supporting Development in Europe. *Front. Med.* 4. doi:10.3389/fmed.2017.00053.

Frautschi, R. S., Hashem, A. M., Halasa, B., Cakmakoglu, C., and Zins, J. E. (2016). Current Evidence for Clinical Efficacy of Platelet Rich Plasma in Aesthetic Surgery: A Systematic Review. *Aesthetic Surg. J.*, sjw178. doi:10.1093/asj/sjw178.

Gallico, G. G., O'Connor, N. E., Compton, C. C., Kehinde, O., and Green, H. (1984). Permanent Coverage of Large Burn Wounds with Autologous Cultured Human Epithelium. *N. Engl. J. Med.* 311, 448–451. doi:10.1056/NEJM198408163110706.

Golebiewska, E. M., and Poole, A. W. (2015). Platelet secretion : From haemostasis to wound healing and beyond. *YBLRE* 29, 153–162. doi:10.1016/j.blre.2014.10.003.

Gurtner, G. C., Werner, S., Barrandon, Y., and Longaker, M. T. (2008). Wound repair and regeneration. *Nature* 453, 314–21. doi:10.1038/nature07039.

Kisch, T., Klemens, J. M., Hofmann, K., Liodaki, E., Gierloff, M., Moellmeier, D., et al. (2015). Collection of Wound Exudate From Human Digit Tip Amputations Does Not Impair Regenerative Healing. *Medicine (Baltimore).* 94, e1764. doi:10.1097/MD.0000000000001764.

Kreuger, J., and Phillipson, M. (2015). Targeting vascular and leukocyte communication in angiogenesis, inflammation and fibrosis. *Nat. Rev. Drug Discov.* 15, 125–142. doi:10.1038/nrd.2015.2.

Laver, L., Marom, N., Dnyanesh, L., Mei-Dan, O., Espregueira-Mendes, J., and Gobbi, A. (2017). PRP for Degenerative Cartilage Disease: A Systematic Review of Clinical Studies. *Cartilage* 8, 341–364. doi:10.1177/1947603516670709.

Mantovani, A., Biswas, S. K., Galdiero, M. R., Sica, A., and Locati, M. (2013). Macrophage plasticity and polarization in tissue repair and remodelling. *J. Pathol.* 229, 176–185.

doi:10.1002/path.4133.

Martin, P., and Leibovich, S. J. (2005). Inflammatory cells during wound repair: the good, the bad and the ugly. *Trends Cell Biol.* 15, 599–607. doi:10.1016/j.tcb.2005.09.002.

Martinez-Zapata, M. J., Martí-Carvajal, A. J., Solà, I., Expósito, J. A., Bolíbar, I., Rodríguez, L., et al. (2012). Autologous platelet-rich plasma for treating chronic wounds. *Cochrane Database Syst. Rev.* 10, CD006899. doi:10.1002/14651858.CD006899.pub2.

Mihaylova, Z., Mitev, V., Stanimirov, P., Isaeva, A., Gateva, N., and Ishkitiev, N. (2017). Use of platelet concentrates in oral and maxillofacial surgery: an overview. *Acta Odontol. Scand.* 75, 1–11. doi:10.1080/00016357.2016.1236985.

Pellegrini, G., Traverso, C. E., Franzi, A. T., Zingirian, M., Cancedda, R., and De Luca, M. (1997). Long-term restoration of damaged corneal surfaces with autologous cultivated corneal epithelium. *Lancet* 349, 990–993. doi:10.1016/S0140-6736(96)11188-0.

Quarto, R., Mastrogiacomo, M., Cancedda, R., Kutepov, S. M., Mukhachev, V., Lavroukov, A., et al. (2001). Repair of large bone defects with the use of autologous bone marrow stromal cells. *N. Engl. J. Med.* 344, 385–6. doi:10.1056/NEJM200102013440516.

Romagnoli, G., De Luca, M., Faranda, F., Bandelloni, R., Franzi, A. T., Cataliotti, F., et al. (1990). Treatment of Posterior Hypospadias by the Autologous Graft of Cultured Urethral Epithelium. *N. Engl. J. Med.* 323, 527–530. doi:10.1056/NEJM199008233230806.

Salo, E., Abril, J. F., Adell, T., Cebria, F., Eckelt, K., Fernandez-Taboada, E., et al. (2009). Planarian regeneration: achievements and future directions after 20 years of research. *Int. J. Dev. Biol.* 53, 1317–1327. doi:10.1387/ijdb.072414es.

Suryanarayan, S., Budamakuntala, L., Suresh, D., and Sarvajnamurthy, S. (2013). Autologous platelet rich plasma in chronic venous ulcers: Study of 17 cases. *J. Cutan. Aesthet. Surg.* 6, 97. doi:10.4103/0974-2077.112671.

Suthar, M., Gupta, S., Bukhari, S., and Ponemone, V. (2017). Treatment of chronic non-healing ulcers using autologous platelet rich plasma: a case series. *J. Biomed. Sci.* 24, 16. doi:10.1186/s12929-017-0324-1.

Tanaka, H. V., Ng, N. C. Y., Yang Yu, Z., Casco-Robles, M. M., Maruo, F., Tsonis, P. A., et al. (2016). A developmentally regulated switch from stem cells to dedifferentiation for limb muscle regeneration in newts. *Nat. Commun.* 7, 11069. doi:10.1038/ncomms11069.

Wynn, T. A., and Ramalingam, T. R. (2012). Mechanisms of fibrosis: therapeutic translation for fibrotic disease. *Nat. Med.* 18, 1028–1040. doi:10.1038/nm.2807.

Yuan, T., Zhang, C.-Q., and Wang, J. H.-C. (2013). Augmenting tendon and ligament repair with platelet-rich plasma (PRP). *Muscles. Ligaments Tendons J.* 3, 139–49.

doi:10.11138/mltj/2013.3.3.139.

2. PLATELET LYSATE EFFECT ON HUMAN UMBILICAL VEIN ENDOTHELIAL CELLS: INHIBITION OF ACTIVATED NF-κB, INDUCTION OF PROLIFERATION AND ACTIVATION OF ANGIOGENESIS-RELATED STAT3 AND HIF-1α – *SUBMITTED PAPER*

Alessio Romaldini[1*], Valentina Ulivi[1*], Maddalena Mastrogiacomo[1], Ranieri Cancedda[1,2], and Fiorella Descalzi[2]

[1] Department of Experimental Medicine, University of Genova, Genova, Italy;
[2] Biorigen Srl, Genova, Italy;

***** These authors contributed equally to the paper

2.1. Abstract

Injured blood vessel repair and blood circulation re-establishment are crucial events for tissue repair. In this study, we investigated the effects of platelet lysate (PL) on primary human umbilical vein endothelial cells (HUVECs) in order to elucidate the contribution of molecules contained in isolated platelets on the activation of endothelial cells in an *in vitro* system. The PL is a well-balanced cocktail of bioactive factors possibly representing the factors physiologically released by activated platelets following blood vessel disruption and involved in triggering wound-healing process. We found that PL exerted a protective effect on HUVECs in inflammatory milieu by inhibiting IL-1α-activated NF-κB pathway and by inducing the secretion of PGE_2, described as a pro-resolving factor towards macrophages in the wound microenvironment. Moreover, PL enhanced the proliferation of HUVECs, without affecting their capability of forming tube-like structures on matrigel, and activated resting quiescent cells to re-enter cell cycle and proliferate reaching a cell density significantly higher than the un-stimulated cells. In agreement with these findings, proliferation-related pathways Akt and ERKs were activated as well as the expression of the cell-cycle activator Cyclin D1 was enhanced demonstrating that quiescent cells, at a stage of basic metabolism, were activated by PL and resumed proliferation possibly contributing to vessel restoration. Finally, PL induced in HUVECs the stabilization of HIF-1α and the phosphorylation of STAT3, which are involved in the angiogenesis, suggesting the possible *in vivo* contribution of PL to new vessel formation by activation of resident progenitor cells located in the vessel walls. Our findings provide a rationale for the clinical use of PL in the treatment of wound healing-related pathologies.

2.2. Introduction

The wound healing is the physiological response of the body to injury or disease in order to restore tissue or organ integrity and homeostasis. Adult mammals, including humans, have a limited regenerative potential and tend to repair wounds by fibrosis and scarring. Scarring is the result of a prolonged or chronic inflammatory response. Therefore, an early inflammatory response represents the critical point for a successful regeneration process (Atala et al., 2010). The scar tissue is characterized by an aberrant structure, which prevents the repaired tissue from recovering its original function. A fibrotic repair may determine a complex medical case with severe clinical complications for the patients. For example, the myocardial fibrosis, due to heart infarction, is the main cause of arrhythmias and heart failure (Chin and Murry, 2012). Biotechnological research related to wound healing process is strongly involved in the search of innovative and effective treatments, but the obtained results are not satisfying yet. In November 2017, the European Union

introduced the Regulation on Advanced Therapies with the goal of better defining rules for production and application of Advanced Therapy Medicinal Products (ATMPs), i.e. innovative therapies that encompass gene therapy, somatic cell therapy and tissue engineering techniques for the treatment of severe chronic conditions (https://ec.europa.eu/health/human-use/advanced-therapies_en). However, so far, only four ATMPs with orphan designation (Glybera, Strimvelis, Zalmoxis, and Holoclar) have been successful in obtaining a market authorization and a 10-year market exclusivity. Three had ongoing Pediatric Investigation Plans (PIPs) at the time of submission for marketing authorization. One, namely Strimvelis, has obtained a 2-year extension of the market exclusivity (Farkas et al., 2017).

The new frontier of regenerative medicine aims at re-activating and enhancing endogenous regeneration pathways, which have been lost during evolution and human ontogenesis. In this scenario, platelet by-products are a promising perspective because they are based on a well-balanced cocktail of more than 300 bioactive factors released by activated platelets following clot formation and platelet degranulation. Physiologically, these factors trigger the tissue regeneration/repair process and are involved in all subsequent steps of the wound healing (Cancedda et al., 2017; Golebiewska and Poole, 2015). Therefore, they could be used as a powerful therapeutic tool to trigger and enhance the healing process. Encouraging results have been already achieved by the use of different platelet by-products for clinical applications, such as in dental and maxillofacial surgery (Kumar et al., 2013) (Cortese et al., 2016), in orthopaedics (Mishra and Pavelko, 2006), (Kon et al., 2010) (Randelli et al., 2011), in ophthalmology (Avila, 2014), (Carreras et al., 2015). Clinical trials were conducted with Platelet-Rich Plasma (PRP) (Xie et al., 2014) and also with autologous Platelet Lysate (PL) (Al-Ajlouni et al., 2014) for the treatment of degenerative cartilage diseases demonstrating beneficial effects.

In the last years, we evaluated the activity of platelet-contained molecules on different tissue cells in order to investigate activated pathways leading to tissue healing. In particular, we focused our attention on the effects of PL on human locally resident cells such as keratinocytes (El Backly et al., 2011), osteoblasts (Ruggiu et al., 2013), and chondrocytes (Pereira et al., 2013) or mouse bone marrow-derived mesenchymal stem cells (Ulivi et al.,2014). Indeed, not only tissue-specific progenitors are activated and take part in the wound healing process, but also circulating cells, possibly from bone marrow, could be recruited in the wound site (Lo Sicco et 2015). In the studied cell systems, we observed a strong initial and transient pro-inflammatory activity of a Platelet Lysate (PL) leading to NF-κB activation and secretion of pro-inflammatory cytokines (El Backly et al., 2011; Pereira et al., 2013; Ruggiu et al., 2013), the closure of a scratch wound in culture (El

Backly et al., 2011) and a strong activation of quiescent cells, which resumed proliferation keeping the ability to differentiate in permissive conditions (Ruggiu et al., 2013).

In this study, we evaluated the *in vitro* effects of PL on primary human umbilical vein endothelial cells (HUVECs) because the endothelial cells represent the first cell population responding to blood extravasation, coagulation, platelet activation and degranulation, and inflammatory milieu. Several studies have reported the effects of different platelet derivatives in endothelial cells, such as PRP (Kakudo et al., 2014; Martínez et al., 2015; Zahn et al., 2017) and the content of isolated platelets in the form of platelet-released supernatant (Kandler et al., 2004) or PL (Barsotti et al., 2013; Ranzato et al., 2010). In this study, we focused our attention on the activity of PL obtained by the lysis of platelets, which were washed in physiological saline, and consequently not contaminated by plasmatic molecules in order to specifically investigate the effects of human platelet content on HUVECs. To mimic as much as possible the wound microenvironment, we also included an inflammatory stimulus, represented by IL-1α, in our *in vitro* system. This *in vitro* system allowed to dissect the endothelial cell responses induced during the early stages of the wound healing process. We believe that the approach of this study would be useful for providing a rationale for the therapeutic use of PL in the treatment of wound healing-related pathologies. In particular, we investigated the activity of PL on the modulation of the inflammation-related NF-κB pathway and on the secretion of cytokines and factors under both physiological and inflammatory conditions. We monitored the proliferation of HUVECs in presence of PL and verified the *in vitro* angiogenic capability of the cells expanded in PL. We focused our attention on the activation of quiescent cells by PL investigating the induction of cell proliferation and proliferation-related pathways. Finally, we studied the effect of PL on angiogenesis-related pathways covering thus a broad range of cell responses induced by the molecules contained in PL and potentially involved in the restoration of injured blood vessels.

2.3. Materials and Methods

2.3.1. Materials

Medium 199 with Earle's Salts, foetal bovine serum (FBS), L-glutamine, penicillin G-streptomycin sulphate and trypsin-EDTA were all obtained from Euroclone Life Sciences Division (Milan, Italy). 10 cm Petri dish, 96-well plate, 24-well plate were derived from Eppendorf S.r.l. (Milan, Italy). Recombinant human FGF-acidic (FGF-acidic), recombinant human FGF-basic (FGF-basic), animal-free recombinant human EGF and recombinant human interleukin-1α (IL-1α) were purchased from Peprotech (London, UK). PHAREPA 25000 U.I./5 mL heparin sodium-salt was obtained from PharmaTex Italia (Milan, Italy). Hydrocortisone-water soluble, Bright-LineTM

hemacytometer and protease inhibitor cocktail were purchased from Sigma-Aldrich (St. Louis, MO, USA). Corning® Matrigel® Growth Factor Reduced Basement Membrane Matrix was acquired from Corning (Bedford, MA, USA). TransAMTM NF-κB p65 kit was purchased from Active Motif (La Hulpe, Belgium). Prostaglandin E_2 ELISA kit was from Cayman Chemical (Ann Arbor, MI, USA). NuPAGETM 4-12% Bis-Tris gels were from Invitrogen (Milano, Italy). AmershamTM ProtranTM 0.45 μm NC, AmershamTM ECLTM western blotting detection reagents and AmershamTM hyperfilmTM ECL were obtained from GE Healthcare (Buckinghamshire, UK). Antibodies anti-interleukin-8 (IL-8), anti-interleukin-6 (IL-6), anti-cyclin D1 and anti-actin were purchased from Santa Cruz Biotechnology Inc. (Dallas, TX, USA). Antibodies anti-phospho-Akt, anti-Akt, anti-phospho-$ERK_{1/2}$, anti-$ERK_{1/2}$ and anti-phospho-STAT3 were acquired from Cell Signalling Technology (Danvers, MA, USA). Antibody anti-HIF-1α was obtained from BD Biosciences (San Jose, CA, USA).

2.3.2. HUVEC harvest and culture

Primary Human Umbilical Vein Endothelial Cells (HUVEC) were obtained from "Centro di Risorse Biologiche" (CRB) of IRCCS Ospedale Policlinico San Martino (Genova, Italy) following the approval of this study by the institutional ethics committee. The CRB obtained the written informed consent by every umbilical cord donor. The HUVECs were CD31- and CD106-positive (endothelial cell-specific markers) and CD90- and CD45-negative (fibroblast-specific and leukocyte-specific markers, respectively) as guaranteed by CRB. The cells were seeded at the density of $6.0x10^3$ cells/cm^2 into gelatine-coated 10 cm Petri dishes and cultured in Medium 199 with Earle's Salts supplemented with 10% (v/v) FBS, 2 mM L-glutamine, 100 U/mL penicillin G, 100 μg/mL streptomycin sulfate, 100 mg/L heparin, 10 μg/L FGF-acidic, 10 μg/L FGF-basic, 10 μg/L EGF, 1 mg/L hydrocortisone (complete culture medium). Cells were incubated at 37°C in a humidified atmosphere with 5% CO_2. Medium was changed 3 times per week and at 80% confluence cells were split 1:2 by trypsinization with trypsin-EDTA. For the described experiments, HUVECs at passages from 3 to 6 were used.

2.3.3. Platelet lysate preparation

Platelet lysate was produced starting from buffy coat samples obtained from the whole blood of healthy donors and considered as a waste by Blood Transfusion Centre of IRCCS Ospedale Policlinico San Martino (Genova, Italy) within the frame of an agreement between Biorigen Srl and IRCCS Ospedale Policlinico San Martino signed on September 2012 and renewed on 2nd February 2017 ("Deliberazione" n°0084). At the time of blood donation, all donors provided the written informed consent for the use of donated blood for clinical and scientific applications. The buffy

coats of 5 to 10 donors were pooled for minimizing the variations among donors and centrifuged at low speed. Platelet-rich plasma (PRP) was separated and centrifuged at high speed in order to sediment the platelets. The pellet was washed 3 times with physiological saline (0.9% w/v NaCl), in order to eliminate possible contaminants from plasma. Platelets were suspended in physiological saline at a concentration of $10x10^6$ platelets/μL and the suspension was subjected to 3 freeze/thaw cycles followed by high-speed centrifugation. The supernatant, containing the cocktail of factors released by the platelets re-suspended in physiological saline (Platelet Lysate, PL), was collected and stored in aliquots at -20°C until use. Platelet lysate was supplemented to complete culture medium at a final concentration of 5% (v/v), approximately corresponding to the highest physiological concentration of platelets in the human blood, without adding heparin.

2.3.4. Proliferation assays

1) Crystal violet assay: HUVECs were seeded at the density of $2.5x10^3$ cells/well on gelatine-coated 96-well plate and incubated in complete culture medium for 24h to enable cell adhesion. The next day, medium was replaced with complete medium not supplemented (control cells) or supplemented with 5% PL (treated cells). The assay was performed in quintuplicate for each culture condition after 0, 2, 4 and 6 days of PL stimulation. At each time point, the culture media were removed and replaced with 50 μL/well of 0.75% (w/v) crystal violet staining solution. After 20 min incubation, the staining solution was discarded and wells were extensively washed. When the plate was dry, 100 μL/well of elution solution was added and dye absorbance was measured at 595 nm. The average of three independent experiments performed on different single-donor primary HUVEC cultures and the fold increase of the signal revealed after 6 days of PL treatment over control (mean ± SD) is shown.

2) Cell count: HUVECs were seeded on gelatine-coated 24-well plate and cultured in complete culture medium until reaching confluence. The medium was then replaced with complete medium supplemented (treated culture) or not supplemented (control culture) with 5% PL. At 0, 3, 6, 10 days of PL stimulation, cell density was monitored in triplicate by cell counting using a Bright-Line™ Hemacytometer with an improved Neubauer chamber. Values are expressed as fold increase with respect to the value obtained at the time of the PL addition (first considered time point - day 0). Results are expressed as the average of three independent experiments performed on different single-donor primary HUVEC cultures (mean ± SD). Cell density ratio between PL-treated and control cells at 10th day of PL

treatment is also reported. Ratio was separately calculated in 3 independent experiments and expressed as mean ± SD.

2.3.5. Tube formation assay

Proliferating HUVECs were cultured in complete culture medium un-supplemented (control) or supplemented with 5% PL for a week. The cells were then trypsinized, re-suspended in serum-free medium (no supplements) and seeded at the density of 70,000 cells/well on matrigel-coated 24-well plate. Images were taken after 6h incubation at 37°C in a humidified atmosphere with 5% CO_2.

2.3.6. Western blot analysis

To analyse the cytokine production in cell culture media, sub-confluent HUVECs were treated for 1, 5 or 24h with complete culture medium supplemented with 5% PL, or 100 U/mL IL-1α, or 5% PL + 100 U/mL IL-1α, or without any supplement. Cells were then extensively washed with PBS for removing residual factors and incubated in serum-free medium (medium 199 with Earle's Salts supplemented only with 2 mM L-glutamine, 100 U/mL penicillin G and 100 µg/mL streptomycin sulphate) for 24h. The different media were collected, clarified at 2000 rpm for 10 min at room temperature and stored at -20°C. To investigate the PL effect on proliferation-related pathways and on cell cycle activation, sub-confluent HUVECs were treated for multiple time intervals with complete culture medium supplemented with 5% PL, washed with PBS, and lysed by incubating the cell layers on ice for 5 min with an ice-cold buffer containing 50 mM Tris HCl pH 7.5, 150 mM NaCl, 1% (w/v) sodium deoxycholate, 1% (v/v) Triton X-100, 0.1% (w/v) sodium dodecyl sulphate, 0.2% (w/v) sodium azide and protease inhibitor cocktail. Cell lysates were harvested with a cell scraper, clarified at 10000 rpm for 15 min at 4°C and stored at -20°C. For studying HIF-1α pathway, cell layers were washed with cold PBS on ice, incubated overnight at -80°C, lysed as described above and harvested with cold cell scraper. They were sonicated at 30 amplitude microns for 5 seconds, clarified at 10000 rpm for 15 min at 4°C and immediately analysed by western blot. The protein content of both conditioned media and cell lysates was quantified by Bradford protein assay (Bradford, 1976).

Electrophoresis was performed in reducing conditions using 25-60 µg of protein loaded on a NuPAGE™ 4-12% Bis-Tris gel and proteins were transferred to a Amersham™ Protran™ 0.45 µm NC nitrocellulose blotting membrane. The blot was saturated with 5% skimmed cow milk in TTBS (20 mM Tris HCl pH 7.5, 500 mM NaCl, 0.1% Tween 20) for 2h at room temperature and washed several times with TTBS and probed in a cold room overnight with specific primary antibodies raised against IL-8 (1:250 dilution) and IL-6 (1:250 dilution) for the conditioned media or against phospho-Akt (1:1000 dilution), Akt (1:1000 dilution), phospho-$ERK_{1/2}$ (1:1000 dilution), $ERK_{1/2}$

(1:1000 dilution), phospho-STAT3 (1:1000 dilution), Cyclin D1 (1:250 dilution), HIF-1α (1:500 dilution) and Actin (1:500 dilution) for the cell lysates. After washing, the detection was obtained by incubating the blot with secondary horseradish peroxidase-conjugated immunoglobulins G (IgGs) for 1h at room temperature. The blot was then washed and incubated with Amersham™ ECL™ western blotting detection reagents following manufacturer's instructions and finally exposed to Amersham™ hyperfilm™ ECL to capture the image. For each considered marker, western blot was performed on 3 independent experiments corresponding to different single-donor primary HUVEC cultures. Densitometric analysis was performed by scanning the film using the Epson Perfection V330 Photo scanner (Epson, Italy) and quantifying the band densities using ImageJ software (https://imagej.nih.gov/ij/download.html). Presented results are the average of 3 independent experiments ± SD values.

2.3.7. NF-κB activity assay

To evaluate the nuclear factor-κB (NF-κB) activity, TransAMTM NF-κB p65 kit was used. This ELISA-based kit is based on the binding of NF-κB active form to an oligonucleotide, containing NF-κB consensus decameric sequence 5'-GGGACTTTCC-3', immobilized on a 96-well plate. Sub-confluent HUVECs were treated for 1h or 16h with complete culture medium supplemented with 5% PL, 100 U/mL IL-1α, or 5% PL + 100 U/mL IL-1α, or without any supplement (control). Media were removed and cells washed with PBS. Whole-cell extracts were prepared following manufacturer's instructions. The NF-κB active form contained in the whole-cell extracts specifically binds to the consensus sequence and the primary antibody recognizes an epitope on subunit p65, which is accessible only when NF-κB is activated and bound to its target site. An HRP-conjugated secondary antibody provides a colorimetric signal quantified by spectrophotometry. Specificity of the assay was checked by adding soluble wild-type and mutated consensus oligonucleotides acting as competitors for NF-κB binding. For the reported representative experiment, results are expressed as the absorbance values measured in the presence of the mutated oligonucleotide minus those measured in the presence of the wild-type oligonucleotide. This assay was performed in triplicate on 3 independent experiments corresponding to different single-donor primary HUVEC cultures. For each stimulation time, the over the control fold increase of NF-κB activity induced by IL-1α stimulation and the percentage value of NF-κB activity induced by PL+IL-1α treatment with respect to IL-1α net increase are reported (means ± SD).

2.3.8. PGE_2 quantification

To quantify the PGE_2 production, Prostaglandin E_2 ELISA kit was used. This assay is based on the

competition between PGE_2 present in the sample and a PGE_2 tracer for a limited amount of anti-PGE_2 monoclonal antibody. Sub-confluent HUVECs were treated for 24h with complete culture medium supplemented with 5% PL, 100 U/mL IL-1α, or 5% PL + 100 U/mL IL-1α, or without any supplement (control). Cells were then extensively washed with PBS for removing residual factors and then incubated in serum-free medium for 24h. The different conditioned media were collected and assayed following manufacturer's instructions. Results are expressed as fold change referring to control. This assay was performed in duplicate on 3 independent experiments corresponding to different single-donor primary HUVEC cultures.

2.3.9. Statistical analysis

All data are presented as means and standard deviations based on independent experiments performed on three different primary HUVEC cultures, each of them derived from a single donor. The statistical analysis was performed using the unpaired t-Test for NF-κB activity and proliferation assays or using the ordinary one-way ANOVA for IL-8, IL-6, Cyclin D1, HIF-1α and phospho-STAT-3 densitometric analysis and PGE_2 quantification. If ANOVA detected statistically significant differences within the data set, Tukey's or Dunnett's multiple comparison tests were used to calculate the significant differences for IL-8 and IL-6 densitometric analysis and PGE_2 quantification or for Cyclin D1, HIF-1α and phospho-STAT-3 densitometric analysis, respectively. All tests were run setting a confidence interval of 95% ($p<0,05$).

2.4. Results

2.4.1. PL down-regulates NF-κB pathway in an inflammatory milieu

Having in mind that bioactive molecules released by platelets trigger the wound healing process and that this process takes place in an inflammatory microenvironment, we focused our attention on the response of endothelial cells to PL in both normal conditions and in the presence of inflammatory cytokines. In particular, we evaluated the activation of NF-κB pathway, a key player in the inflammatory phase response (Lawrence, 2009), in sub-confluent HUVECs treated for 1h or 16h with complete culture medium supplemented with 5% PL, or 100 U/mL IL-1α, or 5% PL+100 U/mL IL-1α or un-supplemented (control, CTR). Figure 1, Panel A, reports the NF-κB activity in a representative experiment where cells were exposed to different culture conditions. Panels B shows the over the control fold increase of NF-κB activity induced by IL-1α stimulation for 1 hour and the percentage reduction in the IL-1α-induced NF-κB activity when the culture was supplemented also with PL. Panel C shows the fold increase and the percentage reduction after 16h stimulation of the cells. Values are reported as average values ± SD values of 3 independent experiments. The NF-κB activity increase was statistically significant with respect to control after both 1h and 16h cell

stimulation with IL-1α (p=0.0413 and p=0.0062, respectively, Figure 1B,C), and statistically significantly decreased after both 1h and 16h stimulation in cells treated with PL+IL-1α with respect to the IL-1α treated cells (p=0.0018 and p=0.0292, respectively, Figure 1B,C). These results indicate an anti-inflammatory activity of PL on HUVECs both at early and late times.

Considering the negative regulation of NF-κB pathway by PL in an inflammatory milieu, we evaluated the production of two pro-inflammatory cytokines, IL-8 and IL-6, following 1h and 24h stimulations with PL under both physiological and inflammatory conditions. By western blot analysis of conditioned media, we did not observe a significant variation of pro-inflammatory cytokine secretion induced by IL-1α in PL+IL-1α treated cells. The reported densitometric analyses refer to the average of 3 or 4 independent experiments performed on different primary HUVEC cultures for 1h or 24h stimulations, respectively (Figure 2A,B).

2.4.2. PL increases PGE_2 secretion by HUVEC in an inflammatory milieu

In a previous publication from our laboratory, we demonstrated a pro-resolving activity of Platelet Rich Plasma on cells of the immune system to create an anti-inflammatory microenvironment related to PGE_2 production (Papait et al, 2017). A quantitation of PGE_2 released by HUVECs in the presence of PL was performed in order to detect a possible protective activity in an inflammatory environment. Results reported in Figure 3 show a significant increase of PGE_2 secretion in PL+IL-1α treated cells with respect to the control (p=0.0191) indicating that PL-activated HUVECs could contribute to resolution of tissue inflammation also by a paracrine mechanism.

2.4.3. PL enhances proliferation of HUVECs retaining their differentiation capability

The PL effect on HUVEC viability and proliferation was evaluated at different times from the PL addition by crystal violet staining assay performed on 3 independent primary cultures. Cells treated with the complete culture medium supplemented with 5% PL had a higher proliferation rate with respect to control cells in complete medium with no supplement, with a significant (1.83±0.31)-fold increase of the signal induced by PL at day 6^{th} with respect to the control signal (p=0.0092; Figure 4A,B). We did not observe any significant change in the cell morphology between PL-treated cells and control cells. We did not observe qualitative differences between treated and control cells about their angiogenic capability. Cells grown in PL for 1 week kept the ability to form capillary-like structures when seeded on matrigel (Figure 4 C, D).

2.4.4. PL promotes the proliferation of quiescent HUVECs, activates Akt and ERK pathways, and induces Cyclin D1 expression

Considering the enhancement of cell proliferation induced by PL on HUVECs and our previous study on human osteoblasts demonstrating an activation of quiescent cells by PL (Ruggiu et al., 2013), we cultured HUVECs in complete culture medium until reaching the confluence state, and we treated the cells with complete medium supplemented with 5% PL or not supplemented (control) for 10 days. We monitored cell growth by cell counting at different time intervals. PL induced proliferation of confluent cells that reached a higher (1.72 ± 0.33)-fold cell density then control cells ($p=0.0201$) at day 10^{th} (Figure 5A,B). For each experimental condition, we report the values expressed as fold increase with respect to the first considered time point (day 0). The average values ± SD of 3 independent experiments are shown. We also investigated the modulation of proliferation-related Akt and ERK pathways (Mebratu and Tesfaigzi, 2009; Yu and Cui, 2016) and the expression of the cell cycle associated Cyclin D1 following PL treatment. Sub-confluent cells maintained in complete medium were treated with 5% PL. Cell lysates were collected at different times from the PL addition and analysed by western blot. Activation of both Akt and ERK pathways was observed already 10 min after PL treatment followed by a progressive decrease, more rapid for Akt than for ERK (Figure 5C). Three independent experiments performed on different primary HUVEC cultures yielded the same results. The analysis of the Cyclin D1 expression showed that the expression level of Cyclin D1 was significantly enhanced already after 1h of PL treatment reaching its maximum level at 4h ($p=0.0274$ for 0h versus 1h and $p=0.0049$ for 0h versus 4h, Figure 5D) and decreasing at later times. The densitometric analysis of western blots for Cyclin D1 expression as the average of 3 independent experiments performed on different primary HUVEC cultures (mean ± SD) is reported in Figure 5D.

2.4.5. PL activates the angiogenesis-related HIF-1α and STAT3

In tissue wound, the vascular injury leads to a stop of the blood flow and a consequent ischemia and hypoxia. The re-establishment of a blood vasculature through the process of angiogenesis is necessary for delivering oxygen and nutrients to the healing site. Hypoxia induces activation of HIF-1α, a transcription factor that accumulates in the wounded tissue cells and also in endothelial cells (Ahluwalia and Tarnawski, 2012; Dal Monte et al., 2011), and induces VEGF gene expression. In addition to oxygen depletion, HIF-1α activation can be induced also in normoxic conditions by several factors such as cytokines, growth factors and microbe-derived components. Indeed, HIFs are transcription factors able to induce the expression of genes necessary for cell survival and metabolism under a variety of hostile conditions (for a review see Shi et al., 2017).

We investigated a possible involvement of PL in wound re-vascularization. We here report that PL

significantly induced HIF-1α in HUVECs after 24h stimulation (0h versus 24h p=0.0123, Figure 6A). In agreement with a possible implication of PL in restoring blood vasculature in wounded tissues, we also observed a very rapid and transient activation of STAT3 (0h versus 10' p=0.0405, Figure 6B), a critical transcription pathway in angiogenesis (Chen and Han, 2008).

2.5. Discussion

Injured blood vessel repair and blood circulation re-establishment are crucial events for tissue repair. Our work focuses on the behaviour of endothelial cells in a wound-like microenvironment physiologically characterized by the presence of inflammatory cytokines and by the transition from plasma to serum, i.e. from plasma to a mixture of plasma proteins and growth factors and bioactive molecules released by activated platelets. The new microenvironment plays a major role in restoring tissue function, but, at the end of the healing process, when the blood circulation is restored in the newly formed tissue, cells are again exposed to plasma. Indeed, the plasma to serum transition is necessary for proper healing, but serum must be replaced by plasma for reactivation of tissue function (LeBrasseur, 2006).

In this paper, we showed that Platelet Lysate (PL), used at a concentration approximately corresponding to the highest physiological concentration of platelets in the human blood, could modify the behaviour of endothelial cells, thus playing a significant role in the different phases of tissue healing:

i) *PL induced resolution of inflammation by inhibiting IL-1α-activated NF-κB pathway.*

Physiologically, after an injury, platelets leak from damaged blood vessels and the inflammatory phase is initiated by the platelet degranulation leading to the release of growth factors acting as key players in the tissue healing process. The inflammatory phase is characterized by the clearance of microbial contamination and the removal of devitalized tissue by migrating macrophages. We previously investigated the effect of PL in an inflammatory milieu in several cell systems and we demonstrated an early and transient activation of the pro-inflammatory NF-κB pathway induced by IL-1α in human keratinocytes, osteoblasts, chondrocytes, and murine BMSC (El Backly et al., 2011; Pereira et al., 2013; Ruggiu et al., 2013; Ulivi et al., 2014). This early activation was paralleled by an early and increased secretion of pro-inflammatory cytokines IL-6 and IL-8 and, in keratinocytes, also by an increased production of the antimicrobial lipocalin NGAL. This effect was transient because, after the early inflammatory burst, PL inhibited IL-1α-induced NF-κB activation (Pereira et al., 2013). This finding was in agreement with other reports that showed a pro-resolving activity of PL and/or PRP (Xie et al., 2014). We believe that platelet released factors exerts an immediate pro-inflammatory effect causing an immediate

antimicrobial response by the tissue that releases antimicrobial proteins such as NGAL (El Backly et al., 2011), and the migration of neutrophils and macrophages (Tasso et al., 2013a) that engulf contaminant microorganisms and remove the devitalized tissue. At later time PL exerts an opposite effect by inhibiting NF-κB activation and promoting resolution of the inflammatory phase.

Given that endothelial cells are the first cells in contact with PL after vessel injury, we treated HUVECs with PL for different times in presence or not of IL-1α. The PL inhibited IL-1α-induced NF-κB activation already after 1-hour treatment as well as after 16-hours treatment showing an anti-inflammatory activity at both the early and the late considered times. This finding is in agreement with the anti-inflammatory activity of PRP described in literature (Mazzocca et al., 2013) and provides a possible rationale to this effect. We also observed that, at variance with the other so far investigated cell systems, PL did not significantly enhance the production of IL-6 and IL-8 induced by IL-1α, nor induce a significant repression, although the trend was a decrease in the secretion of these two cytokines. The response of the different assayed primary cultures was quite variable as demonstrated by the standard deviation. Taken together, the data suggest that endothelial cells are protected by PL in the inflammatory milieu of the wound.

ii) *PL increased PGE_2 secretion in the presence of inflammatory cytokines.*

A significant increase of PGE_2 secretion in inflammatory conditions was detected indicating that PL activated HUVECs possibly to contribute to resolution of tissue inflammation. Indeed, an anti-inflammatory activity of PGE_2 was demonstrated toward macrophages, inducing the functional switch from M1 inflammatory phenotype to M2 pro-resolving phenotype (Maggini et al., 2010). In a previous publication from our laboratory, it was also demonstrated a pro-resolving activity of Platelet Rich Plasma on cells of the immune system to create an anti-inflammatory microenvironment related to PGE_2 production (Papait et al., 2017). The presented results provide an additional indication that PL exerts an early anti-inflammatory activity on HUVECs.

iii) *PL enhanced proliferation of HUVECs without affecting their differentiation capability.*

Our goal was to dissect the system and to specifically investigate the effect of human platelet-contained molecules on endothelial cells maintained in standard culture conditions, i.e. in the presence of foetal bovine serum. Platelet lysate enhanced the proliferation of HUVECs, without affecting their capability of forming tube-like structures on matrigel. Our findings are in agreement with reported data referring that platelet-released molecules support proliferation of cells from different tissues, including endothelial cells, showing a

significantly lower apoptosis and increased proliferation rates (Denecke et al., 2015). The maintained capacity of endothelial cells expanded in PL to form tube-like structures on matrigel is in agreement with Tasev et al., 2015, although, in that study, the platelet lysate was made in human plasma and was used as serum substitute.

iv) *PL induced proliferation of quiescent HUVECs*.

We previously reported that quiescent cultured osteoblasts exposed to PL resumed proliferation retaining their differentiation capability (Ruggiu et al., 2013). In the present study, we observed that resting confluent HUVECs were activated by PL that induced cell proliferation up to a cell concentration approximately double than the one of not PL stimulated, control cells. This observation also suggested a possible change in the HUVEC size as reported for human MSCs (Chevallier et al., 2010) and for human osteoblasts (Ruggiu et al., 2013). In agreement with these findings, proliferation-related pathways Akt and ERK were activated as well as the expression of the cell cycle activator Cyclin D1 enhanced. We consider this an important finding because clot formation and platelet degranulation are the first tissue's response to an injury and, in particular, the multitude of platelet-released factors able to attract circulating cells and to restore the proliferation of resting resident cells physiologically leads to the tissue repair through the complex series of events typical of the wound healing process. Eventually, only after the effective repair of the injured tissue, normal blood perfusion resumes.

It was demonstrated that HUVECs and HAECs (Human Aortic Endothelial Cells) derived from vessel walls, considered normally differentiated endothelial cells, contain a complete hierarchy of endothelial progenitor cells (EPCs) and that a diversity of EPCs exists in human vessel playing an important role in maintaining vessel integrity (Ingram, 2005). We demonstrated that resting cultured confluent HUVECs are activated and resume proliferation following a PL treatment suggesting that an activation of the resident cell population, possibly progenitors and differentiated cells, could occur also *in vivo* after an injury.

Several studies reported that EPCs can be isolated also from adult peripheral and umbilical cord blood. These progenitors are thought to originate from bone marrow, to circulate in the peripheral blood and to be involved in neovascularization and wound healing (Tasso et al., 2010, Balaji et al., 2013; Shi et al., 2017). However, mechanisms for vessel repair in wound are not currently well defined. Cells from bone marrow are recruited to the site of injury by migration trough the blood circulation, whereas cell activation and recruitment from vessel walls occurs via direct activation of local cells. We believe that, in the process of injury

repair, cells recruited from bone marrow and resident cells contribute to new vessel formation in an extent that may vary depending on the type of injury and possibly on the tissue type involved.

v) *PL induced HIF-1α protein stabilization and STAT3 activation: implication in angiogenesis.*

Tissue injury leads to the destruction of blood vessels and the disruption of local blood perfusion resulting in a hypoxic state that requires the adaptive response of local cells, including vascular precursor cells, responding to the produced stimuli. Hypoxia-inducible transcription factors (HIFs) are a complex of factors that regulate the cell response to hypoxia. The HIF-1α subunit, present in the cell, is physiologically degraded by the ubiquitine system, but is stabilized by hypoxia and migrate to the nucleus as a complex with HIF-1β and co-activators, which together activate transcription of over 100 responding genes (Liu et al., 2012). These genes are important for cell survival and metabolism. Indeed, HIFs can be induced also in normoxic conditions by various stimuli, such as cytokines, growth factors, reactive oxygen or nitrogen species and microbial components, occurring in injury and hostile conditions (Richard et al., 2000). The activation of HIF pathway by PL was recently reported in cartilage cells by a paper from our laboratory (Nguyen et al., 2017). Angiogenesis, i.e. the formation of new blood vessels from the pre-existing vasculature, is a complex process regulated by signal transduction pathways leading to the expression and activation of angiogenic molecules. It was demonstrated that in HUVECs the hypoxia induced the HIF-1α stabilization driving angiogenesis (Dal Monte et al., 2011; Yu et al., 2015) and that bFGF in normoxic condition induced HIF-1α stabilization and tubular structure formation (Calvani et al., 2006). It was also shown that STAT3 signalling is important and necessary for endothelial cell proliferation, migration, and microvascular tube formation (Chen and Han, 2008) and also for *in vivo* angiogenesis induction (Valdembri et al., 2002).

We reported that platelet-released factors induced the stabilization of HIF-1α and the phosphorylation of STAT3 in agreement with an involvement of PL in the activation of angiogenesis.

In conclusion, in this paper, we demonstrated a beneficial activity of PL treatment on HUVECs by the inhibition of inflammation, the enhancement of proliferation of cells, which retained the differentiation capability, the resumption of proliferation of quiescent cells and the activation of angiogenesis-related pathways, thus providing a rationale for the clinical use of PL in wound healing.

2.6. Conflict of interest statement

RC and MM are shareholders of Biorigen Srl, a spin off company of the University of Genova, with an interest in Regenerative Medicine.

2.7. Author contributions

FD and VU conceived and designed the work. MM provided the reagents. AR and VU performed the experiments and elaborate the data. RC, FD and MM participate to the interpretation and discussion of data. AR and FD wrote the article. RC, MM and VU revised the article. All authors agree to be accountable for the content of the work and approved the final version of this article.

2.8. Acknowledgements and Funding

We thank Dr. Alessandra Ruggiu for performing the cell proliferation experiment by crystal violet assay and for helpful discussion.

This study was supported by the international project E! 8119 Re.Me.Pro EUROSTARS.

2.9. References

Ahluwalia, A., and Tarnawski, A. S. (2012). Critical role of hypoxia sensor--HIF-1α in VEGF gene activation. Implications for angiogenesis and tissue injury healing. *Curr. Med. Chem.* 19, 90–7.

Al-Ajlouni, J., Awidi, A., Samara, O., Al-Najar, M., Tarwanah, E., Saleh, M., et al. (2014). Safety and Efficacy of Autologous Intra-articular Platelet Lysates in Early and Intermediate Knee Osteoarthrosis in Humans. *Clin. J. Sport Med.*, 1. doi:10.1097/JSM.0000000000000166.

Atala, A., Irvine, D. J., Moses, M., and Shaunak, S. (2010). Wound Healing Versus Regeneration: Role of the Tissue Environment in Regenerative Medicine. *MRS Bull.* 35, 597–606. doi:10.1557/mrs2010.528.

Avila, M. Y. (2014). Restoration of Human Lacrimal Function Following Platelet-Rich Plasma Injection. *Cornea* 33, 18–21. doi:10.1097/ICO.0000000000000016.

Balaji, S., King, A., Crombleholme, T. M., and Keswani, S. G. (2013). The Role of Endothelial Progenitor Cells in Postnatal Vasculogenesis: Implications for Therapeutic Neovascularization and Wound Healing. *Adv. Wound Care* 2, 283–295. doi:10.1089/wound.2012.0398.

Barsotti, M. C., Losi, P., Briganti, E., Sanguinetti, E., Magera, A., Al Kayal, T., et al. (2013). Effect of Platelet Lysate on Human Cells Involved in Different Phases of Wound Healing. *PLoS One* 8, e84753. doi:10.1371/journal.pone.0084753.

Bradford, M. M. (1976). A rapid and sensitive method for the quantitation of microgram quantities of protein utilizing the principle of protein-dye binding. *Anal. Biochem.* 72, 248–254. doi:10.1016/0003-2697(76)90527-3.

Calvani, M., Rapisarda, A., Uranchimeg, B., Shoemaker, R. H., and Melillo, G. (2006). Hypoxic induction of an HIF-1alpha-dependent bFGF autocrine loop drives angiogenesis in human endothelial cells. *Blood* 107, 2705–12. doi:10.1182/blood-2005-09-3541.

Cancedda, R., Bollini, S., Descalzi, F., Mastrogiacomo, M., and Tasso, R. (2017). Learning from Mother Nature: Innovative Tools to Boost Endogenous Repair of Critical or Difficult-to-Heal Large Tissue Defects. *Front. Bioeng. Biotechnol.* 5, 1–13. doi:10.3389/fbioe.2017.00028.

Carreras, E., Nadal, J., Suarez Figueroa, M., Pujol, P., Canut, M. I., and Barraquer, R. I. (2015). Autologous platelet concentrate in surgery for macular detachment associated with congenital optic disc pit. *Clin. Ophthalmol.*, 1965. doi:10.2147/OPTH.S81976.

Chen, Z., and Han, Z. C. (2008). STAT3: a critical transcription activator in angiogenesis. *Med. Res. Rev.* 28, 185–200. doi:10.1002/med.20101.

Chevallier, N., Anagnostou, F., Zilber, S., Bodivit, G., Maurin, S., Barrault, A., et al. (2010). Osteoblastic differentiation of human mesenchymal stem cells with platelet lysate. *Biomaterials* 31, 270–8. doi:10.1016/j.biomaterials.2009.09.043.

Chin, M. T., and Murry, C. E. (2012). Is it possible to transform cardiac scar tissue into beating heart muscle in humans? *Regen. Med.* 7, 623–625. doi:10.2217/rme.12.54.

Cortese, A., Pantaleo, G., Borri, A., Caggiano, M., and Amato, M. (2016). Platelet-rich fibrin (PRF) in implant dentistry in combination with new bone regenerative technique in elderly patients. doi:10.1016/j.ijscr.2016.09.022.

Dal Monte, M., Martini, D., Ristori, C., Azara, D., Armani, C., Balbarini, A., et al. (2011). Hypoxia effects on proangiogenic factors in human umbilical vein endothelial cells: functional role of the peptide somatostatin. *Naunyn. Schmiedebergs. Arch. Pharmacol.* 383, 593–612. doi:10.1007/s00210-011-0625-y.

Denecke, B., Horsch, L. D., Radtke, S., Fischer, J. C., Horn, P. A., and Giebel, B. (2015). Human endothelial colony-forming cells expanded with an improved protocol are a useful endothelial cell source for scaffold-based tissue engineering. *J. Tissue Eng. Regen. Med.* 9, E84–E97. doi:10.1002/term.1673.

El Backly, R., Ulivi, V., Ph, D., Tonachini, L., Ph, D., Mastrogiacomo, M., et al. (2011). Platelet Lysate Induces In Vitro Wound Healing of Human Keratinocytes Associated with a Strong Proinflammatory Response. 17. doi:10.1089/ten.tea.2010.0729.

Farkas, A. M., Mariz, S., Stoyanova-Beninska, V., Celis, P., Vamvakas, S., Larsson, K., et al. (2017). Advanced Therapy Medicinal Products for Rare Diseases: State of Play of Incentives Supporting Development in Europe. *Front. Med.* 4. doi:10.3389/fmed.2017.00053.

Golebiewska, E. M., and Poole, A. W. (2015). Blood Reviews Platelet secretion : From haemostasis

to wound healing and beyond. *YBLRE* 29, 153–162. doi:10.1016/j.blre.2014.10.003.

Ingram, D. A. (2005). Vessel wall-derived endothelial cells rapidly proliferate because they contain a complete hierarchy of endothelial progenitor cells. *Blood* 105, 2783–2786. doi:10.1182/blood-2004-08-3057.

Kakudo, N., Morimoto, N., Kushida, S., Ogawa, T., and Kusumoto, K. (2014). Platelet-rich plasma releasate promotes angiogenesis in vitro and in vivo. *Med. Mol. Morphol.* 47, 83–89. doi:10.1007/s00795-013-0045-9.

Kandler, B., Fischer, M. B., Watzek, G., and Gruber, R. (2004). Platelet-Released Supernatant Increases Matrix Metalloproteinase-2 Production, Migration, Proliferation, and Tube Formation of Human Umbilical Vascular Endothelial Cells. *J. Periodontol.* 75, 1255–1261. doi:10.1902/jop.2004.75.9.1255.

Kon, E., Buda, R., Filardo, G., Di Martino, A., Timoncini, A., Cenacchi, A., et al. (2010). Platelet-rich plasma: intra-articular knee injections produced favorable results on degenerative cartilage lesions. *Knee Surgery, Sport. Traumatol. Arthrosc.* 18, 472–479. doi:10.1007/s00167-009-0940-8.

Kumar, K. A. J., Rao, J. B., Pavan Kumar, B., Mohan, A. P., Patil, K., and Parimala, K. (2013). A Prospective Study Involving the Use of Platelet Rich Plasma in Enhancing the Uptake of Bone Grafts in the Oral and Maxillofacial Region. *J. Maxillofac. Oral Surg.* 12, 387–394. doi:10.1007/s12663-012-0466-3.

Lawrence, T. (2009). The Nuclear Factor NF- B Pathway in Inflammation. *Cold Spring Harb. Perspect. Biol.* 1, a001651–a001651. doi:10.1101/cshperspect.a001651.

LeBrasseur, N. (2006). Serum keeps order in the wound. *J. Cell Biol.* 172, 957a–957a. doi:10.1083/jcb.1727iti1.

Liu, W., Shen, S.-M., Zhao, X.-Y., and Chen, G.-Q. (2012). Targeted genes and interacting proteins of hypoxia inducible factor-1. *Int. J. Biochem. Mol. Biol.* 3, 165–78.

Lo Sicco, C., Tasso, R., Reverberi, D., Cilli, M., Pfeffer, U., and Cancedda, R. (2015). Identification of a New Cell Population Constitutively Circulating in Healthy Conditions and Endowed with a Homing Ability Toward Injured Sites. *Nat. Publ. Gr.*, 1–11. doi:10.1038/srep16574.

Maggini, J., Mirkin, G., Bognanni, I., Holmberg, J., Piazzón, I. M., Nepomnaschy, I., et al. (2010). Mouse Bone Marrow-Derived Mesenchymal Stromal Cells Turn Activated Macrophages into a Regulatory-Like Profile. *PLoS One* 5, e9252. doi:10.1371/journal.pone.0009252.

Martínez, C. E., Smith, P. C., and Palma Alvarado, V. A. (2015). The influence of platelet-derived products on angiogenesis and tissue repair: a concise update. *Front. Physiol.* 6.

doi:10.3389/fphys.2015.00290.

Mazzocca, A. D., McCarthy, M. B. R., Intravia, J., Beitzel, K., Apostolakos, J., Cote, M. P., et al. (2013). An In Vitro Evaluation of the Anti-Inflammatory Effects of Platelet-Rich Plasma, Ketorolac, and Methylprednisolone. *Arthrosc. J. Arthrosc. Relat. Surg.* 29, 675–683. doi:10.1016/j.arthro.2012.12.005.

Mebratu, Y., and Tesfaigzi, Y. (2009). How ERK1/2 activation controls cell proliferation and cell death: Is subcellular localization the answer? *Cell Cycle* 8, 1168–1175. doi:10.4161/cc.8.8.8147.

Mishra, A., and Pavelko, T. (2006). Treatment of Chronic Elbow Tendinosis With Buffered Platelet-Rich Plasma. *Am. J. Sports Med.* 34, 1774–1778. doi:10.1177/0363546506288850.

Nguyen, V. T., Cancedda, R., and Descalzi, F. (2017). Platelet lysate activates quiescent cell proliferation and reprogramming in human articular cartilage: Involvement of hypoxia inducible factor 1. *J. Tissue Eng. Regen. Med.* doi:10.1002/term.2595.

Papait, A., Cancedda, R., Mastrogiacomo, M., and Poggi, A. (2017). Allogeneic platelet-rich plasma affects monocyte differentiation to dendritic cells causing an anti-inflammatory microenvironment, putatively fostering wound healing. *J. Tissue Eng. Regen. Med.* doi:10.1002/term.2361.

Pereira, C., Scaranari, M., Benelli, R., Strada, P., Reis, R. L., Cancedda, R., et al. (2013). Dual effect of platelet lysate on human articular cartilage: a maintenance of chondrogenic potential and a transient pro-inflammatory activity followed by an inflammation resolution. *Tissue Eng. Part A* 19, 1476–1488. doi:10.1089/ten.TEA.2012.0225.

Randelli, P., Arrigoni, P., Ragone, V., Aliprandi, A., and Cabitza, P. (2011). Platelet rich plasma in arthroscopic rotator cuff repair: a prospective RCT study, 2-year follow-up. *J. Shoulder Elb. Surg.* 20, 518–528. doi:10.1016/j.jse.2011.02.008.

Ranzato, E., Boccafoschi, F., Mazzucco, L., Patrone, M., and Burlando, B. (2010). Role of ERK1/2 in platelet lysate-driven endothelial cell repair. *J. Cell. Biochem.* 110, 783–793. doi:10.1002/jcb.22591.

Richard, D. E., Berra, E., and Pouyssegur, J. (2000). Nonhypoxic pathway mediates the induction of hypoxia-inducible factor 1alpha in vascular smooth muscle cells. *J. Biol. Chem.* 275, 26765–71. doi:10.1074/jbc.M003325200.

Ruggiu, A., Ulivi, V., Sanguineti, F., Cancedda, R., and Descalzi, F. (2013). Biomaterials The effect of Platelet Lysate on osteoblast proliferation associated with a transient increase of the in fl ammatory response in bone regeneration. *Biomaterials* 34, 9318–9330. doi:10.1016/j.biomaterials.2013.08.018.

Shi, X., Zhang, W., Yin, L., Chilian, W. M., Krieger, J., and Zhang, P. (2017). Vascular precursor cells in tissue injury repair. *Transl. Res.* 184, 77–100. doi:10.1016/j.trsl.2017.02.002.

Tasev, D., van Wijhe, M. H., Weijers, E. M., van Hinsbergh, V. W. M., and Koolwijk, P. (2015). Long-Term Expansion in Platelet Lysate Increases Growth of Peripheral Blood-Derived Endothelial-Colony Forming Cells and Their Growth Factor-Induced Sprouting Capacity. *PLoS One* 10, e0129935. doi:10.1371/journal.pone.0129935.

Tasso, R., Fais, F., Reverberi, D., Tortelli, F., and Cancedda, R. (2010). The recruitment of two consecutive and different waves of host stem/progenitor cells during the development of tissue-engineered bone in a murine model. *Biomaterials* 31, 2121–2129. doi:10.1016/j.biomaterials.2009.11.064.

Tasso, R., Ulivi, V., Reverberi, D., Lo Sicco, C., Descalzi, F., and Cancedda, R. (2013). In vivo implanted bone marrow-derived mesenchymal stem cells trigger a cascade of cellular events leading to the formation of an ectopic bone regenerative niche. *Stem Cells Dev.* 22. doi:10.1089/scd.2013.0313.

Ulivi, V., Tasso, R., Cancedda, R., and Descalzi, F. (2014). Mesenchymal Stem Cell Paracrine Activity Is Modulated by Platelet Lysate: Induction of an Inflammatory Response and Secretion of Factors Maintaining Macrophages in a Proinflammatory Phenotype. *Stem Cells Dev.* 0, 1–12. doi:10.1089/scd.2013.0567.

Valdembri, D., Serini, G., Vacca, A., Ribatti, D., and Bussolino, F. (2002). In vivo activation of JAK2/STAT-3 pathway during angiogenesis induced by GM-CSF. *FASEB J.* 16, 225–7. doi:10.1096/fj.01-0633fje.

Xie, X., Zhang, C., and Tuan, R. S. (2014). Biology of platelet-rich plasma and its clinical application in cartilage repair. *Arthritis Res. Ther.* 16, 204. doi:10.1186/ar4493.

Yu, F., Lin, Y., Zhan, T., Chen, L., and Guo, S. (2015). HGF expression induced by HIF-1α promote the proliferation and tube formation of endothelial progenitor cells. *Cell Biol. Int.* 39, 310–7. doi:10.1002/cbin.10397.

Yu, J. S. L., and Cui, W. (2016). Proliferation, survival and metabolism: the role of PI3K/AKT/mTOR signalling in pluripotency and cell fate determination. *Development* 143, 3050–3060. doi:10.1242/dev.137075.

Zahn, J., Loibl, M., Sprecher, C., Nerlich, M., Alini, M., Verrier, S., et al. (2017). Platelet-Rich Plasma as an Autologous and Proangiogenic Cell Delivery System. *Mediators Inflamm.* 2017, 1–14. doi:10.1155/2017/1075975.

2.10. Figures & Legends

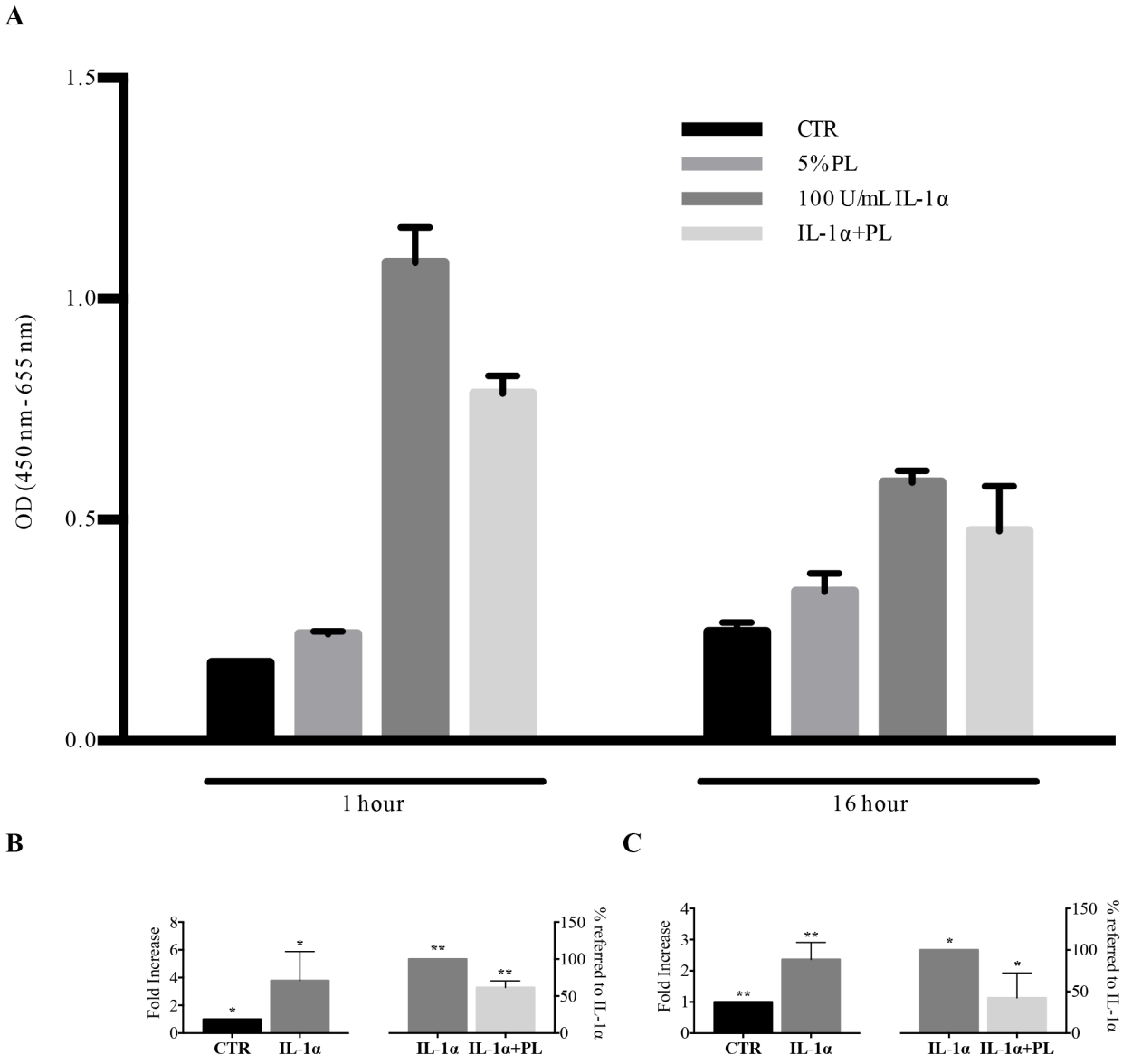

Figure 1: Modulation of NF-κB pathway in HUVEC treated with PL under physiological and inflammatory conditions. Sub-confluent HUVEC were treated for 1h or 16h with complete medium supplemented with 5% PL, or 100 U/mL IL-1α, or 5% PL+100 U/mL IL-1α or un-supplemented (control, CTR). Whole-cell extracts were analysed by ELISA-based TransAMTM NF-κB p65 kit. (A) Absorbance values of NF-κB activity after 1h and 16h stimulation related to a representative experiment. (B), (C) Cell NF-κB activity after 1h and 16h stimulation, respectively, expressed as fold increase over control following IL-1α treatment and percentage value following PL+IL-1α treatment with respect to IL-1α induced net increase (100%, after the subtraction of control value). For each condition, the average of 3 different experiments (mean ± SD) assayed in triplicate on different single-donor primary cultures are reported. For 1h stimulation, * and ** symbols refer to

p=0.0413 and p=0.0018, respectively. For 16h stimulation, * and ** symbols refer to p=0.0292 and p=0.0062, respectively.

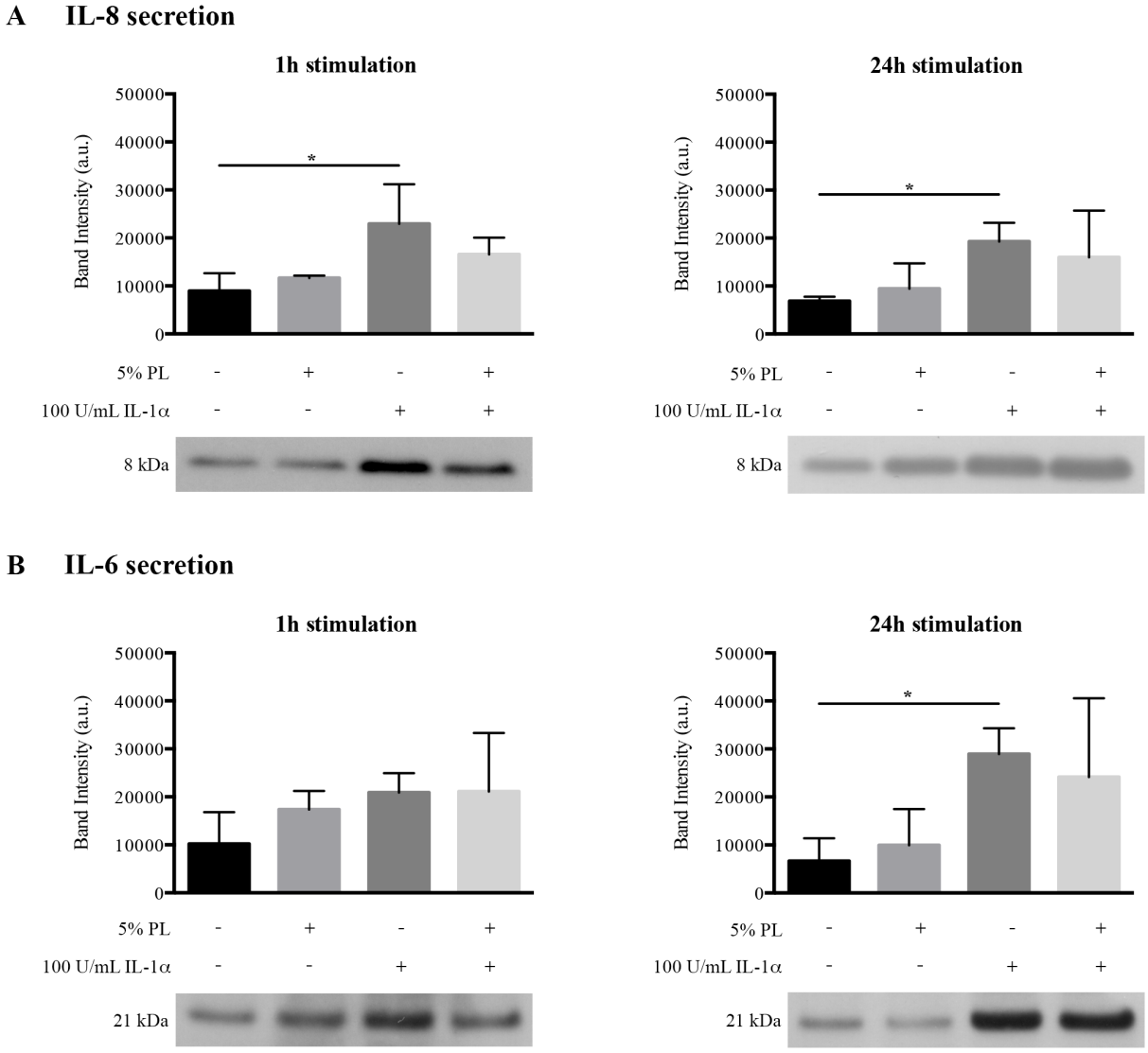

Figure 2: Pro-inflammatory cytokine secretion by HUVEC following PL stimulation under both physiological and inflammatory conditions. Sub-confluent HUVEC were treated for 1h or 24h with complete medium supplemented with 5% PL, or 100 U/mL IL-1α, or 5% PL+100 U/mL IL-1α, or without any supplement (control, CTR). At the end of the different stimulations, the supplemented media were removed and replaced with serum-free medium. After 24h incubation, the conditioned media were collected. Western blot analysis of conditioned media for the secretion of IL-8 (A) and IL-6 (B). The densitometric analysis of western blots was performed on 3 or 4 independent single-donor primary cultures (means ± SD) for 1h or 24h treatments, respectively. The * symbol represents significant differences with $p \leq 0.0494$. Under densitometric analysis histograms, representative western blots are shown.

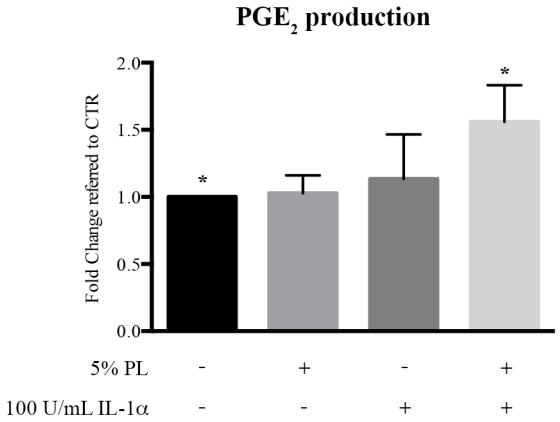

Figure 3. PGE_2 secretion by HUVEC following PL stimulation under both normal and inflammatory conditions. Sub-confluent HUVEC were treated for 24h with complete medium supplemented with 5% PL, or 100 U/mL IL-1α, or 5% PL+100 U/mL IL-1α, or without any supplement (control, CTR). Media were removed and replaced with serum-free medium for 24h incubation. The conditioned media were collected and analysed by Prostaglandin E_2 ELISA kit. For each condition, PGE_2 production is expressed as fold change with respect to CTR. The average values and relative standard deviation values of 4 determinations performed in duplicate on 3 different single-donor primary cultures are presented. The * symbol represents a significant difference with p=0.0191.

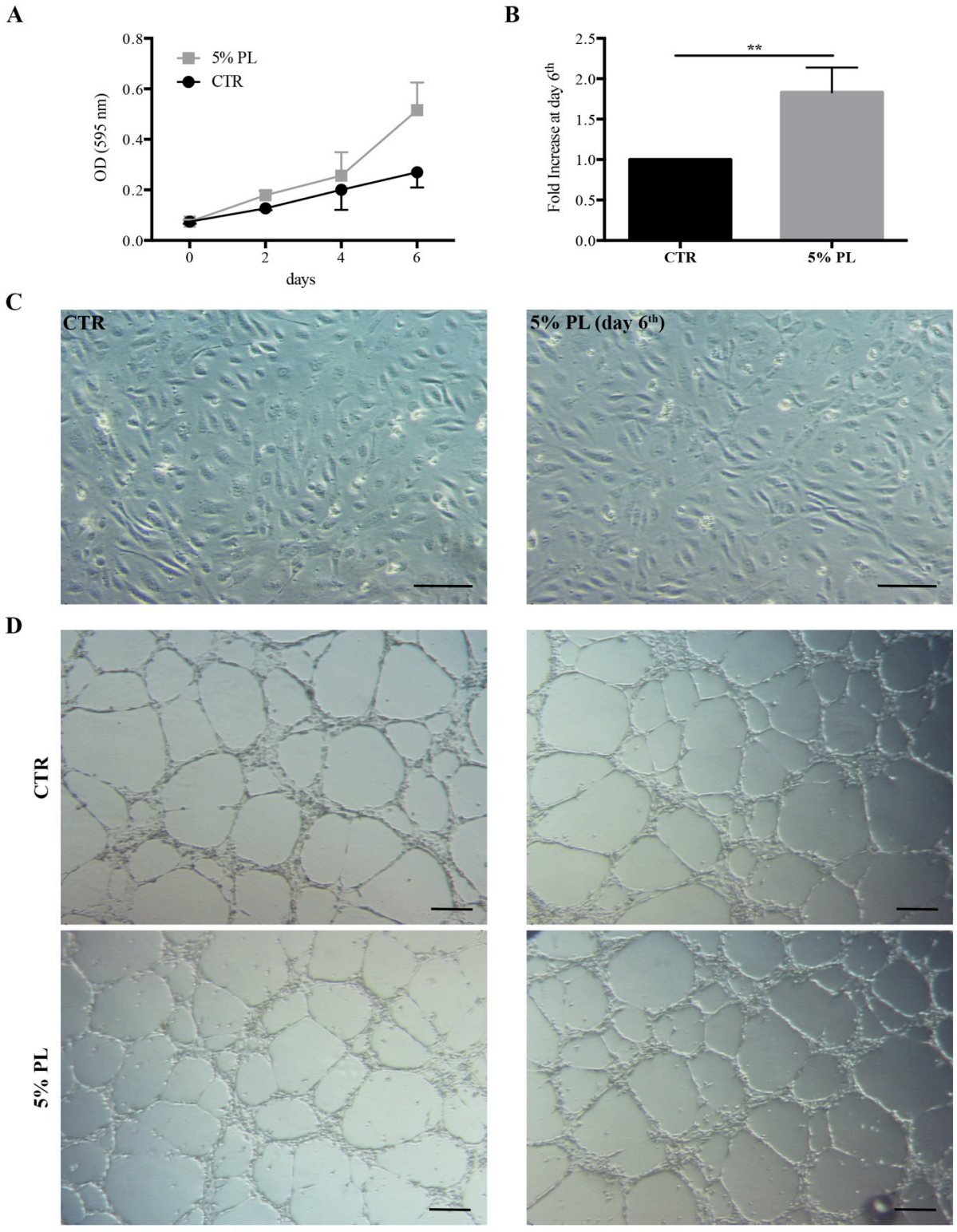

Figure 4: PL effect on proliferation, morphology and angiogenic capability of HUVEC. (A) Proliferation of HUVECs treated with the complete medium supplemented with 5% PL or un-supplemented (control, CTR) evaluated at different time intervals by crystal violet staining assay. The average values ± SD of 3 independent experiments performed in quintuplicate on different single-donor primary cultures are reported. (B) Fold increase of the signal revealed after 6 days of PL treatment over control (CTR) expressed as mean ± SD of 3 independent experiments. The **

symbol refers to p=0.0092. (C) Morphology of HUVECs cultured in complete medium un-supplemented (control cells, CTR) or supplemented with 5% PL for 6 days. Scale bar = 150 μm. (D) Tube-like structure formation assay performed on matrigel using HUVECs grown in complete medium un-supplemented (control cells, CTR) or supplemented with 5% PL for 7 days. The assay was performed in the absence of PL. Two pictures related to different positions in the well per condition are reported. Scale bar = 250 μm.

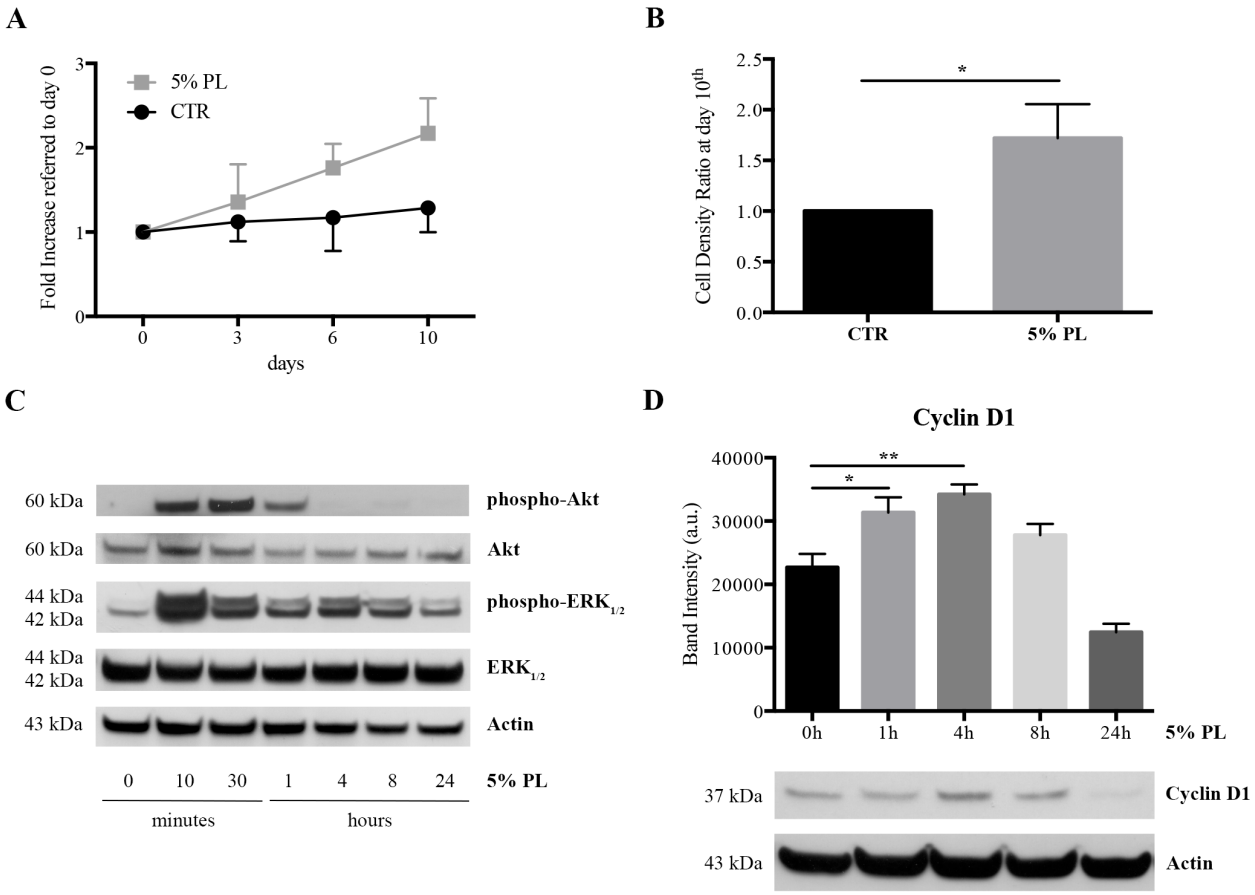

Figure 5: Proliferation of quiescent HUVEC in the presence of PL, modulation of Akt and ERK pathways and activation of cell cycle by PL. (A) Proliferation of confluent HUVEC maintained in complete medium (CTR) or treated with complete medium supplemented with 5% PL monitored by cell counting. The values were expressed as fold increase related to the value obtained at the first considered time point (day 0). The average values ± SD of 3 determinations performed in triplicate on 3 different single-donor primary HUVEC cultures are shown. (B) Cell density ratio between PL-treated and control cells (CTR) at day 10^{th} of PL treatment. Ratio was separately calculated in 3 independent experiments and expressed as mean ± SD. The * symbol refers to p=0.0201. (C) Western blot analysis of sub-confluent HUVEC treated with complete medium supplemented with 5% PL for multiple times. Cell lysates were analysed by western blot with antibodies raised against

phospho-Akt, Akt, phospho-$ERK_{1/2}$, $ERK_{1/2}$ and Actin. The Akt, $ERK_{1/2}$ and Actin were used as internal controls. Three independent experiments performed on different primary HUVEC cultures yielded the same results. (D) The PL effect on cell cycle of sub-confluent cells treated with 5% PL in complete medium for different times. A western blot analysis of the cell lysates was performed to evaluate the Cyclin D1 expression. In the upper panel, the densitometric analysis of Cyclin D1-probed western blots performed on 3 independent single-donor primary cultures is reported (means ± SD). The * and ** symbols represent significant differences with p=0.0274 and p=0.0049, respectively. In the lower panel, a representative western blot for Cyclin D1 is shown. Actin was blotted as an internal control.

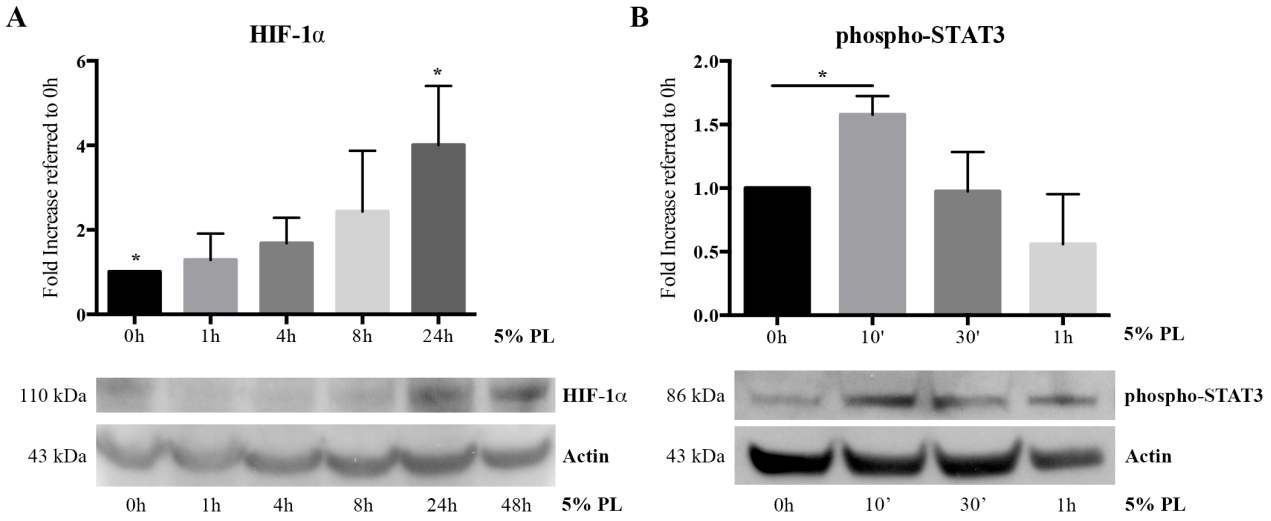

Figure 6: Stabilization of HIF-1α and activation of STAT3 in HUVECs by PL. (A) Western blot analysis of HUVECs incubated at sub-confluence in serum-free medium for 2h and treated for multiple time intervals with serum-free medium supplemented with PL. Corresponding cell lysates were analysed by western blot with antibody raised against HIF-1α. Actin was probed as internal control. In the upper panel, the densitometric analysis of HIF-1α-probed blots shows means ± SD of 3 independent single-donor primary cultures. The significant difference 0h versus 24h corresponds to p=0.0123 (*). In the lower panel, a representative western blot for HIF-1α is shown. (B) Western blot analysis of sub-confluent HUVECs treated with complete medium supplemented with 5% PL for multiple time intervals. Corresponding cell lysates were analysed by western blot with antibody raised against phospho-STAT3. Actin was probed as internal control. In the upper panel, the densitometric analysis of pospho-STAT3-probed blots performed on 3 independent single-donor primary cultures is reported (means ± SD). The significant difference 0h versus 10' corresponds to p = 0.0405 (*). In the lower panel, a representative western blot for pospho-STAT3 is shown.

3. PLATELET LYSATE EFFECT ON HUMAN SUBCUTANEOUS ADIPOSE TISSUE: INDUCTION OF PROGENITOR CELL PROLIFERATION AND SECRETION OF INFLAMMATION-RELATED CYTOKINES AND FACTORS – *PAPER IN PREPARATION*

Alessio Romaldini[1] et al.

[1] Department of Experimental Medicine, University of Genova, Genova, Italy;

3.1. Introduction

When tissue or organ is affected by injury or disease, the human body responds immediately by activating the wound-healing cascade. However, large and deep lesions and organ failure determine fibrosis and scar formation, which are causes of reduction or loss of functionality. Regenerative medicine was born and grew up with the aim of delaying scarring process and promoting as much as possible regeneration of tissue or organ structure and homeostasis. "Classical" regenerative strategies are based on separated or combined use of biomaterials and stem/progenitor cells but they are still not broadly used in the clinical practice. We strongly think the new frontier of regenerative medicine should head towards approaches able to reactivate and enhance dormant endogenous regenerative mechanisms (Cancedda, Bollini, Descalzi, Mastrogiacomo, & Tasso, 2017). The fundamental condition for designing clinically suitable tools is to know in detail tissue's natural response to injury or disease in order to be able to identify those pathways, among the all, to be activated and those ones to be limited.

In the humans, postnatal epidermis is one of the tissues with the highest regenerative potential. However, when an injury affects the underlying dermal layer, the wound healing leads to scar formation. In some circumstances, an aberrant repair process of skin lesions can determine serious consequences, such as pathological scarring (hypertrophic scar or keloid) or chronic wounds (Eming, Martin, & Tomic-Canic, 2014). In particular, chronic wounds are non-healing ulcerative defects of the skin, which arise in association with disease states (e.g. vascular diseases or diabetes mellitus) or in presence of systemic factors (e.g. advanced age), and represent a very important worldwide medical and economic issue. In the United States alone, chronic wounds affect around 6.5 million patients with estimated US$ 25 billions for the healthcare system. In Western countries, it has been estimated that 1-2% of the population will experience a chronic wound during their lifetime (Sen et al., 2009). For the treatment of chronic wounds, the new therapeutic approaches are based on *in situ* administration of bioactive molecules, incorporated or not in wound dressings, for enhancing the physiological healing process. In this scenario, platelet by-products could be promising clinical tools. In particular, it was reported that platelet-rich plasma (PRP), which is an autologous blood platelet-based derivative, can improve the healing of chronic wounds even if there are in literature some contradictory outcomes considering the aetiologies of wounds (Martinez-Zapata et al., 2012; Suryanarayan, Budamakuntala, Suresh, & Sarvajnamurthy, 2013; Suthar, Gupta, Bukhari, & Ponemone, 2017). Focusing our attention on the molecular mechanism of platelet-derived factors in skin wound healing, we previously studied the effects of human platelet lysate on human keratinocytes showing that platelet lysate stimulated resting cells to produce

increased levels of IL-8 and of the antimicrobial peptide NGAL in inflammatory condition, via p38 MAPK and NF-κB activation, and promoted an accelerated wound closure in an *in vitro* scratch assay (El Backly et al., 2011).

Starting from these findings, we addressed our interest in the role of human subcutaneous adipose tissue in supporting the repair process of skin wounds because such tissue is located beneath the skin and physiologically contribute to re-establish the homeostasis of the damaged skin. In this study, we investigated the *in vitro* response of subcutaneous adipose tissue to human platelet content in order to shed light on those endogenous pathways potentially activated following the injury. For this purpose, we defined a clinically relevant model using the early injury-associated stimuli, which are Human Serum (HS), Platelet Lysate (PL) and Interleukin-1α (IL-1α), in order to reproduce *in vitro* as much as possible *in situ* microenvironment establishing during deep skin injury. In particular, HS played the role of serum, which is the physiological fluid at the wound site, while PL corresponded to that well-balanced cocktail of more than 300 bioactive molecules physiologically released by activated platelets during haemostasis and involved in all steps of the wound healing process (Cancedda et al., 2017; Golebiewska & Poole, 2015). Because of the manufacturing procedures, HS was not contaminated by platelet-derived factors and PL did not contain plasmatic molecules allowing to study their separated and combined effects on adipose tissue. The IL-1α is physiologically involved in the induction and the maintenance of local inflammatory responses (Di Paolo & Shayakhmetov, 2016) and was used to create an inflammatory microenvironment. In this manner, we wanted to dissect the system and specifically elucidate the effects of platelet content on subcutaneous adipose tissue in order to give a rationale to the therapeutic use of PL for the treatment of chronic wounds. The considered stimuli were tested in two types of adipose tissue culture: primary culture of human adipose-derived stromal cells (hASCs), used as *in vitro* paradigm of resident progenitor cells, and *ex vivo* culture of *in toto* human adipose tissue (hAT). We, first, examined the proliferative and differentiation capabilities of hASCs expanded in HS in comparison with cells expanded in foetal bovine serum (FBS). We, then, studied PL effect on the proliferation of HS-expanded cells, in absence or presence of IL-1α, focusing our attention on the activated growth-related pathways. We also investigated the hASC inflammatory response to PL, in both physiological and inflammatory microenvironment, in terms of released bioactive factors and activated pathways. We, finally, studied the proliferative response of hAT cultured *ex vivo* with HS in presence or absence of PL under normal or inflammatory conditions in order to reduce the gap between *in vitro* results and *in vivo* events associated with adipose tissue repair process.

3.2. Materials and Methods

3.2.1. Materials

Type I collagenase was purchased from Worthington (Lakewood, NJ, USA). The MEM Alpha Medium (1X) GlutaMAX™ without nucleosides (αMEM) was from Gibco (Thermo Fisher Scientific, Waltham, MA, USA). Foetal bovine serum (FBS), penicillin G-streptomycin sulphate solution and normal goat serum were from Euroclone Life Sciences Division (Milan, Italy). Dimethyl sulphoxide (DMSO) was obtained from Panreac (Barcelona, Spain). Human interleukin-1alpha (IL-1α) was from PeproTech (London, UK). Bright-Line™ Hemacytometer with an improved Neubauer chamber, crystal violet powder, thiazolyl blue tetrazolium bromide (MTT), insulin from bovine pancreas, dexamethasone, L(+)-ascorbic acid sodium salt, β-glycerophosphate disodium salt hydrate, Oil Red O (ORO), Alizarin Red S (ARS), paraformaldehyde, protease inhibitor cocktail and poly-L-lysine solution were purchased from Sigma-Aldrich (St. Louis, MO, USA). Formaldehyde 37% weight solution was from Chem-Lab (Zedelgem, Belgium). Methylene blue hydrate powder was purchased from Honeywell Riedel-de Haën® (Seelze, Germany). The RNeasy® Plus Micro Kit and Omniscript® RT Kit were from Qiagen (Milan, Italy). Power SYBR® Green PCR Master Mix and 7500 Fast Real-Time PCR System were from Applied Biosystems® Life Technologies (Thermo Fisher Scientific, Waltham, MA, USA). The NuPAGE™ 4-12% Bis-Tris gels and streptavidin-peroxidase of HistoMouse™-SP kit were from Invitrogen (Thermo Fisher Scientific, Waltham, MA, USA). Amersham™ Protran™ 0.45 μm NC, secondary anti-rabbit and anti-mouse horseradish peroxidase-linked immunoglobulins G (IgGs), Amersham™ ECL™ western blotting detection reagents and Amersham™ Hyperfilm™ ECL were obtained from GE Healthcare (Buckinghamshire, UK). Primary antibodies raised against interleukin-8 (IL-8), interleukin-6 (IL-6), Cyclin D1 and Actin were purchased from Santa Cruz Biotechnology Inc. (Dallas, TX, USA). Primary antibodies raised against phospho-Akt, Akt, phospho-$ERK_{1/2}$, $ERK_{1/2}$ and phospho-STAT3 were acquired from Cell Signalling Technology (Danvers, MA, USA). Primary antibodies raised against cyclooxygenase-2 (COX-2) and microsomal prostaglandin E synthase-1 (mPGES-1) and Prostaglandin E_2 ELISA kit were from Cayman Chemical (Ann Arbor, MI, USA). Secondary anti-goat peroxidase-conjugated immunoglobulins G (IgGs) were from Jackson ImmunoResearch (Bar Harbor, MA, USA). Primary antibody raised against PCNA was from Abnova (Taipei City, Taiwan). Secondary biotinylated immunoglobulins G (IgGs) and 3,3'-diaminobenzidine (DAB) were from Dako (Carpinteria, CA, USA).

3.2.2. HS and PL production

The Human Serum (HS) and the Platelet Lysate (PL) were obtained from healthy blood wastes of Blood Transfusion Centre of IRCCS Ospedale Policlinico San Martino (Genova, Italy) within the frame of an agreement between Biorigen Srl and IRCCS Ospedale Policlinico San Martino signed on September 2012 and renewed on 2nd February 2017 ("Deliberazione" n°0084). At the time of blood donation, all donors provided the written informed consent for the use of donated blood for clinical and scientific applications. In particular, both reagents were produced as pool of several blood donors (at least 3 donors for HS or 25 donors for PL) in order to minimize the variations among donors. According to the standard procedure, the whole blood units were centrifuged at high speed obtaining different phases: the plasma at the top, the buffy coat layer (enriched in platelets and leukocytes) at the interface and the red blood cell fraction at the bottom. The HS was produced starting from fresh frozen plasma (FFP) units, which are *de facto* devoid of platelets. Each FFP unit was slowly thawed at 4°C in order to produce a cryoprecipitate containing fibrinogen and other coagulation factors. The complete clotting was obtained by adding calcium chloride (2 mg/mL) to the liquid phase and incubating at 37°C for 6 hours. After a high-speed centrifugation, the supernatant (i.e. HS) was collected and pooled with the others. The pool was divided into aliquots then lyophilized and stored at -20°C until use. In this work, HS was added in the complete culture medium at the same concentration of FBS (10%, v/v) used in the control medium according to the gold standard for expanding hASCs. The PL was produced starting from buffy coat samples, which were pooled and centrifuged at low speed. After this centrifugation, the lower phase, enriched in platelets and indicated as platelet-rich plasma (PRP), was separated and centrifuged at high speed in order to sediment the platelets. The platelet pellet was washed 3 times with physiological saline (0.9% w/v NaCl), in order to eliminate possible plasma-derived contaminants. The platelets were re-suspended and concentrated to $10x10^6$ platelets/μL. The platelet concentrate was subjected to 3 consecutive freeze/thaw cycles for breaking the cell plasma membranes. After a high-speed centrifugation, the supernatant containing the cocktail of platelet-released factors (PL) was collected and combined with the other supernatants. The pool was divided in aliquots, lyophilized and stored at -20°C. For the described treatments, the complete culture medium was supplemented with PL reaching the final concentration of 5% (v/v), approximately corresponding to the highest physiological concentration of platelets in the human blood, without adding heparin.

3.2.3. Primary hASC cultures

Primary human adipose-derived stromal cell (hASC) cultures were obtained from subcutaneous adipose tissue liposuction wastes derived from healthy female donors. All donors provided the written informed consent. Protocol and procedures were approved by the Local Ethical Committee.

The hASCs were isolated following the protocol reported by Estes, Diekman, Gimble, & Guilak, 2010, with some modifications. Briefly, liposuction aspirate was extensively washed with phosphate-buffered saline (PBS, composed by 136.9 mM NaCl, 2.7 mM KCl, 8.0 mM Na_2HPO_4, 1.5 mM KH_2PO_4, with pH 7.4) (1:1 volume). After that, the fat sample was digested with 0.1% type I collagenase in PBS (1:1 volume) at 37°C for 1h shaking the mix by hand every 5-10 minutes. The digested sample was centrifuged at 290g for 5 minutes at room temperature and, at the end of centrifugation, shacked vigorously to ensure all the stromal cells could be properly released and separated from the remaining tissue. After a further centrifugation, the upper mature adipocyte and middle collagenase/PBS layers were aspirated off leaving the pellet, which were composed by the stromal vascular fraction (SVF). The pellet was re-suspended in αMEM supplemented with 10% (v/v) FBS, 100 U/mL penicillin G and 100 µg/mL streptomycin sulphate for neutralizing the residual collagenase. The SVF was centrifuged, re-suspended in PBS and splitted in two half. After a final centrifugation, one half was re-suspended with a volume of αMEM supplemented with 10% (v/v) HS, 100 U/mL penicillin G and 100 µg/mL streptomycin sulphate (*complete medium*) corresponding to half of initial volume of lipoaspirate, while the other half with an identical volume of αMEM supplemented with 10% (v/v) FBS, 100 U/mL penicillin G and 100 µg/mL streptomycin sulphate (control medium). The SVF cells were plated at an equivalent to about 0,04 mL of liposuction aspirate per cm^2 for every condition. Adhering hASC cultures were incubated at 37°C in a humidified atmosphere with 5% CO_2 and media were changed 3 times per week. At 80% confluence, cells were harvested by trypsinization and frozen in liquid nitrogen using αMEM supplemented with 50% (v/v) HS or FBS, 10% (v/v) DMSO, 100 U/mL penicillin G and 100 µg/mL streptomycin sulphate for long-term storage (passage 0, P0). After to be thawed, cells were expanded for one passage (P1) and used at passage 2 (P2) for all the described experiments, except for CFE assay and differentiation assays of PL-expanded cells. In particular, for differentiation assays of PL-expanded cells, HS-isolated hASCs were expanded for one passage with complete medium and for further 3 passages with complete medium supplemented with 5% PL and used at passage 5 (P5).

3.2.4. *In toto* hAT cultures

In toto human adipose tissue (hAT) samples were obtained from resection material of abdominoplasty on healthy female donors. All donors provided the written informed consent. The inner portion of subcutaneous fat was minced into pieces with the diameter of 3-4 mm, paying attention to avoid visible blood vessels. Such pieces were cultured in complete culture medium supplemented with 5% PL, 100 U/mL IL-1α, or 5% PL + 100 U/mL IL-1α, or without any

supplement, for 14 days. *In toto* hAT cultures were incubated at 37°C in a humidified atmosphere with 5% CO_2 and media were changed 3 times per week.

3.2.5. Proliferation assays

I. Cell counting: HS- and FBS-isolated hASCs at P2 were plated at 4157 cells/cm^2/well in 6-well plates using the complete or control culture medium according to their isolation condition. They were incubated for 24h to enable cell adhesion to wells and, the next day (day 0), medium was replaced with complete medium, un-supplemented or supplemented with 5% PL, or control medium. For each culture condition, the cell number was measured in two different wells, after 0, 2, 4, 6 and 8 days of stimulation, using a Bright-Line™ Hemacytometer with an improved Neubauer chamber. The final result was expressed as the average of 3 independent experiments performed on different single-donor primary hASC cultures ± SD value.

II. Crystal violet staining assay: HS-isolated hASCs were plated at $2.5x10^3$ cells/well in 96-well plate and incubated in complete medium for 24h. The next day (day 0), medium was replaced with complete medium un-supplemented or supplemented with 5% PL, 100 U/mL IL-1α, or 5% PL + 100 U/mL IL-1α. Crystal violet staining assay was performed in quintuplicate for each culture condition after 0, 1, 2, 3 and 4 days of the different stimulations. At every time point, the culture media were removed and replaced with 50 µL/well of 0.75% (w/v) crystal violet staining solution (prepared using 0.375 g crystal violet powder, 0.175 g NaCl, 16.15 mL absolute ethanol and 4.32 mL formaldehyde 37% weight solution and bringing to 50 mL with distilled water). After 20-minute incubation, the staining solution was discarded and wells were extensively washed with distilled water. When the plates were dry, 100 µL/well of elution solution (composed by 50% v/v absolute ethanol and 1% v/v acetic acid in PBS) was added. For each well, the optical density (OD) was measured at 595 nm. As final result, it was reported the n-fold increase of OD respect to day 0, for each culture condition, expressed as the average of 3 independent experiments performed on different single-donor primary hASC cultures ± SD value.

3.2.6. Viability assay

The hASC viability under the same culture conditions assayed with the cell counting was evaluated in a parallel set of experiments by colorimetric MTT assay. This assay is based on the reduction of MTT, a yellow water-soluble substrate, in formazan, a blue alcohol-soluble reaction product, by mitochondrial succinate dehydrogenase of living cells. Formazan is then dissolved in alcohol and spectrophotometrically measured. Therefore, the optical density (OD) is strictly correlated with

viable cell number. In particular, HS- or FBS-isolated hASCs at P2 were plated at 4157 cells/cm^2/well in 24-well plates and, after an incubation of 24h, medium was replaced with complete medium, un-supplemented or supplemented with 5% PL, or control medium, respectively. After 0, 2, 4, 6 and 8 days of stimulation, cell layers were incubated with 5 mg/mL MTT in serum-free medium for 3h at 37°C in a humidified atmosphere with 5% CO_2 in the dark. The MTT solution was then removed and formazan was dissolved in absolute ethanol. The OD of the resulting solution was measured using a test wavelength of 570 nm and a reference wavelength of 670 nm. For each culture condition, the OD was measured in three different wells and expressed as the average of 3 independent experiments performed on different single-donor primary hASC cultures ± SD value.

3.2.7. Colony-forming efficiency assay

Immediately after their isolation (P0), hASCs were plated at 100 µL of lipoaspirate/Petri dish in complete medium, un-supplemented or supplemented with 5% PL, or in control medium in duplicate per each culture condition. After 9 days, colonies were fixed by 10% neutral buffered formalin (comprised of 10 mL formaldehyde 37% weight solution, 90 mL PBS) for 10 min at room temperature and stained with 1% methylene blue solution at pH 8.8 (prepared with 1% w/v methylene blue hydrate powder, 0.2 M boric acid, 0.05 M sodium tetraborate decahydrate, distilled water up to the final volume) for 45 min at room temperature. The dye excess was washed away with distilled water and dishes were allowed to air dry. In each dish, the colony number was counted by naked eye. The CFE was also quantified by using the ImageJ-plugin "ColonyArea", which calculates two output parameters: 'colony area percentage', i.e. the percentage of dish area covered by colonies, and 'colony intensity percentage' that takes into account both the area covered by colonies and the density of the colonies (Guzmán, Bagga, Kaur, Westermarck, & Abankwa, 2014). The number of colonies/condition and both the ColonyArea-derived parameters were expressed as mean values ± SD calculated on the basis of 5 independent experiments relative to different single-donor primary cultures for all tested culture conditions.

3.2.8. Adipogenic and osteogenic differentiation

To induce adipogenic and osteogenic differentiation, HS-isolated hASCs at P2 or PL-expanded hASCs at P5 were plated at 8314 cells/cm^2/well in 24-well plates and were expanded for at least 4 days in complete medium. After this expansion step, one half of sub-confluent cell wells was treated with specific induction media for adipogenic and osteogenic differentiation for 14 days and the other half was cultured with complete medium as control. Adipogenic differentiation medium was composed by complete medium supplemented with 6 ng/mL insulin and 10^{-7} M dexamethasone

(Scott, Nguyen, Levi, & James, 2011). Osteogenic differentiation medium was composed by complete medium supplemented with 50 μg/mL ascorbic acid, 10 mM β-glycerophosphate and 10^{-7} M dexamethasone (Muraglia et al., 2017). The media were changed 3 times per week. At day 14, the presence of intracellular lipid droplets was detected in all the cell cultures induced to adipogenesis and in half of those induced to osteogenesis, with their relative control cultures, by Oil Red O (ORO) staining. Cell layers were fixed with a formol-calcium solution (comprised of 10 mL formaldehyde 37% weight solution, 1 g calcium chloride, 90 mL distilled water) for 10 min at room temperature. They were extensively washed with distilled water and stained with 0,5% (w/v) ORO in propan-2-ol, diluted 3:2 in distilled water, for 20 min at room temperature. The dye excess was washed away with distilled water and photos of stained cell layers were taken by Hamamatsu Color Chilled 3CCD Camera C5810. For adipogenic induction experiment, incorporated ORO was extracted by incubating stained cell layers in 100% propan-2-ol for 10 min at room temperature with mild agitation. For control and induction conditions, the optical density (OD) was measured at 530 nm in triplicate and expressed as the average of 3 independent experiments performed on different single-donor primary hASC cultures ± SD value. Analogously, the amount of incorporated ORO was also evaluated in hASCs plated at P2 at 4157 cells/cm^2/well in 24-well plates and cultured in complete medium, un-supplemented or supplemented with 5% PL, or in control medium for 0, 4 and 8 days, without any induction. The final result is expressed as means ± SD values considering at least 3 independent experiments assayed in triplicate on different single-donor primary cultures. At the end of osteogenic induction, the matrix mineralization in the induced cultures was valuated by Alizarin Red S (ARS) staining. Cell layers were fixed with 4% (w/v) paraformaldehyde in PBS for 10 min at room temperature. They were washed with distilled water and stained with 2% (w/v) ARS in distilled water at pH 4.2 for 10 min at room temperature. After a washing step with absolute ethanol and others with distilled water, the stained wells were allowed to air dry and finally scanned by Epson Perfection V330 Photo Scanner. The osteogenic differentiation was assayed in duplicate on 3 different single-donor primary cultures.

3.2.9. Real Time quantitative PCR analysis

To analyse the expression of adipogenesis-related genes, total RNA was extracted from HS- and FBS-cultured hASCs used for cell counting experiment at 0, 4 and 8 culture days and from HS-cultured cells stimulated with 5% PL for 4 days by RNeasy® Plus Micro Kit following manufacturer's instructions. Total RNA concentrations were measured at 260 nm and total RNA purity was checked considering 260 nm/280 nm ratio with values included in 1.9-2.1 range. Total RNA was reverse-transcribed to cDNA using Omniscript® RT Kit according to manufacturer's protocol. Transcript levels of target genes were measured by Real Time quantitative PCR using

Power SYBR® Green PCR Master Mix on 7500 Fast Real-Time PCR System. Primer sequences were: forward 5'-CCTATTGACCCAGAAAGCGA-3' and reverse 5'-GGGAGTGGTCTTCCATTACG-3' for PPARγ2 (designed by Primer-BLAST, Ye et al., 2012); forward 5'-CAGAGGGACCGGAGTTATGA-3' and reverse 5'-TTCACATTGCACAAGGCACT-3' for C/EBPα (Russo, Yu, Belliveau, Hamilton, & Flynn, 2014); forward 5'-GACTCAACACGGGAAACCTCACC-3' and reverse 5'-ACCAGACAAATCGCTCCACCAACT-3' for 18S rRNA (Schiller, Schiele, Sims, Lee, & Kuo, 2013). The expression of 18S rRNA was used as endogenous control (normalizer). For each primer pair, the production of single amplicon was checked by generating a melting curve. Transcript levels were extrapolated from a standard curve, generated using a dilution series of all total RNA sample mixture, and divided by normalizer quantity. Each sample was assayed in triplicate. The final results are expressed as the average of 3 independent experiments performed on different single-donor primary hASC cultures ± SD values.

3.2.10. Western blot analysis

To analyse the cytokine production, HS-isolated hASCs at P2 were seeded in 60 mm dishes, cultured in complete medium until 80% confluence and treated for 24h with serum-free medium supplemented with 5% PL, 100 U/mL IL-1α, or 5% PL + 100 U/mL IL-1α, or without any supplement. Cells were then extensively washed with PBS for removing residual factors and then incubated in serum-free medium for 24h. The different media were collected, clarified at 2000 rpm for 10 min at room temperature and stored at -20°C. The incubation in serum-free medium for 24h and the collection of conditioned media were consecutively repeated twice more on the same cell layers obtaining media at 48h and 72h. To investigate the activation of inflammation-related pathways, HS-isolated hASCs were treated as described above and, at the end of 24h stimulation, cells were extensively washed with PBS and lysed by incubating the cell layers on ice for 5 min with ice-cold RIPA buffer (containing 50 mM Tris HCl pH 7.5, 150 mM NaCl, 1% w/v sodium deoxycholate, 1% v/v Triton X-100, 0.1% w/v sodium dodecyl sulphate and 0.2% w/v sodium azide) supplemented with protease inhibitor cocktail. Cell lysates were harvested with cell scrapers, clarified at 10000 rpm for 15 min at 4°C and stored at -20°C. The same procedure was followed for preparing cell lysates corresponding to cell layers used for collecting conditioned media at 72h. To study the PL effect on proliferation-related pathways and on cell cycle activation, sub-confluent HS-isolated hASCs were incubated in serum-free medium for 1h (serum starvation) and treated for multiple time intervals with serum-free medium supplemented with 5% PL. Cells were washed with cold PBS on ice and incubated at -80°C for at least 1h. Cell layers were then incubated on ice with ice-cold RIPA buffer supplemented with protease inhibitor cocktail, immediately harvested with ice-cold cell scraper, clarified at 10000 rpm for 15 min at 4°C and stored at -20°C. The protein

content of both conditioned media and cell lysates was quantified by Bradford protein assay (Bradford, 1976). Electrophoresis was performed in reducing conditions using 6 μg of total protein/sample for conditioned media and 30 μg or 100 μg for cell lysates for studying inflammation-related or proliferation-related pathways, respectively. Proteins were loaded on NuPAGE™ 4-12% Bis-Tris gel and transferred to Amersham™ Protran™ 0.45 μm NC nitrocellulose blotting membrane. The blot was saturated with 5% skimmed cow milk in TTBS (composed by 20 mM Tris HCl pH 7.5, 500 mM NaCl and 0.1% Tween 20 in distilled water) for 2h at room temperature and probed in a cold room overnight with primary antibodies raised against IL-8 (1:250 dilution) and IL-6 (1:250 dilution) for conditioned media or against COX-2 (1:1000 dilution), mPGES-1 (1:200 dilution), phospho-Akt (1:1000 dilution), Akt (1:1000 dilution), phospho-$ERK_{1/2}$ (1:1000 dilution), $ERK_{1/2}$ (1:1000 dilution), Cyclin D1 (1:250 dilution), phospho-STAT3 (1:1000 dilution) and Actin (1:500 dilution) for cell lysates. After washing, the detection was obtained by incubating the blot with specific secondary horseradish peroxidase-linked IgGs (1:6000 dilution) for 1h at room temperature. The blot was then washed with TTBS, incubated with Amersham™ ECL™ western blotting detection reagents following manufacturer's instructions and finally exposed to Amersham™ hyperfilm™ ECL to capture the image. For each considered marker, western blot was performed on 3 independent experiments corresponding to different single-donor primary hASC cultures. The densitometric analysis for IL-6 and IL-8 secretion and for Cyclin D1 synthesis was performed by scanning the relative films using Epson Perfection V330 Photo scanner (Epson, Italy) and quantifying the band densities using ImageJ software (https://imagej.nih.gov/ij/download.html). The relative shown results are the average of 3 independent experiments ± SD values.

3.2.11. PGE_2 quantification

For the quantification of PGE_2 in conditioned media, Prostaglandin E_2 ELISA kit was used. This assay is based on the competition between PGE_2 present in the sample and a PGE_2-acetylcholinesterase (AChE) conjugate (PGE_2-tracer) for a limited amount of anti-PGE_2 monoclonal antibody. By adding the substrate of AChE, a colorimetric reaction occurs and the relative absorbance is measured spectrophotometrically at 405 nm. The PGE_2 concentration relative to the sample is calculated using a standard curve. The hASC 24h,72h-conditioned media were prepared in the same way reported for western blot analysis and assayed following manufacturer's instructions. For each culture condition, the PGE_2 concentration is reported as average value of 3 independent experiments performed in duplicate on different single-donor primary cultures ± SD.

3.2.12. Histological analysis

After 14 culture days, *in toto* hAT samples were fixed with a formol-calcium solution overnight at 4°C, rinsed extensively with PBS, dehydrated with increasing ethanol concentrations, cleared in xylol and embedded in paraffin. As control, some *in toto* hAT pieces were fixed and paraffin-embedded immediately after their isolation from the resection material (un-stimulated hAT). All samples were cut into sections of 5 µm, which were placed on poly-L-lysine-coated glasses and dried overnight at 37°C. Sectioned samples were stained with Hematoxylin and Eosin (H&E). For immunohistochemical investigations, sections were deparaffinised, hydrated to water with decreasing ethanol concentrations, incubated with 0.2% Triton in PBS for 10 min to permeabilize cell membranes, incubated with 0.3% H_2O_2 in distilled water for 30 min to block endogenous peroxidase activity and covered with 10% normal goat serum in PBS for 1h to reduce non-specific staining. Sections were incubated with primary antibody raised against PCNA (1:200 dilution) diluted in 5% normal goat serum in PBS overnight at 4°C in a humid chamber. As negative control, one section per slide was incubated only with 5% normal goat serum in PBS. For detection of primary antibody, sections were incubated first with biotinylated IgGs (1:200 dilution), diluted in 5% normal goat serum in PBS, and then with streptavidin-peroxidase (1:500 dilution), diluted in 5% normal goat serum in PBS, each for 30 min at room temperature. The peroxidase was visualized using DAB following manufacturer's instructions. A complete histological analysis was performed on each of 3 different single-donor hAT samples.

3.2.13. Statistical analysis

All data are presented as means and standard deviations based on independent experiments performed on at least three different primary hASC cultures, each of them derived from a single donor. The statistical analysis was performed using the unpaired t-Test for cell counting assay, real time quantitative PCR analysis, CFE assay and ORO quantification or using the ordinary one-way ANOVA for IL-8, IL-6 and Cyclin D1 densitometric analysis, PGE_2 quantification and crystal violet assay. If ANOVA detected statistically significant differences within the data set, Tukey's multiple comparison test was used to calculate the significant differences for IL-8 and IL-6 densitometric analyses, PGE_2 quantification and crystal violet assay. Dunnett's multiple comparison test was used for Cyclin D1 densitometric analysis. All tests were run setting a confidence interval of 95% ($p<0,05$).

3.3. Results

3.3.1. HS sustains hASC proliferation more efficiently than FBS

Since our attempt was to study *in vitro* the cell behaviour in the wound microenvironment, primary hASCs were isolated in presence of HS, which was devoid of platelet-derived factors, and characterized respect to cells isolated with FBS. In particular, the cells were isolated using a culture medium supplemented with 10% HS or 10% FBS (complete or control medium, respectively) and were frozen in liquid nitrogen at P0 for long-term storage. After thawing, (92.8±8.1)% and (88.6±9.6)% of viable cells were obtained with complete and control medium, respectively, by trypan blue exclusion test. The proliferation of HS- and FBS-expanded hASCs was monitored at P2 for 8 days by cell counting. The HS-expanded hASCs had a higher proliferation rate respect to FBS-expanded cells, showing a significant (5.75±1.35)-fold increase of cell density after 8 culture days (**Figure 1a**, p=0.0006 for 10%FBS vs. 10%HS at day 8). In parallel experiments, we evaluated cell viability in the same conditions used for cell counting by MTT assay, obtaining trends similar to those relative to cell proliferation (**Figure 1b**). This finding indicates that hASCs were metabolically active independently from the cell density. Cell morphology was different depending on culture conditions (**Figure 1c**). In agreement with the reported cell density, HS-expanded hASCs were smaller than FBS-expanded cells, which showed a spreading and flatter shape.

Although HS sustained cell proliferation more efficiently than FBS, we did not find a significant difference in the number of colony-forming unit-fibroblasts (CFU-fs) between complete and control medium by CFE assay (**Figure 1d,e**). For the quantitative analysis of CFE assay, we used the ImageJ-plugin "ColonyArea", which calculates the percentage of dish area covered by colonies (colony area percentage) and the intensity-weighted area percentage (colony intensity percentage). Both the output parameters increased with the complete medium respect to the control one but these differences were not significant (**Figure 1f**).

3.3.2. HS induces spontaneous adipogenic differentiation in hASCs

During hASC culture in presence of HS, we observed spherical deposits within the cells increasing in number and dimension with time while they were absent in hASCs cultured with FBS. The ORO staining of hASCs at P2 cultured with 10% HS for 0, 4 and 8 days showed ORO-positive cells with red-stained lipid deposits increasing with time while FBS-expanded hASCs were totally negative (**Figure 2a,b**). Quantitation of the amount of incorporated ORO, normalized per cell number, showed a trend of increase with time in agreement with the observation of the progressive increase of deposits (**Figure 2c**), suggesting the spontaneous differentiation of ASCs towards adipogenesis. Analysis of total RNA extracted from hASCs cultured with HS and FBS for 0, 4 and 8 days showed

that transcript levels of *pparγ2* and *c/ebpα*, two master regulators of adipogenesis, gradually increased with time in HS-expanded hASCs at variance with FBS-expanded cells in which they remained at a basal level with time (**Figure 2d,e**). At 8th day, *pparγ2* and *c/ebpα* expression reached a level significantly higher in HS-cultured cells with respect to FBS-cultured ones (p=0.0422 and p=0.0318 for 10%HS vs. 10%FBS, respectively).

3.3.3. Committed HS-expanded hASCs differentiate towards adipogenesis and osteogenesis

From observing HS-expanded hASC cultures after ORO staining, we realized that cell layers contained some regions with ORO-negative cells also at high cell density after 8 culture days. For this reason, we induced committed HS-expanded hASCs to differentiate into the adipogenic lineage in order to investigate qualitatively the capability of ORO-negative cells to differentiate towards adipogenesis. Sub-confluent hASCs at P2 were treated with complete medium supplemented with 6 ng/mL insulin and 10^{-7} M dexamethasone or un-supplemented (control) for 14 days obtaining in induced cultures ORO-positive cells with intracellular lipid droplets morphologically similar to those recognised in control cultures at the end of induction (**Figure 3a**). The amount of incorporated ORO in the treated cells did not significantly vary between induced and control cultures although a trend of increase was shown (**Figure 3b**). However, we still found several ORO-negative cells in induced cell layers.

To verify the presence of immature or less committed cells in HS-expanded hASC cultures, we induced the osteogenic differentiation in sub-confluent HS-expanded hASCs containing lipid droplets at P2 by using complete medium supplemented with 50 μg/mL ascorbic acid, 10 mM β-glycerophosphate and 10^{-7} M dexamethasone or un-supplemented (control) for 14 days. At the end of induction, ARS staining revealed a great amount of calcium-rich deposits in the extracellular matrix of induced cells but not in the control cultures (**Figure 3c**). In a parallel set of experiments, we still found ORO-stained lipid droplets within induced ASCs. Surprisingly, these droplets were qualitatively very similar to those found in the control cultures (**Figure 1Sa,b**). Interestingly, when chondrogenic differentiation was induced on HS-expanded hASCs at P2 by pellet-culture method using serum-free medium supplemented with 6.25 μg/mL insulin, 6.25 μg/mL human apo-transferrin, 1.25 μg/mL linoleic acid, 5.35 μg/mL bovine serum albumin, 1 mM sodium pyruvate, 50 μg/mL ascorbic acid, 10^{-7} M dexamethasone and 10 ng/mL TGF-β1 for 21 days, poor metachromatic toluidine blue staining and no collagen type II production were detected in the extracellular matrix of pellets by histological analysis (**Figure 2Sa,b**).

3.3.4. Proliferation in the wound microenvironment: PL increases the proliferation of HS-expanded hASCs

Considering that platelets release a cocktail of bioactive molecules by degranulation as soon as an injury occurs, we evaluated the effect of PL, possibly representing the content released by platelets, on the proliferation of hASCs isolated and cultured in HS in order to mimic the wound microenvironment. Cell proliferation and viability were determined in HS-expanded cells at P2 stimulated with 5% PL by cell counting and MTT, respectively. The presence of PL in the complete medium induced a significant increase of cell proliferation and, at the same time, a similar increase of cell viability, revealing that proliferating cells were metabolically active (**Figure 4a,b**, p=0.0004 for 10%HS+5%PL vs. 10%HS at day 4). After 4 days of PL treatment, cell density in presence of PL was (2.76±0.58)-fold higher than that reached in absence of PL. At longer time, confluent hASC layers detached starting from borders forming each a spheroidal cell mass. The PL treatment determined spindle-like morphology and smaller dimensions compared to cells cultured in the absence of PL (**Figure 4c**). Interestingly, the differences in cell morphology were evident immediately after the cultures were established.

In presence of PL, the number of CFU-fs did not significantly vary compared to un-supplemented culture condition (**Figure 4d,e**). Instead, colony area percentage and colony intensity percentage, calculated by ImageJ-plugin "ColonyArea", were significantly higher when PL was added to complete medium respect to the values recovered for the un-supplemented condition (p=0.0001 for 10%HS vs. 10%HS+5%PL regarding colony area percentage; p<0.0001 for 10%HS vs. 10%HS+5%PL regarding colony intensity percentage) (**Figure 4f**).

3.3.5. PL activates Akt, ERK and STAT3 pathways and induces Cyclin D1 synthesis in hASCs

Starting from the findings about the strong increase of proliferation rate induced by PL treatment, we focused our attention on the PL effect on three common proliferation-related pathways and on cell cycle activation. In particular, sub-confluent HS-isolated hASCs were serum starved for 1h in order to reduce cell metabolism and treated for multiple time intervals with serum-free medium supplemented with 5% PL. At the end of stimulation, cell layers were harvested and analysed by western blot. We found a strong and transient activation of Akt and ERK pathways by phosphorylation starting from 30 min of PL stimulation and decreasing after 1h. The activation of STAT3 pathway was gradual starting from 30 min and arriving to 24h of PL treatment corresponding to the maximum level of phospho-STAT3 (**Figure 5a**). We revealed an analogous activation of these three pathways also in cell lysates derived from sub-confluent HS-isolated hASCs treated with PL in presence of HS (data not shown). Regarding cell cycle activation, PL

induced a significant increase of Cyclin D1 after 4h of treatment (p=0.0009 for 0h vs. 4h) reaching a level (3.43±0.92)-fold higher than basal level. After that, Cyclin D1 decreased at 8h (p=0.0065 for 0h vs. 8h) and disappeared at 24h (**Figure 5b**). An analogous trend in the Cyclin D1 synthesis was observed when hASCs were treated with PL in presence of HS (data not shown).

3.3.6. PL-activated hASCs retain differentiation capability towards adipogenesis and osteogenesis

Since HS-expanded hASCs showed spontaneous adipogenic differentiation and further increased adipogenesis in permissive conditions, we studied the capability to differentiate of PL-activated cells. The HS-expanded hASCs at P2 stimulated with 5% PL for 4 days retained the capability to differentiate spontaneously towards adipogenesis, as shown by ORO staining, but the quantitation of incorporated ORO, referred to the ratio between the cell number in PL-supplemented complete medium and the cell number in complete medium, showed a significant decrease in PL-treated cells (**Figure 6a,b**, p=0.0230 for 10%HS vs. 10%HS+5%PL). At the same time, we also found a significant decrease of *pparγ2* transcript level in PL-treated cells respect to un-treated cells (**Figure 6c**, p=0.0024 for 10%HS vs. 10%HS+5%PL).

Moreover, we expanded HS-isolated hASCs with complete medium supplemented with 5% PL for further 3 passages and induced them to differentiate towards adipogenesis and osteogenesis. Sub-confluent PL-expanded hASCs at P5 were treated with complete medium supplemented with 6 ng/mL insulin and 10^{-7} M dexamethasone or un-supplemented (control) for 14 days, obtaining in the induced cultures ORO-positive cells with intracellular lipid droplets morphologically similar but of greater dimensions respect to those recognised in the control cultures at the end of induction (**Figure 7a**). Regarding osteogenic differentiation, sub-confluent PL-expanded hASCs at P5 were treated with complete medium supplemented with 50 μg/mL ascorbic acid, 10 mM β-glycerophosphate and 10^{-7} M dexamethasone or un-supplemented (control) for 14 days. At the end of induction, ARS staining demonstrated the capability of these cells to produce a mineralized extracellular matrix in response to permissive conditions (**Figure 7b**). In a parallel set of experiments, we found ORO-positive lipid droplets within osteogensis-induced hASCs even though they were fewer and smaller respect to those present in the control condition (**Figure 3Sa,b**).

3.3.7. PL exerts the mitogenic effect in both physiological and inflammatory milieu

Having in mind that the recruitment of stem/progenitor cells out from their tissue niche takes place in inflammatory milieu at the wound site, we investigated the PL effect on hASC growth under both physiological and inflammatory conditions. The HS-expanded hASCs were treated with complete medium un-supplemented or supplemented with 5% PL, 100 U/mL IL-1α, or 5% PL + 100 U/mL

IL-1α for multiple times and the cell proliferation was monitored by crystal violet staining. We found that PL significantly increased cell proliferation respect to reference condition in physiological milieu in agreement with the results obtained with cell counting (p=0.0024 for 10%HS vs. 10%HS+5%PL at 4th treatment day). Regarding inflammatory milieu, PL significantly induced an increase of the proliferation rate respect to reference condition (p=0.0445 for 10%HS+100U/mLIL-1α vs. 10%HS+5%PL+100 U/mLIL-1α at 4th treatment day). No significant differences were detected between HS+PL and HS+PL+IL-1α conditions or between HS and HS+IL1α (**Figure 8a,b**).

3.3.8. PL induces a transient pro-inflammatory response in HS-expanded hASCs in inflammatory milieu

Considering that platelet content is not only involved in the proliferative response of resident cells but also in triggering and modulating the inflammatory state at the wound site, we investigated the PL effect on the inflammatory response of hASCs in both physiological and inflammatory condition. For this reason, sub-confluent HS-expanded hASCs were treated for 24h with serum-free medium supplemented or not with 5% PL for physiological conditions and supplemented with 100 U/mL IL-1α and/or 5% PL for inflammatory conditions. At the end of stimulation, the media were replaced every 24h with serum-free medium collecting conditioned media at 24, 48 and 72h. By western blot analysis of conditioned media, we found a significantly increased secretion of pro-inflammatory cytokines IL-6 and IL-8 with PL+IL-1α respect to IL-1α at 24h of serum-free incubation (p<0.0001 and p=0.0002 for 100U/mLIL-1α vs. 5%PL+100U/mLIL-1α at 24h regarding IL-6 and IL-8, respectively). Their secretion in PL+IL-1α gradually decreased up to basal level after 72h of serum-free incubation (p<0.0001 and p=0.0002 for 24h vs. 72h of 5%PL+100U/mLIL-1α regarding IL-6 and IL-8, respectively) (**Figure 9a**). Moreover, cell lysates were harvested at the end of 24h stimulation and after 72h of incubation with serum-free medium. By western blot analysis, we observed a strongly increased production of COX-2 after 24h of PL and IL-1α treatment and the complete disappearance of the signal after 72h of serum-free incubation. Regarding mPGES-1 production, we revealed a remarkable basal level enhanced by PL in both physiological and inflammatory condition after 24h treatment. After serum-free incubation, mPGES-1 level increased with all tested conditions (**Figure 9b**). As a consequence of COX-2 and mPGES-1 induction, we found a significantly increased concentration of PGE_2 with PL+IL-1α respect to IL-1α (p=0.0029) as regards 24h conditioned media by ELISA analysis, indicating a synergistic activity of IL-1α and PL in hASCs. After 72h serum-free incubation, PGE_2 levels with PL+IL-1α decreased reaching the basal level (p=0.0060) (**Figure 9c**).

3.3.9. PL induces cell proliferation also in *in toto* hAT cultured *ex vivo*

To confirm *in vitro* results obtained with hASCs, we decided to culture *ex vivo in toto* hAT samples using complete medium supplemented with 5% PL, 100 U/mL IL-1α, or 5% PL + 100 U/mL IL-1α, or without any supplement, for 14 days. During the culture, we did not revealed any change of hAT morphology and colour in all tested conditions. We observed spindle-like cells to come out, adhere to plastic and proliferate in all conditions, especially under PL stimulation (**Figure 10**). After 14 culture days, every hAT piece was collected, paraffin-embedded and examined by histological analysis. In particular, H&E staining revealed the presence of small and elongated cells in the outer layer of the pieces in every tested condition, especially with PL (**Figure 11a**). Moreover, the immunohistochemical analysis with specific antibody directed against the proliferation marker PCNA demonstrated small outlying cells were actively proliferating (**Figure 11b**). This outcome indicates that PL is able to exert the mitogenic effect, observed already with hASC culture, also in *in toto* hAT.

3.4. Discussion

Wound-healing process consists of a sequence of finely orchestrated events leading to the repair of the damaged tissue. When the progression of this process is impaired, chronic (or acute) wounds take place, especially in patients with underlying pathologies, affecting millions people around the world. The failure of the wounds to heal is largely related to vascular insufficiency, diabetes mellitus and local excessive pressure (Demidova-Rice, Hamblin, & Herman, 2012). Our interest is focused on the molecular basis of the wound-healing process in order to identify the endogenous pathways naturally activated following the injury and envisage a therapeutic approach able to re-order the impaired process of the chronic wounds. Starting from the previous findings obtained investigating the platelet lysate effects on human keratinocytes (El Backly et al., 2011), we studied the response of human subcutaneous adipose tissue to platelet-derived factors under conditions mimicking as much as possible the wound microenvironment in order to evaluate its contribute in supporting the repair process of skin lesions. For this purpose, we defined a clinically relevant model using Human Serum (HS), Platelet Lysate (PL) and Interleukin-1α (IL-1α) as effectors and primary human adipose-derived stromal cells (hASCs) and *in toto* human adipose tissue (hAT) cultured *ex vivo* as targets. Considering the manufacturing procedures of the used supplements, it is necessary to make some considerations of HS and PL composition. In particular, HS was un-contaminated by platelet-derived factors, as Muraglia et al. (2017) already reported. Analogously, the PL did not contain any plasmatic molecule since it has been prepared using platelets extensively washed with physiological saline before to have been disrupted. Consequently, such supplements allowed us to study rigorously their separated and combined effects on adipose tissue.

Considering that serum is the physiologic fluid present at the wound site following the coagulation process, we first evaluated the effect of HS on *in vitro* proliferation and differentiation of hASCs in comparison with FBS, normally used as gold standard for hASC culture. In particular, we found that HS sustained hASC proliferation with a rate significantly higher than FBS in agreement with data reported in literature (Hui et al., 2012; Kocaoemer, Kern, Klüter, & Bieback, 2007; Witzeneder et al., 2013). However, no statistically significant difference was observed in the number of isolated CFU-fs between HS and FBS, in agreement with Kocaoemer et al. (2007), demonstrating that the increased proliferation induced by HS was not related to a greater number of clonogenic progenitor cells. Moreover, we found that HS allowed adipogenic programme to carry on in hASCs by inducing the expression of two master regulators of adipogenesis PPARγ2 and C/EBPα and the accumulation of lipid droplets within the cells while no induction was observed with FBS. This finding was not previously reported in studies on cell differentiation in presence of human serum (Kocaoemer et al., 2007; Lindroos et al., 2010), possibly because such studies were performed using serum prepared from total blood instead of serum from plasma devoid of platelets, but it is in agreement with Hui et al. (2012) showing that HS decreased the expression of stemness-related genes although proliferation was induced. Considering both the morphology and the amount of incorporated lipid droplets, the HS-induced adipogenesis showed to be qualitatively similar to adipogenesis obtained following a traditional differentiation protocol normally used for hASCs cultured in FBS (Scott et al., 2011). By promoting the osteogenic differentiation with a traditional protocol (Muraglia et al., 2017), we obtained a strong deposition of mineralized matrix by HS-committed hASCs even though lipid droplets were still revealed within cells by ORO staining, as also reported by Lindroos et al. (2010). These findings suggest HS-expanded hASCs could represent a heterogeneous cell population constituted by progenitor cells at different stages of commitment. In this scenario, we speculate that in presence of human plasmatic molecules more committed cells would be able to continue their adipogenic cell fate while less committed cells would remain immature and would respond to exogenous stimuli differentiating towards the osteogenic lineage, as shown above. Hypothetically, HS could exert a “niche” effect on hASCs regulating self-renewal and differentiation of stem/progenitor cells included in this cell population. Interestingly, no differentiation towards chondrogenesis was observed at variance with the reports in literature for hASCs expanded in FBS (Zuk, 2002), possibly because HS-expanded cells were more committed to adipogenesis.

The coagulation process determines physiologically not only the conversion of plasma to serum but also the release of bioactive molecules from activated platelets by degranulation. For this reason, we studied the proliferative response of hASCs to platelet content. In particular, the presence of PL

in the culture medium supplemented with HS significantly enhanced cell growth reaching at confluence state a higher cell density and determining spindle-like morphology and smaller dimensions in comparison with cells cultured in the absence of PL, in agreement with an earlier study about bone marrow-stromal cells stimulated with PL (Chevallier et al., 2010). Under PL stimulation, the number of CFU-fs did not significantly vary respect to un-supplemented condition but PL-cultured colonies showed greater dimension and cell density than reference condition, such as output parameters of ImageJ-plugin "ColonyArea" revealed, in agreement with increased cell proliferation reported above. According to the these findings, PL determined in HS-expanded hASCs the early activation of proliferation-related Akt and ERK pathways, known to be involved in promoting cell growth (reviewed in Manning & Cantley, 2007) and implicated in the induction of Cyclin D1 expression and in the repression of anti-proliferative gene transcription (reviewed in Chambard, Lefloch, Pouysségur, & Lenormand, 2007), respectively. This outcome is supported by our previous study about human osteoblasts where we demonstrated the activation of such pathways and their involvement in cell proliferation, when PL was added to culture medium, by using Akt and ERK inhibitors (Ruggiu, Ulivi, Sanguineti, Cancedda, & Descalzi, 2013). In agreement with these findings, PL also induced the synthesis of Cyclin D1 after 4h treatment confirming the mitogenic role of PL in hASCs. Interestingly, we also observed that STAT3, which is involved in the cell-cycle progression (Hirano, Ishihara, & Hibi, 2000), was activated by PL and the maximum level of the phosphorylated form was reached after 24h treatment. Taken together, these data suggest that quiescent progenitor cells could be possibly activated and induced to proliferate by platelet-derived factors also at the wound site. No significant variations in hASC growth were found between physiological and inflammatory conditions when PL was supplemented or not to culture medium containing HS thus suggesting IL-1α was not involved in cell proliferation, in agreement with our previous study showing that human osteoblast proliferation was enhanced by adding PL to culture medium containing FBS, independently of the presence of IL-1α (Ruggiu et al., 2013). Interestingly, we observed that hASCs treated with PL for 4 days showed a significant decrease of incorporated ORO in parallel with a significant decrease of *pparγ2* transcript level. Taken together, these data suggest that PL treatment would favour the presence of un-differentiated cells in cultures of committed hASCs. In particular, PL could possibly induce the de-differentiation of cells already committed in HS or induce the proliferation of un-committed cells. Moreover, we found that hASCs expanded in presence of PL for 3 passages retained differentiation capability towards adipogenesis and osteogenesis.

In the human body, adipose tissue is not simply an inert tissue for energy storage but functions as an endocrine organ producing soluble mediators, indicated as adipokines, which are involved in the

regulation of many physiological and pathological processes (Kershaw & Flier, 2004). By using mouse models, Schmidt & Horsley (2013) demonstrated that mature adipocytes repopulated the skin wounds in parallel with fibroblast migration during the proliferative phase of healing. Moreover, they reported some evidences regarding a direct intercellular communication between adipocytes and fibroblasts that might contribute to fibroblast migration during dermal healing. Considering a putative role of adipogenic lineage cells in the healing of damaged skin also in humans, we evaluated the activation of adipogenic progenitor cells following inflammation and induction by platelet lysate. In particular, we investigated the secretory and inflammatory response of HS-expanded hASCs to PL under both normal and inflammatory conditions. We found the strong increase of pro-inflammatory cytokine IL-6 and IL-8 secretion from hASCs in presence of PL in inflammatory milieu respect to IL-1α condition, in agreement with our previously reported data regarding other cell systems (El Backly et al., 2011; Pereira et al., 2013; Ruggiu et al., 2013). Considering that the release of platelet-derived molecules is limited in time, we monitored the secretion of such cytokines up to 72h after the removal of PL stimulation finding the gradual decrease of their secretion with time. The production of COX-2, an enzyme involved in causing inflammation (Chen, 2010), was also temporarily induced in presence of IL-1α by a burst of PL (24h). As a consequence of COX-2 increase, we revealed the synergistic induction of mPGES-1 by PL and IL-1α even though mPGES-1 was already present at a remarkable basal level in the un-treated cells. The mPGES-1 levels increased with time under all tested conditions, included the control condition. The activation of COX-2/mPGES-1 pathway by PL under inflammatory condition led to a massive production of PGE_2, a prostaglandin able to induce the functional switch of macrophages towards the alternatively activated M2 phenotype, involved in the dampening of inflammation, as previously described in literature (Tasso et al., 2013; Vasandan et al., 2016). The strong but temporally transient increase of IL-6 and IL-8, already described as present in ASC secretome in physiological conditions and involved in wound healing (J. Braga Osorio Gomes Salgado et al., 2010), the transient induction of COX-2 and the production of PGE_2 following PL treatment under inflammatory condition suggest a possible contribution *in vivo* of subcutaneous adipose tissue first in establishing an inflammatory microenvironment and then in preparing the inflammation resolution during body's response to an injury.

The *ex vivo* culture of *in toto* hAT showed that PL was able to induce the proliferation of small and elongated cells on the surface of hAT pieces under both physiological and inflammatory conditions, while the presence of such cells was limited in absence of PL. The presence of IL-1α in the culture medium did not influence the cell proliferation. Moreover, PL induced cells to come out from hAT pieces, adhere to plastic and proliferate. The nature of cells coming out from hAT pieces is under

investigation. Overall, these findings supported further the capability of platelet-derived factors of inducing in culture the cell growth not only of primary hASCs but also of *in toto* hATs and possibly in *in vivo* subcutaneous adipose tissue.

3.5. References

Bradford, M. M. (1976). A rapid and sensitive method for the quantitation of microgram quantities of protein utilizing the principle of protein-dye binding. *Analytical Biochemistry*, *72*(1–2), 248–254. http://doi.org/10.1016/0003-2697(76)90527-3

Cancedda, R., Bollini, S., Descalzi, F., Mastrogiacomo, M., & Tasso, R. (2017). Learning from Mother Nature: Innovative Tools to Boost Endogenous Repair of Critical or Difficult-to-Heal Large Tissue Defects. *Frontiers in Bioengineering and Biotechnology*, *5*(April), 1–13. http://doi.org/10.3389/fbioe.2017.00028

Chambard, J.-C., Lefloch, R., Pouysségur, J., & Lenormand, P. (2007). ERK implication in cell cycle regulation. *Biochimica et Biophysica Acta (BBA) - Molecular Cell Research*, *1773*(8), 1299–1310. http://doi.org/10.1016/j.bbamcr.2006.11.010

Chen, C. (2010). COX-2's new role in inflammation. *Nature Chemical Biology*, *6*(6), 401–402. http://doi.org/10.1038/nchembio.375

Chevallier, N., Anagnostou, F., Zilber, S., Bodivit, G., Maurin, S., Barrault, A., … Rouard, H. (2010). Osteoblastic differentiation of human mesenchymal stem cells with platelet lysate. *Biomaterials*, *31*(2), 270–8. http://doi.org/10.1016/j.biomaterials.2009.09.043

Demidova-Rice, T. N., Hamblin, M. R., & Herman, I. M. (2012). Acute and Impaired Wound Healing. *Advances in Skin & Wound Care*, *25*(7), 304–314. http://doi.org/10.1097/01.ASW.0000416006.55218.d0

Di Paolo, N. C., & Shayakhmetov, D. M. (2016). Interleukin 1[alpha] and the inflammatory process. *Nat Immunol*, *17*(8), 906–913. Retrieved from http://dx.doi.org/10.1038/ni.3503

El Backly, R., Ulivi, V., Ph, D., Tonachini, L., Ph, D., Mastrogiacomo, M., & Ph, D. (2011). Platelet Lysate Induces In Vitro Wound Healing of Human Keratinocytes Associated with a Strong Proinflammatory Response, *17*. http://doi.org/10.1089/ten.tea.2010.0729

Eming, S. A., Martin, P., & Tomic-Canic, M. (2014). Wound repair and regeneration: mechanisms, signaling, and translation. *Science Translational Medicine*, *6*(265), 265sr6. http://doi.org/10.1126/scitranslmed.3009337

Estes, B., Diekman, B., Gimble, J., & Guilak, F. (2010). Isolation of adipose derived stem cells and

their induction to a chondrogenic phenotype. *Nature Protocols*, *5*(7), 1294–1311. http://doi.org/10.1038/nprot.2010.81.Isolation

Golebiewska, E. M., & Poole, A. W. (2015). Platelet secretion : From haemostasis to wound healing and beyond. *YBLRE*, *29*(3), 153–162. http://doi.org/10.1016/j.blre.2014.10.003

Guzmán, C., Bagga, M., Kaur, A., Westermarck, J., & Abankwa, D. (2014). ColonyArea: An ImageJ Plugin to Automatically Quantify Colony Formation in Clonogenic Assays. *PLoS ONE*, *9*(3), e92444. http://doi.org/10.1371/journal.pone.0092444

Hirano, T., Ishihara, K., & Hibi, M. (2000). Roles of STAT3 in mediating the cell growth, differentiation and survival signals relayed through the IL-6 family of cytokine receptors. *Oncogene*, *19*(21), 2548–2556. http://doi.org/10.1038/sj.onc.1203551

Hui, C. K., Safwani, W. K. Z. W., Chin, S. S., Malek, A. A. S. A., Hassan, N., Fazil, M. S., … Sathappan, S. (2012). Human serum promotes the proliferation but not the stemness genes expression of human adipose-derived stem cells. *Biotechnology and Bioprocess Engineering*, *17*(6), 1306–1313. http://doi.org/10.1007/s12257-012-0354-1

J. Braga Osorio Gomes Salgado, A., L. Goncalves Reis, R., Jorge Carvalho Sousa, N., M. Gimble, J., J. Salgado, A., L. Reis, R., & Sousa, N. (2010). Adipose Tissue Derived Stem Cells Secretome: Soluble Factors and Their Roles in Regenerative Medicine. *Current Stem Cell Research & Therapy*, *5*(2), 103–110. http://doi.org/10.2174/157488810791268564

Kershaw, E. E., & Flier, J. S. (2004). Adipose Tissue as an Endocrine Organ. *The Journal of Clinical Endocrinology & Metabolism*, *89*(6), 2548–2556. http://doi.org/10.1210/jc.2004-0395

Kocaoemer, A., Kern, S., Klüter, H., & Bieback, K. (2007). Human AB Serum and Thrombin-Activated Platelet-Rich Plasma Are Suitable Alternatives to Fetal Calf Serum for the Expansion of Mesenchymal Stem Cells from Adipose Tissue. *Stem Cells*, *25*(5), 1270–1278. http://doi.org/10.1634/stemcells.2006-0627

Lindroos, B., Aho, K.-L., Kuokkanen, H., Räty, S., Huhtala, H., Lemponen, R., … Miettinen, S. (2010). Differential Gene Expression in Adipose Stem Cells Cultured in Allogeneic Human Serum Versus Fetal Bovine Serum. *Tissue Engineering Part A*, *16*(7), 2281–2294. http://doi.org/10.1089/ten.tea.2009.0621

Manning, B. D., & Cantley, L. C. (2007). AKT/PKB Signaling: Navigating Downstream. *Cell*, *129*(7), 1261–1274. http://doi.org/10.1016/j.cell.2007.06.009

Martinez-Zapata, M. J., Martí-Carvajal, A. J., Solà, I., Expósito, J. A., Bolíbar, I., Rodríguez, L., &

Garcia, J. (2012). Autologous platelet-rich plasma for treating chronic wounds. *Cochrane Database of Systematic Reviews (Online)*, *10*(10), CD006899. http://doi.org/10.1002/14651858.CD006899.pub2

Muraglia, A., Nguyen, V. T., Nardini, M., Mogni, M., Coviello, D., Strada, P., … Mastrogiacomo, M. (2017). CULTURE MEDIUM SUPPLEMENTS DERIVED FROM HUMAN PLATELET AND PLASMA: CELL COMMITMENT AND PROLIFERATION SUPPORT. *Frontiers in Bioengineering and Biotechnology*, *5*, 66. http://doi.org/10.3389/FBIOE.2017.00066

Pereira, C., Scaranari, M., Benelli, R., Strada, P., Reis, R. L., Cancedda, R., & Gentili, C. (2013). Dual effect of platelet lysate on human articular cartilage: a maintenance of chondrogenic potential and a transient pro-inflammatory activity followed by an inflammation resolution. *Tissue Engineering Part A*, *19*(11–12), 1476–1488. http://doi.org/10.1089/ten.TEA.2012.0225

Ruggiu, A., Ulivi, V., Sanguineti, F., Cancedda, R., & Descalzi, F. (2013). Biomaterials The effect of Platelet Lysate on osteoblast proliferation associated with a transient increase of the in fl ammatory response in bone regeneration. *Biomaterials*, *34*(37), 9318–9330. http://doi.org/10.1016/j.biomaterials.2013.08.018

Russo, V., Yu, C., Belliveau, P., Hamilton, A., & Flynn, L. E. (2014). Comparison of Human Adipose-Derived Stem Cells Isolated from Subcutaneous, Omental, and Intrathoracic Adipose Tissue Depots for Regenerative Applications. *STEM CELLS Translational Medicine*, *3*(2), 206–217. http://doi.org/10.5966/sctm.2013-0125

Schiller, Z. a, Schiele, N. R., Sims, J. K., Lee, K., & Kuo, C. K. (2013). Adipogenesis of adipose-derived stem cells may be regulated via the cytoskeleton at physiological oxygen levels in vitro. *Stem Cell Research & Therapy*, *4*(4), 79. http://doi.org/10.1186/scrt230

Schmidt, B. A., & Horsley, V. (2013). Intradermal adipocytes mediate fibroblast recruitment during skin wound healing. *Development*, *140*(7), 1517–1527. http://doi.org/10.1242/dev.087593

Scott, M. A., Nguyen, V. T., Levi, B., & James, A. W. (2011). Current Methods of Adipogenic Differentiation of Mesenchymal Stem Cells. *Stem Cells and Development*, *20*(10), 1793–1804. http://doi.org/10.1089/scd.2011.0040

Sen, C. K., Gordillo, G. M., Roy, S., Kirsner, R., Lambert, L., Hunt, T. K., … Longaker, M. T. (2009). Human skin wounds: A major and snowballing threat to public health and the economy. *Wound Repair and Regeneration*, *17*(6), 763–771. http://doi.org/10.1111/j.1524-475X.2009.00543.x

Suryanarayan, S., Budamakuntala, L., Suresh, D., & Sarvajnamurthy, S. (2013). Autologous platelet

rich plasma in chronic venous ulcers: Study of 17 cases. *Journal of Cutaneous and Aesthetic Surgery*, *6*(2), 97. http://doi.org/10.4103/0974-2077.112671

Suthar, M., Gupta, S., Bukhari, S., & Ponemone, V. (2017). Treatment of chronic non-healing ulcers using autologous platelet rich plasma: a case series. *Journal of Biomedical Science*, *24*(1), 16. http://doi.org/10.1186/s12929-017-0324-1

Tasso, R., Ulivi, V., Reverberi, D., Lo Sicco, C., Descalzi, F., & Cancedda, R. (2013). In Vivo Implanted Bone Marrow-Derived Mesenchymal Stem Cells Trigger a Cascade of Cellular Events Leading to the Formation of an Ectopic Bone Regenerative Niche. *Stem Cells and Development*, *22*(24), 3178–3191. http://doi.org/10.1089/scd.2013.0313

Vasandan, A. B., Jahnavi, S., Shashank, C., Prasad, P., Kumar, A., & Prasanna, S. J. (2016). Human Mesenchymal stem cells program macrophage plasticity by altering their metabolic status via a PGE2-dependent mechanism. *Scientific Reports*, *6*(1), 38308. http://doi.org/10.1038/srep38308

Witzeneder, K., Lindenmair, A., Gabriel, C., Höller, K., Theiß, D., Redl, H., & Hennerbichler, S. (2013). Human-Derived Alternatives to Fetal Bovine Serum in Cell Culture. *Transfusion Medicine and Hemotherapy*, *40*(6), 417–423. http://doi.org/10.1159/000356236

Ye, J., Coulouris, G., Zaretskaya, I., Cutcutache, I., Rozen, S., & Madden, T. L. (2012). Primer-BLAST: A tool to design target-specific primers for polymerase chain reaction. *BMC Bioinformatics*, *13*(1), 134. http://doi.org/10.1186/1471-2105-13-134

Zuk, P. A. (2002). Human Adipose Tissue Is a Source of Multipotent Stem Cells. *Molecular Biology of the Cell*, *13*(12), 4279–4295. http://doi.org/10.1091/mbc.E02-02-0105

3.6. Figures & Legends

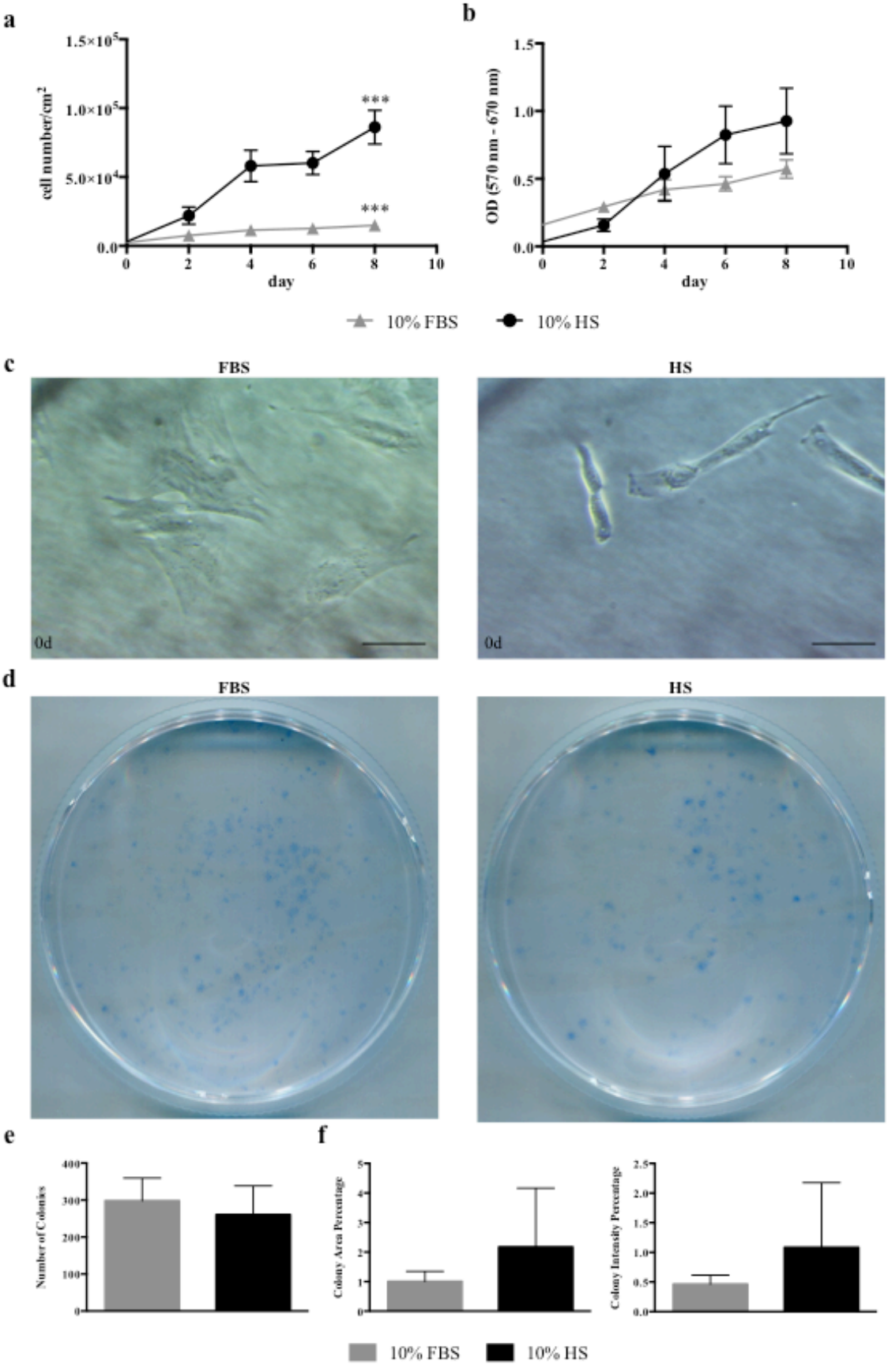

Figure 1: *In vitro* cultures of hASCs isolated and expanded in HS or FBS. **a**) Cell proliferation monitored at different times by cell counting. The average values ± SD of 3 independent experiments performed in duplicate on different single-donor primary cultures are reported. The *** symbol corresponds to p=0.0006. Statistical analysis was performed using the unpaired t-Test. **b**) Cell viability evaluated at different times by MTT assay. The average values ± SD of 3 independent experiments performed each in triplicate are reported. **c**) Morphology of cells in FBS (left photo) and in HS (right photo) one day after the seeding (day 0). Scale bar = 50 μm. **d**) The CFE assay performed on hASCs immediately after their isolation using complete or control medium. Scans of dishes with methylene blue-stained colonies deriving from a representative experiment. **e**) Number of colonies per condition counted by naked eye. The average values ± SD are calculated referring to 5 independent experiments performed each in duplicate. **f**) 'Colony area percentage' and 'colony intensity percentage' calculated by ImageJ-plugin "ColonyArea" and referred to both tested condition. The average values ± SD are calculated referring to 5 independent experiments performed each in duplicate.

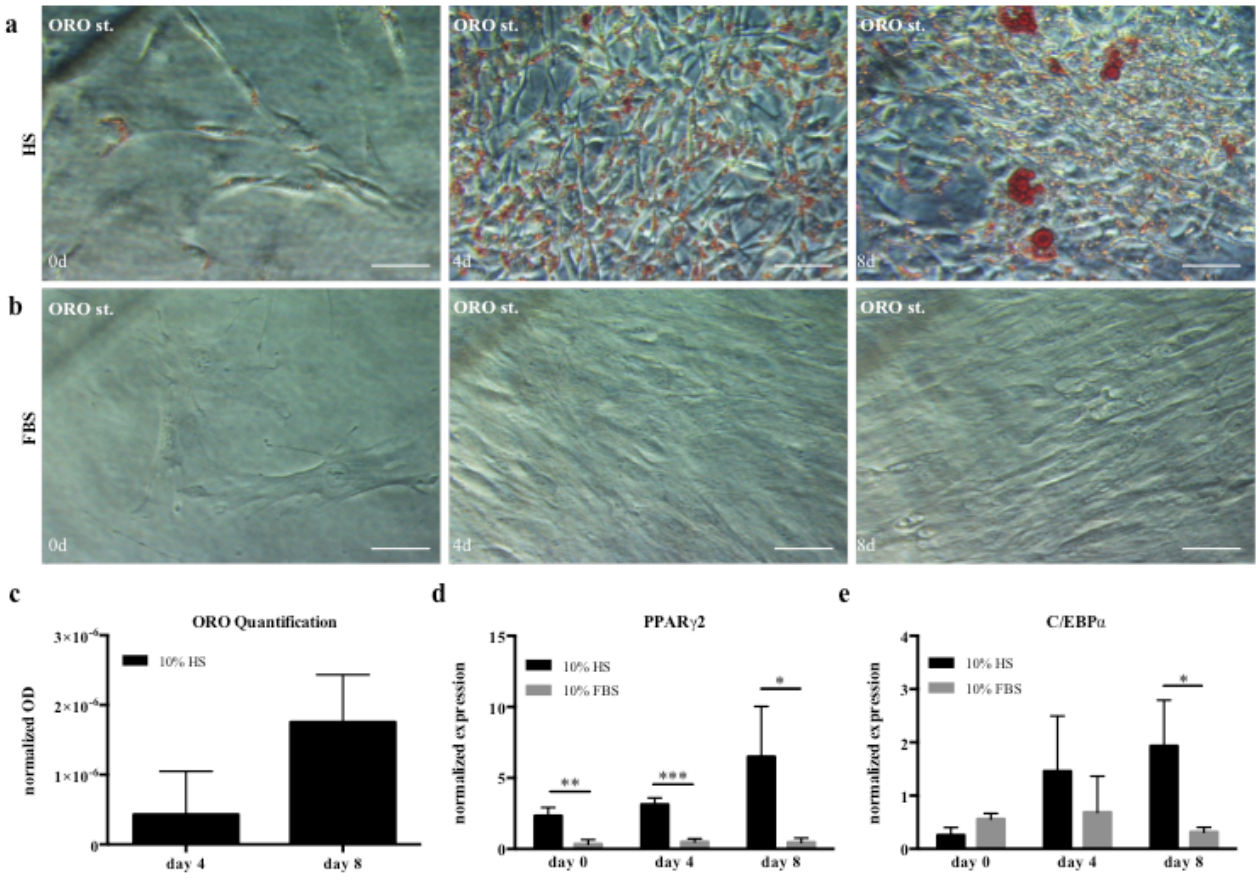

Figure 2: Spontaneous adipogenic differentiation of hASCs cultured in HS with respect to FBS. Representative ORO staining of hASCs cultured with HS (**a**) or FBS (**b**, as control condition) with time. Scale bar = 50 μm. The results were confirmed performing 3 independent experiments with

different single-donor primary hASC cultures. **c**) Quantification of ORO incorporated in HS-expanded hASCs, normalized per cell number, at different times by spectrophotometric analysis. The average values ± SD of 3 independent experiments performed each in triplicate are reported. Real Time quantitative PCR analysis of *pparγ2* (**d**) and *c/ebpα* (**e**) transcript levels in HS or FBS-expanded hASCs at different times. The final results are expressed as means ± SD values considering 3 independent experiments assayed in triplicate. The *, ** and *** symbols refer to p≤0.0422, p=0.0065 and p=0.0009, respectively. Statistical analysis was performed using the unpaired t-Test.

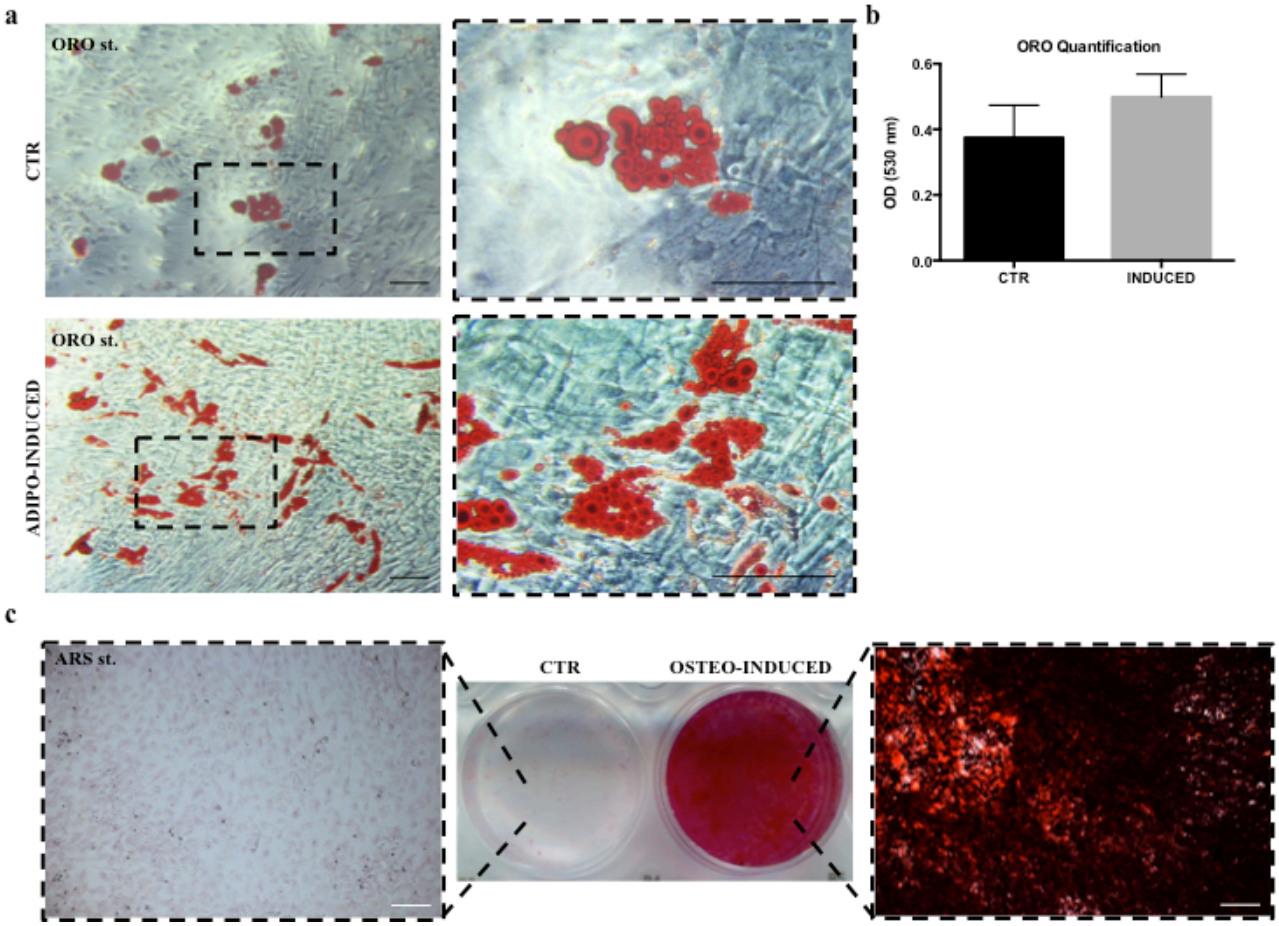

Figure 3: Adipogenic and osteogenic differentiation of HS-committed hASCs at P2 by using traditional differentiation protocols. **a**) Representative experiment assayed with ORO staining of adipogenesis-treated (ADIPO-INDUCED) and control (CTR) cells at the end of induction. The images on the right are magnification of the sections with dashed outline. Scale bar = 100 μm. The results were confirmed performing 3 independent experiments with different single-donor primary hASC cultures. **b**) Quantification of ORO incorporated in adipogenesis-treated (INDUCED) and control (CTR) cells at the end of induction by spectrophotometric analysis. The average values ± SD of 3 independent experiments performed each in triplicate are reported. **c**) Representative experiment assayed with ARS staining of osteogenesis-treated (OSTEO-INDUCED) and control

(CTR) cells at the end of induction. The lateral images with dashed outline are magnification of the treated and control cell layers. Scale bar = 100 μm. The results were confirmed performing 3 independent experiments.

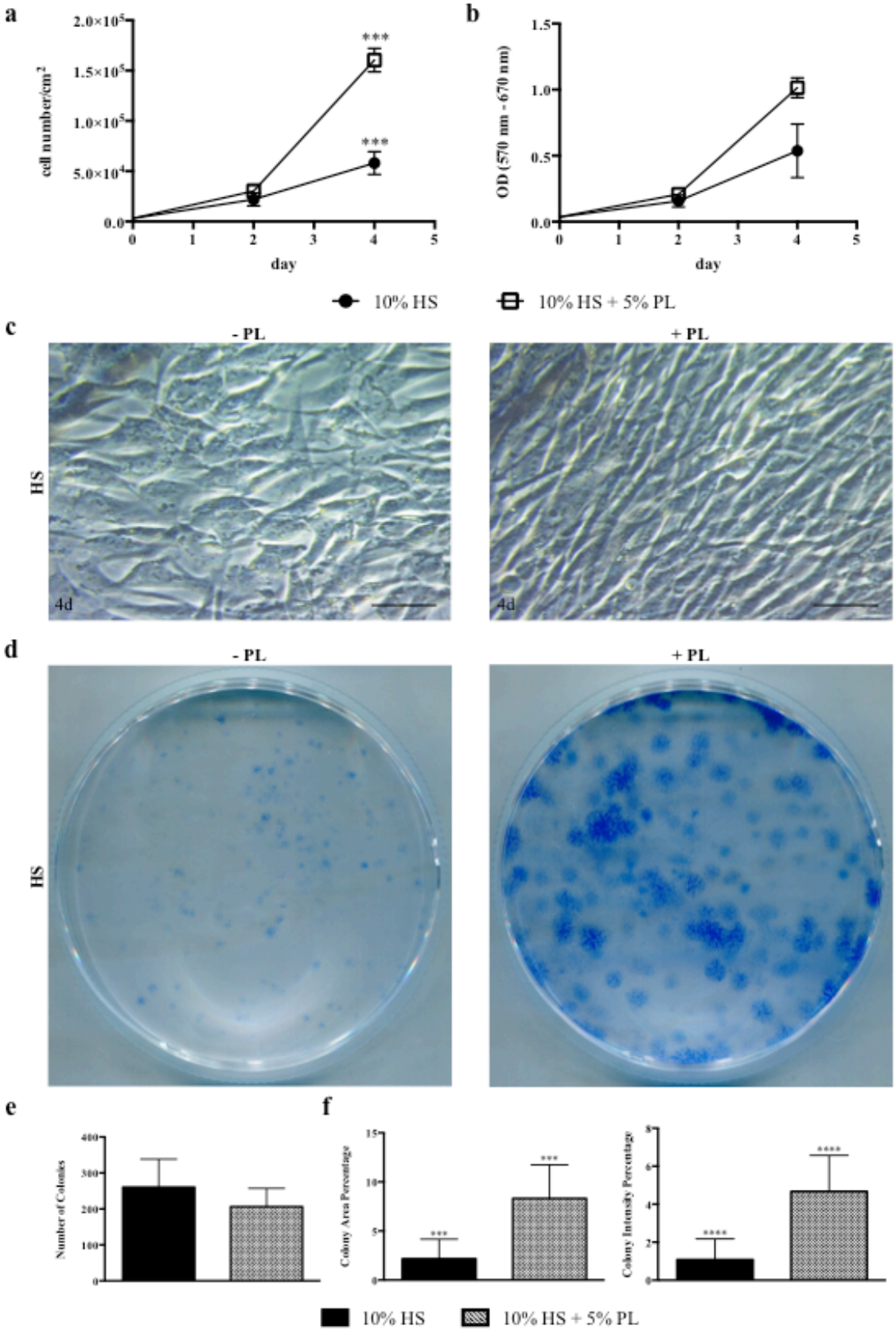

Figure 4: *In vitro* cultures of hASCs isolated and expanded in HS and stimulated with PL. **a**) Cell proliferation monitored at different times by cell counting. The average values ± SD of 3 independent experiments performed in duplicate on different single-donor primary cultures are reported. The *** symbol corresponds to p=0.0004. Statistical analysis was performed using the unpaired t-Test. **b**) Cell viability evaluated at different times by MTT assay. The average values ± SD of 3 independent experiments performed each in triplicate are reported. **c**) Morphology of cells in HS (left photo) and in HS+PL (right photo) after 4-day treatment. Scale bar = 50 μm. **d**) The CFE assay performed on hASCs immediately after their isolation using complete medium supplemented with PL. Scans of dishes with methylene blue-stained colonies deriving from a representative experiment. **e**) Number of colonies per condition counted by naked eye. The average values ± SD are calculated referring to 5 independent experiments performed each in duplicate. **f**) 'Colony area percentage' and 'colony intensity percentage' calculated by ImageJ-plugin "ColonyArea" and referred to both tested condition. The average values ± SD are calculated referring to 5 independent experiments performed each in duplicate. The *** and **** symbols correspond to p=0.0001 and p<0.0001. Statistical analysis was performed using the unpaired t-Test.

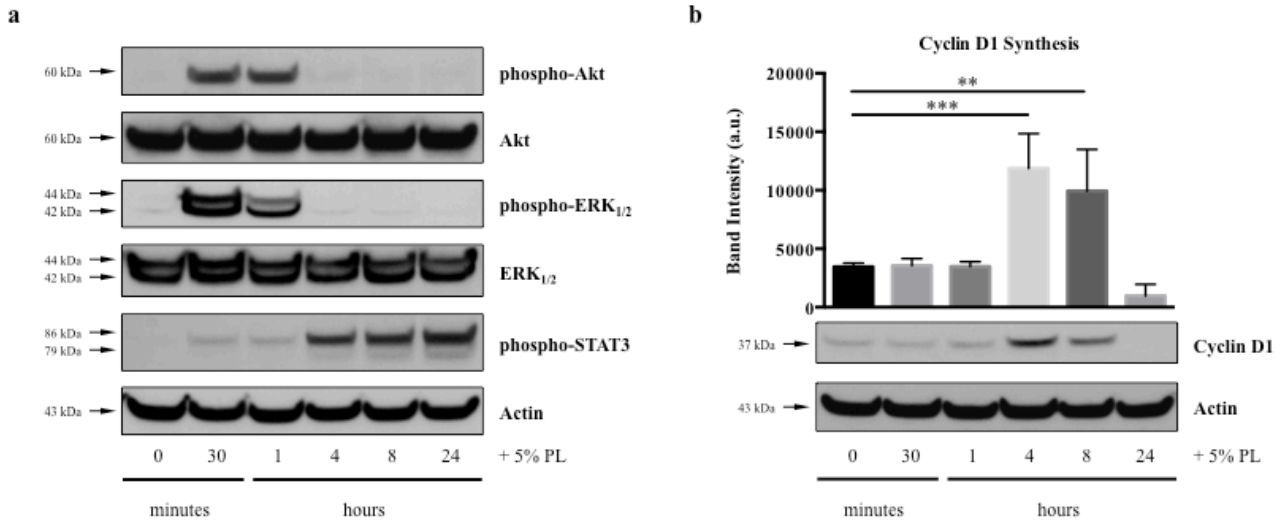

Figure 5: Modulation of proliferation-related pathways and activation of cell cycle in HS-expanded hASCs following multiple time intervals of PL stimulation investigated by western blot analysis. **a**) Representative western blot probed with primary antibodies raised against phospho-Akt, Akt, phospho-$ERK_{1/2}$, $ERK_{1/2}$, phospho-STAT3 and Actin. Actin was used as internal control. The results were confirmed performing 3 independent experiments with different single-donor primary hASC cultures. **b**) Densitometric analysis performed on 3 independent Cyclin D1-probed western blots (means ± SD) deriving from 3 different primary cell cultures (in the upper panel) and a representative western blot probed for Cyclin D1 and Actin (in the lower panel). Actin was used as

an internal control. The ** and *** symbols refer to p=0.0065 and p=0.0009, respectively. Statistical analysis was performed using the ordinary one-way ANOVA.

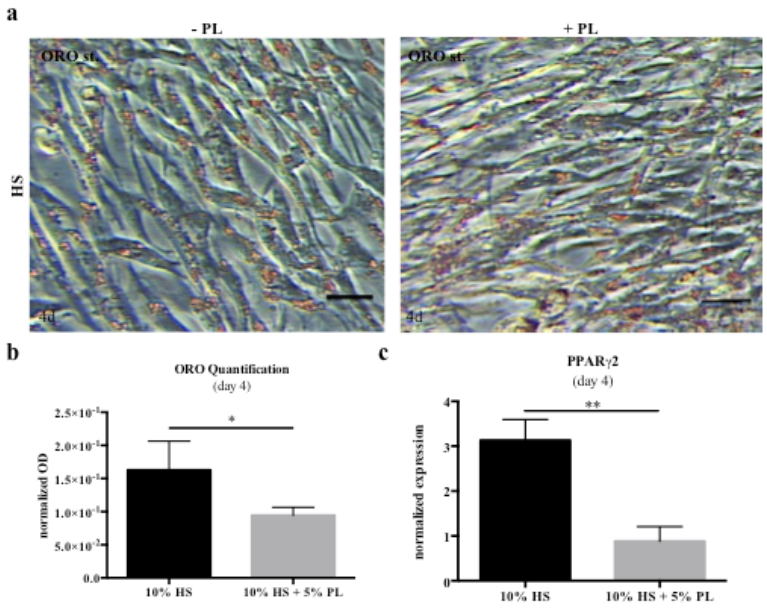

Figure 6: PL effect on adipogenic differentiation of HS-expanded hASCs. **a**) Representative ORO staining of hASCs treated with complete medium supplemented with PL or un-supplemented for 4 days. Scale bar = 25 μm. The results were confirmed performing 3 independent experiments with different single-donor primary hASC cultures. **b**) Quantification of ORO incorporated in HS-expanded hASCs treated or not with PL for 4 days, which were normalized to the ratio between the cell number in PL-supplemented complete medium and the cell number in complete medium, by spectrophotometric analysis. The average values ± SD of 4 independent experiments performed each in triplicate on 3 different primary hASC cultures are reported. The * symbol refers to p=0.0230. Statistical analysis was performed using the unpaired t-Test. **c**) Real Time quantitative PCR analysis of *pparγ2* transcript level in HS-expanded hASCs treated or not with PL for 4 days. The final results are expressed as means ± SD values considering 3 independent experiments assayed in triplicate. The ** symbol refers to p=0.0024. Statistical analysis was performed using the unpaired t-Test.

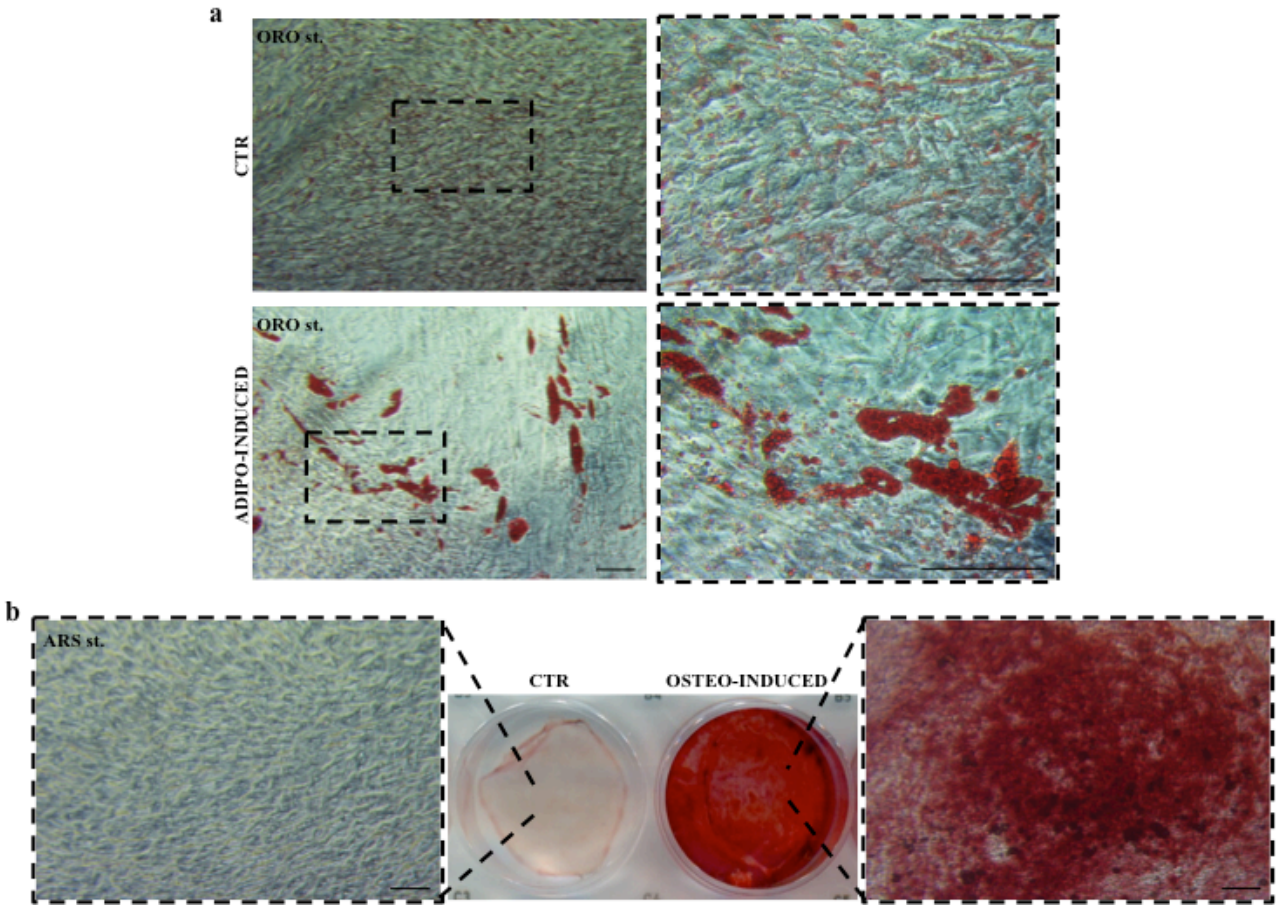

Figure 7: Adipogenic and osteogenic differentiation of hASCs further cultured with complete medium supplemented with PL for 3 passages by using traditional differentiation protocols. **a**) Representative experiment assayed with ORO staining of adipogenesis-treated (ADIPO-INDUCED) and control (CTR) cells at the end of induction. The images on the right are magnification of the sections with dashed outline. Scale bar = 100 μm. The results were confirmed performing 3 independent experiments with different single-donor primary hASC cultures. **b**) Representative experiment assayed with ARS staining of osteogenesis-treated (OSTEO-INDUCED) and control (CTR) cells at the end of induction. The lateral images with dashed outline are magnification of the treated and control cell layers. Scale bar = 100 μm. The results were confirmed performing 3 independent experiments.

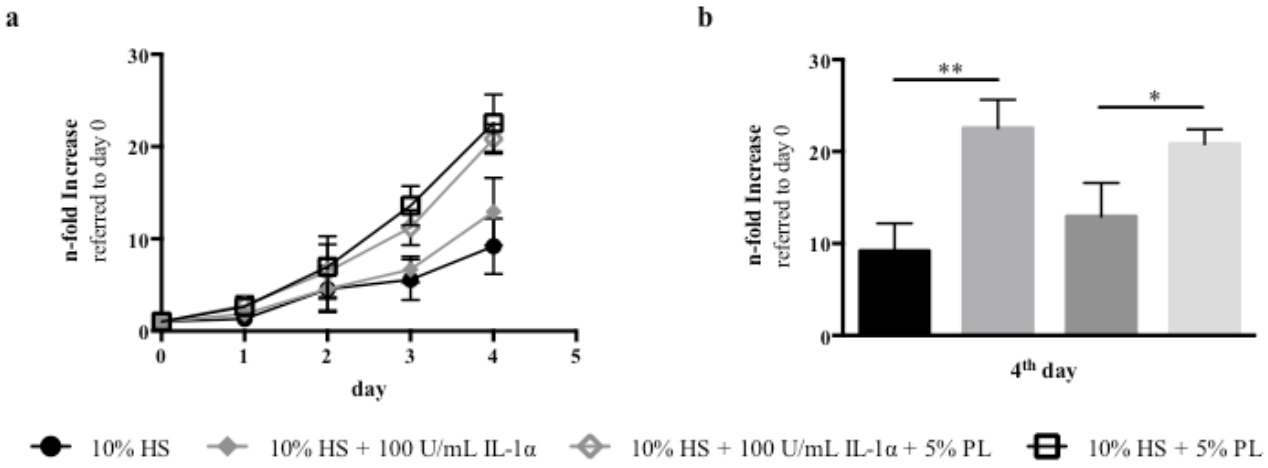

Figure 8: **a**) Effect of PL on HS-expanded hASC proliferation monitored in physiological and inflammatory by using crystal violet staining. For each culture condition, the n-fold increase of OD respect to day 0, expressed as the average of 3 independent experiments performed in quintuplicate on different single-donor primary cultures ± SD, was reported. **b**) The n-fold increase respect to day 0 obtained at 4th treatment day for each culture condition. The * and ** symbols correspond to p=0.0445 and p=0.0024, respectively. Statistical analysis was performed using the ordinary one-way ANOVA.

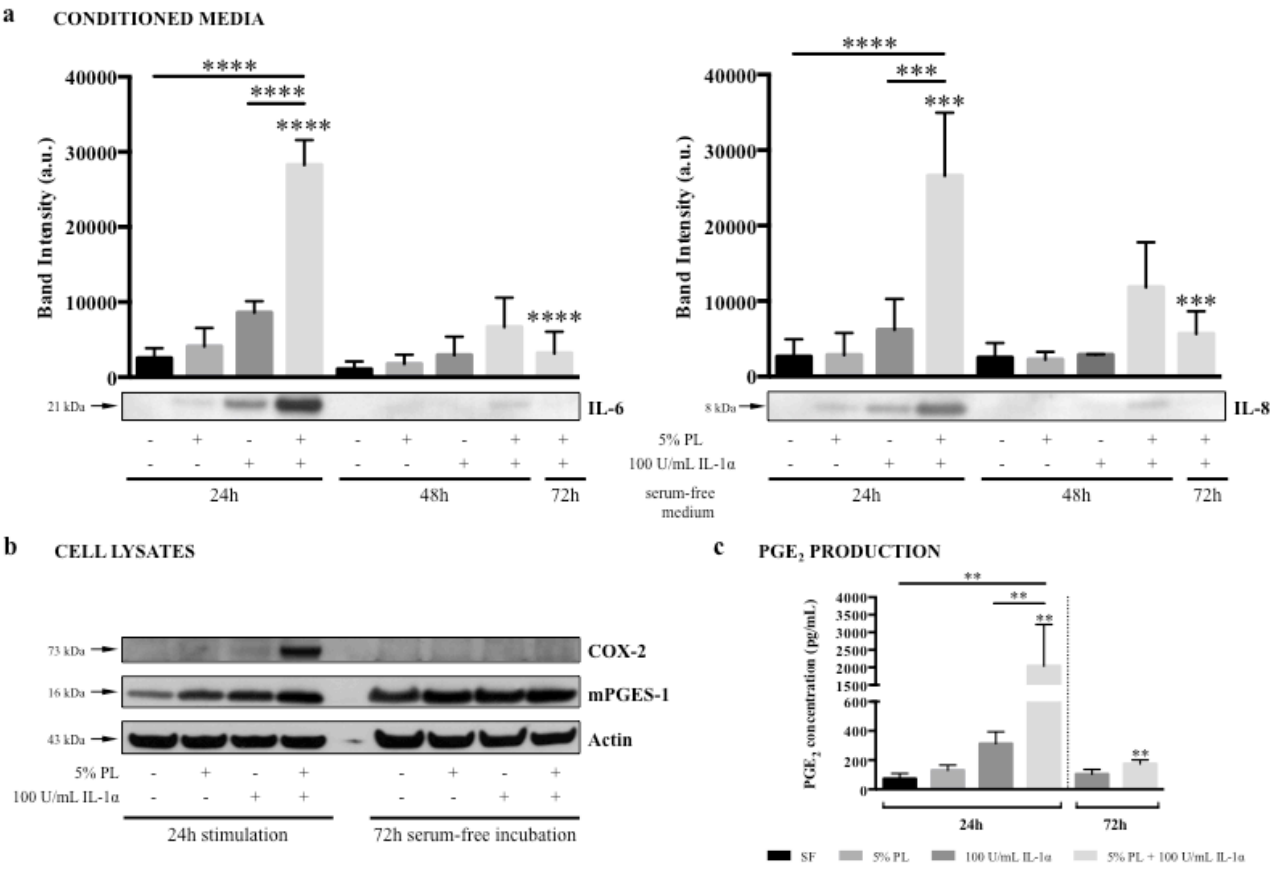

Figure 9: The PL effect on inflammatory response of HS-expanded hASCs under both physiological and inflammatory conditions. **a**) Secretion of IL-6 and IL-8 in hASC-conditioned media collected at 24, 48 and 72h after PL stimulation assayed by western blot. Densitometric analyses performed on 3 independent IL-6- or IL-8-probed western blots (means ± SD) deriving from 3 different single-donor primary cell cultures (in the upper panels) and representative western blots probed with primary antibodies raised against IL-6 and IL-8 (in the lower panels). The *** and **** symbols correspond to p=0.0002 and p<0.0001, respectively. Statistical analysis was performed using the ordinary one-way ANOVA. **b**) Representative western blots probed for COX-2, mPGES-1 and Actin relative to hASC-cell lysates harvested at the end of PL stimulation and after 72h of serum-free incubation. Actin was used as internal control. The results were confirmed performing 3 independent experiments with different primary hASC cultures. **c**) Quantification of PGE_2 in all conditioned media collected at 24h and in IL-1α- and PL+IL-1α-derived media collected at 72h by ELISA analysis. The averages of 3 independent experiments performed in duplicate on different primary cultures ± SD values were reported. The ** symbol refers to p≤0.0060. Statistical analysis was performed using the ordinary one-way ANOVA.

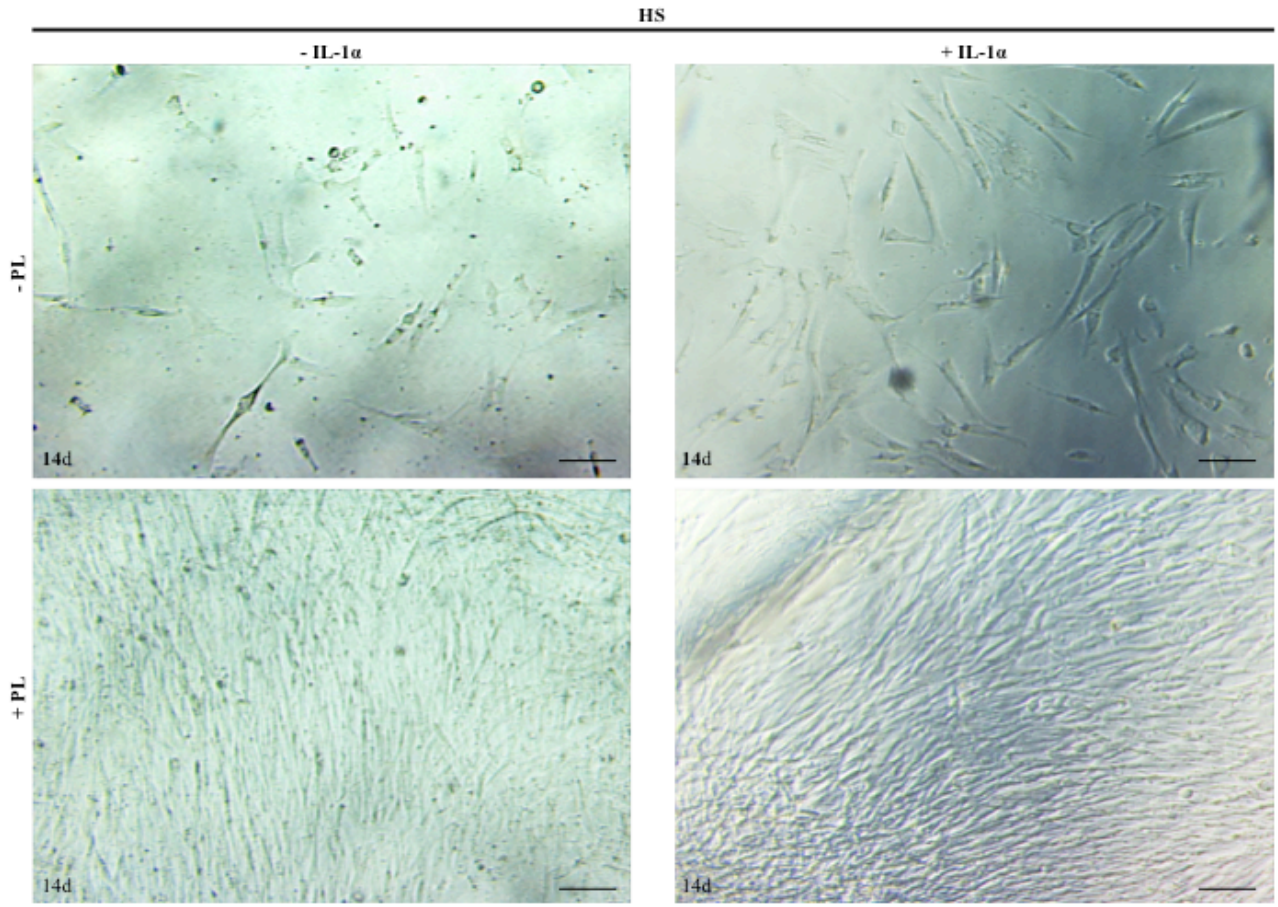

Figure 10: *Ex vivo* culture of *in toto* hAT using complete medium supplemented with PL, IL-1α, or PL+IL-1α, or without any supplement, for 14 days. Cells released by hATs in all tested conditions

during the culture. Scale bar = 100 µm. The reported cell release was observed in 3 independent experiment performed on AT samples deriving from different patients.

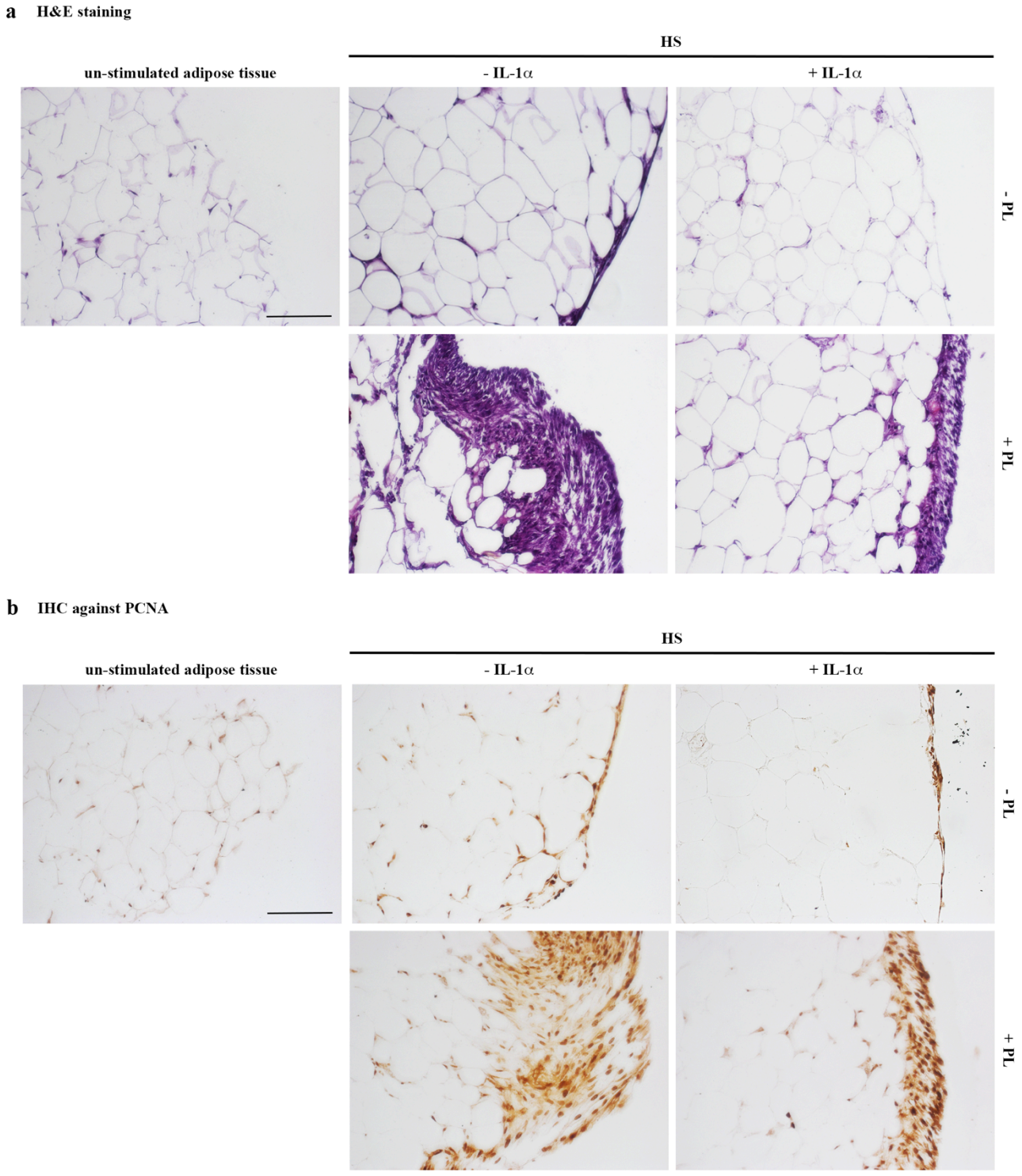

Figure 11: Histological analysis of *in toto* hAT samples cultured *ex vivo* using complete medium supplemented with PL, IL-1α, or PL+IL-1α, or without any supplement, for 14 days. **a**) Hematoxylin and Eosin (H&E) staining of paraffin-embedded hAT pieces at the end of the culture with each tested condition. The sample named 'un-stimulated adipose tissue' refers to hAT pieces

paraffin-embedded immediately after their isolation from the resection material and not cultured. **b**) Immunohistochemical analysis using a specific primary antibody raised against PCNA on paraffin-embedded hAT pieces. Scale bar = 100 μm.

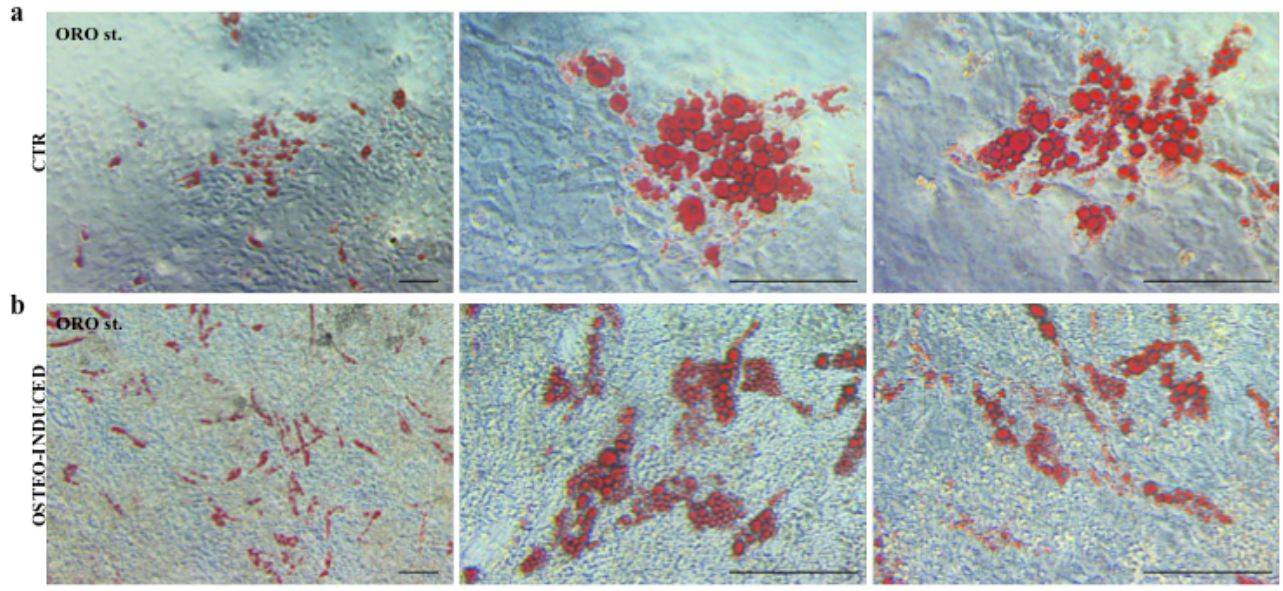

Figure 1S: Osteogenic differentiation of HS-expanded hASCs by using a traditional differentiation protocol. Representative ORO staining of osteogenesis-induced (OSTEO-INDUCED, **b**) and control (CTR, **a**) cells at the end of induction at different magnifications. Scale bar = 100 μm. The results were confirmed performing 3 independent experiments with different single-donor primary cell cultures.

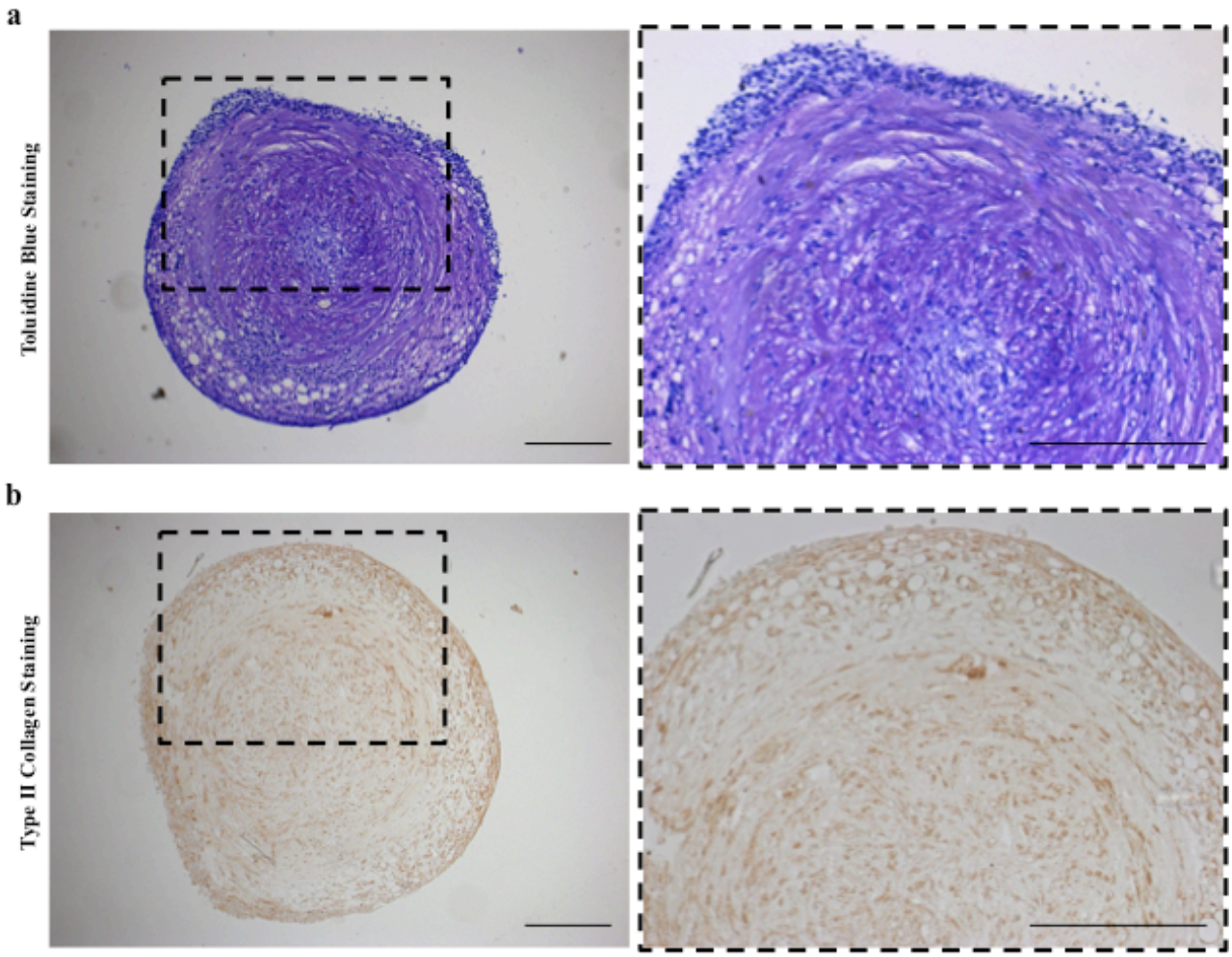

Figure 2S: Chondrogenic differentiation of HS-expanded hASCs by pellet-culture method under permissive conditions. Representative toluidine blue staining (**a**) and immunohistochemical analysis for type II collagen expression (**b**) of paraffin-embedded pellet at the end of induction. The images on the right are magnification of the sections with dashed outline. Scale bar = 200 μm.

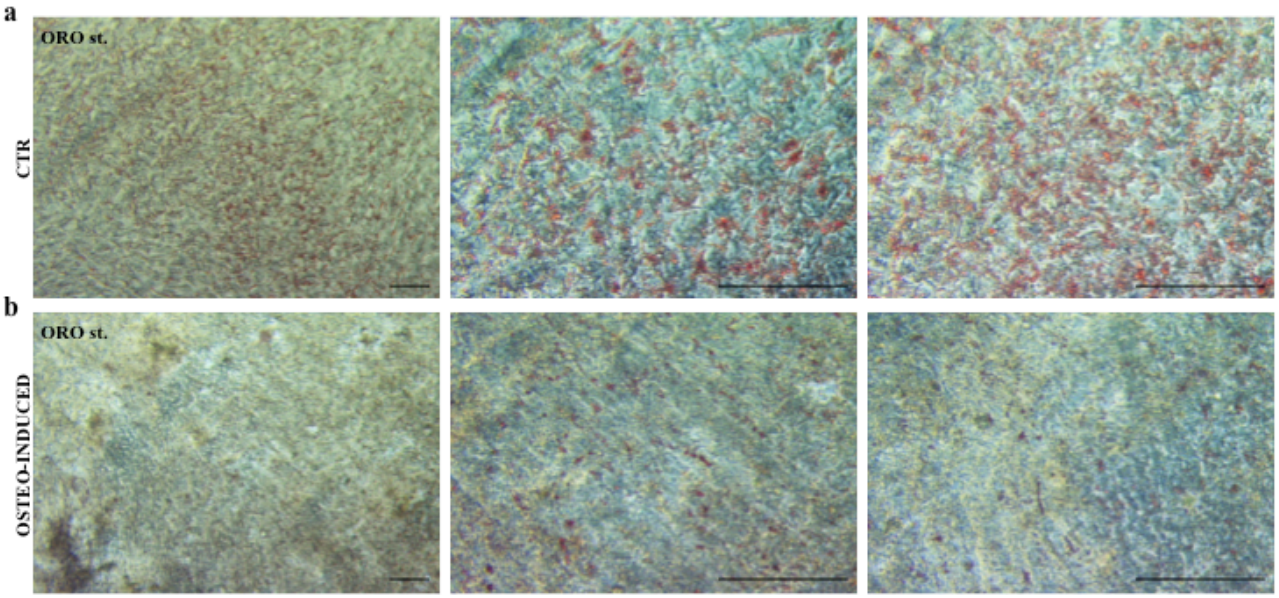

Figure 3S: Osteogenic differentiation of hASCs further cultured with complete medium supplemented with PL for 3 passages by using a traditional differentiation protocol. Representative ORO staining of osteogenesis-induced (OSTEO-INDUCED, **b**) and control (CTR, **a**) cells at the end of induction at different magnifications. Scale bar = 100 μm. The results were confirmed performing 3 independent experiments with different single-donor primary cell cultures.

4. CLOSING REMARKS

My group of research previously investigated the activation of several cell systems in response to platelet lysate (PL) under both physiological and inflammatory conditions in order to elucidate the regenerative mechanisms taking place during wound-healing process. Considering that inflammation is the first body's response to the injury and that platelet content triggers this response, they evaluated the *in vitro* effect of PL on inflammatory response of human keratinocytes, osteoblasts and chondrocytes demonstrating the rapid enhancement of the pro-inflammatory NF-κB pathway activity induced by IL-1α (El Backly et al., 2011; Pereira et al., 2013; Ruggiu et al., 2013). In association with such NF-κB pathway activation, they found the increased expression and secretion of pro-inflammatory cytokines IL-8 (in all investigated cell systems) and IL-6 (in osteoblasts and chondrocytes) and of antimicrobial lipocalin NGAL (in chondrocytes and keratinocytes) in presence of PL under inflammatory conditions. In osteoblasts, the induction of IL-8 and IL-6 expression and secretion was transient as well as the expression and the production of pro-inflammatory COX-2 were temporarily induced by PL in inflammatory milieu. As a consequence of COX-2 activation, they found the strong production of PGE_2, whose it is reported the capability of induce the functional switch of macrophages from pro-inflammatory M1 to pro-resolving M2 phenotype (Maggini et al., 2010; Tasso et al., 2013a; Ulivi et al., 2014). It was also demonstrated that platelet rich plasma (PRP) was able to promote the differentiation of monocytes to a regulatory anti-inflammatory population producing the anti-inflammatory cytokine IL-10 and PGE_2 (Papait et al., 2017). Overall, these findings suggest that platelet-released factors initially exert an immediate pro-inflammatory effect at the wound site and, at later time, an opposite effect by promoting the resolution of the inflammation phase. Considering the transient secretion of IL-8 and IL-6 and the transitory activation of COX-2 in parallel with PGE_2 secretion in presence of PL under inflammatory stimulus, the response of hASCs was consistent with the previous findings. Differently from the previous cell systems, HUVECs were instead protected by PL in the inflammatory milieu of the wound, because PL inhibited IL-1α-induced NF-κB activation already after 1-hour treatment and did not significantly enhance the production of IL-6 and IL-8 induced by IL-1α.

One other important aspect in the tissue repair is the activation and the recruitment of resident progenitor cells. According to its own composition, it was reported that PL was able to induce a strong mitogenic response in the chondrocytes, which maintain a chondrogenic re-differentiation potential (Pereira et al., 2013), and in the osteoblasts without affecting their differentiation potential (Ruggiu et al., 2013). Moreover, Ruggiu et al., 2013 demonstrated that PL resumed the proliferation

of quiescent osteoblasts also with a burst of treatment (24 hour). In agreement with these outcomes, they showed the activation of proliferation-related Akt and ERK pathways, the induction of Cyclin D1 and the phosphorylation of retinoblastoma following PL stimulation. Similarly, HUVECs responded to PL with an increased proliferation rate maintaining their capability of forming tube-like structures on matrigel and quiescent cells resumed proliferation showing the activation of Akt and ERK pathways and the induction of Cyclin D1 following PL treatment. In addition, PL induced also the stabilization of HIF-1α and the phosphorylation of STAT3, two factors involved in the angiogenesis, suggesting the possible *in vivo* contribution of PL to new vessel formation by activation of resident progenitor cells located in the vessel walls. In the adipose-tissue system, the mitogenic effect of PL was observed on hASCs that showed the activation of Akt, ERK and STAT3 pathways and the induction of Cyclin D1 following PL treatment, and also in *in toto* adipose tissue cultured *ex vivo* corroborating the *in vitro* outcomes. Considering the behaviour of these different cell systems in the presence of PL, there are robust evidences regarding the mitogenic effect of PL on resident progenitor cells and possibly on resting differentiated cells in support to the reconstitution of damaged tissue structures.

In the hASC study, I found that human serum (HS) was able to support cell proliferation much better than foetal bovine serum (FBS). However, hASCs expanded in HS showed the accumulation of lipid droplets and the up-regulation of two master regulators of adipogenesis, C/EBPα and PPARγ2, without adding any exogenous stimulus. Interestingly, these cells could be still differentiated towards the osteogenic lineage by using a traditional differentiation protocol. These findings suggest a hierarchy of progenitor cells within the hASC population expanded in HS with cells at different stages of commitment and differently responsive to the surrounding microenvironment. In this scenario, HS could exert a "niche" effect on hASCs regulating self-renewal and differentiation of stem/progenitor cells included in this cell population in order to preserve a reservoir of immature cells.

4.1. References – Chapter 4

El Backly, R., Ulivi, V., Ph, D., Tonachini, L., Ph, D., Mastrogiacomo, M., et al. (2011). Platelet Lysate Induces In Vitro Wound Healing of Human Keratinocytes Associated with a Strong Proinflammatory Response. 17. doi:10.1089/ten.tea.2010.0729.

Maggini, J., Mirkin, G., Bognanni, I., Holmberg, J., Piazzón, I. M., Nepomnaschy, I., et al. (2010). Mouse Bone Marrow-Derived Mesenchymal Stromal Cells Turn Activated Macrophages into a Regulatory-Like Profile. *PLoS One* 5, e9252. doi:10.1371/journal.pone.0009252.

Papait, A., Cancedda, R., Mastrogiacomo, M., and Poggi, A. (2017). Allogeneic platelet-rich

plasma affects monocyte differentiation to dendritic cells causing an anti-inflammatory microenvironment, putatively fostering wound healing. *J. Tissue Eng. Regen. Med.* doi:10.1002/term.2361.

Pereira, C., Scaranari, M., Benelli, R., Strada, P., Reis, R. L., Cancedda, R., et al. (2013). Dual effect of platelet lysate on human articular cartilage: a maintenance of chondrogenic potential and a transient pro-inflammatory activity followed by an inflammation resolution. *Tissue Eng. Part A* 19, 1476–1488. doi:10.1089/ten.TEA.2012.0225.

Ruggiu, A., Ulivi, V., Sanguineti, F., Cancedda, R., and Descalzi, F. (2013). Biomaterials The effect of Platelet Lysate on osteoblast proliferation associated with a transient increase of the in fl ammatory response in bone regeneration. *Biomaterials* 34, 9318–9330. doi:10.1016/j.biomaterials.2013.08.018.

Tasso, R., Ulivi, V., Reverberi, D., Lo Sicco, C., Descalzi, F., and Cancedda, R. (2013a). In vivo implanted bone marrow-derived mesenchymal stem cells trigger a cascade of cellular events leading to the formation of an ectopic bone regenerative niche. *Stem Cells Dev.* 22. doi:10.1089/scd.2013.0313.

Ulivi, V., Tasso, R., Cancedda, R., and Descalzi, F. (2014). Mesenchymal Stem Cell Paracrine Activity Is Modulated by Platelet Lysate: Induction of an Inflammatory Response and Secretion of Factors Maintaining Macrophages in a Proinflammatory Phenotype. *Stem Cells Dev.* 0, 1–12. doi:10.1089/scd.2013.0567.

5. CONGRESS PARTECIPATIONS And OTHER ACTIVITIES

During my Ph.D. period, I participated in the following congresses:

Congress	Organization	Date	Poster Presentation	Oral Presentation
Stem Cells, Cancer, Immunology and Aging	Fondazione Internazionale Menarini	February 12th-14th, 2015 Genova (IT)	-	-
Summer School on Biomaterials and Regenerative Medicine	University of Trento	July 6th-8th, 2015 Riva del Garda (IT)	-	-
GISM Annual Meeting 2015	GISM; Fondazione Poliambulanza; IZSLER	October 8th-9th, 2015 Brescia (IT)	-	-
European Chapter Meeting of TERMIS 2016	TERMIS	June 28th-July 1st, 2016 Uppsala (SE)	-	**x**
GISM Annual Meeting 2016	GISM; Fondazione Poliambulanza; IZSLER	October 20th-21th, 2016 Brescia (IT)	**x**	**x**
Scientific Meeting "Life science for a better future"	Associazione Italiana di Biologia e Genetica	May 11th-13th, 2017 Santa Margherita Ligure (IT)	-	-
Advances in stem cells and regenerative medicine	EMBO Conference	May 23th-26th, 2017 Heidelberg (DE)	**x**	-
European Chapter Meeting of TERMIS 2017	TERMIS	June 26th-30th, 2017 Davos (CH)	**x**	-

I also conducted the following activities:

- Support work for the practical laboratory experiences relative to the following academic courses:

Course	Academic Degree	N° of hours	Academic Year
Biologia Cellulare e dello Sviluppo e Laboratorio di Colture Cellulari e di Biologia dello Sviluppo	Corso di Laurea in Biotecnologie	32	2014/2015
Biologia Cellulare II e Laboratorio	Corso di Laurea Magistrale in Biotecnologie Medico-Farmaceutiche	16	2015/2016
Biologia Cellulare e dello Sviluppo e Laboratorio di Colture Cellulari e di Biologia dello Sviluppo	Corso di Laurea in Biotecnologie	32	2016/2017

- Tutoring activity for students at undergraduate level (Laboratorio per il Medico in Formazione, Corso di Laurea in Medicina e Chirurgia, academic year 2016/2017);
- Attendance at the basic course on "*Animal Experimentation*" organized by the S.S.D. Animal Facility of IRCCS Ospedale Policlinico San Martino in Genova, Italy (successfully completed);
- Attendance at the online non-credit course "*Basics of Extracellular Vesicles*" authorized by University of California, Irvine and offered through Coursera (successfully completed).